Master Thesis

National and Kapodistrian University of Athens

Advanced building materials using nanomaterials in building applications with self-cleaning properties

EVANGELOS KARAGIANNIS

September 2020

National and Kapodistrian University of Athens
School of Science
Department of Physics
Environmental Physics and Meteorology

Master Thesis

Advanced building materials using nanomaterials in building applications with self-cleaning properties

---

Master thesis of:

Evangelos Karagiannis

Supervising Committee

Associate Professor Margarita Niki Assimakopoulos

Associate Professor Dimosthenis Stamopoulos

Professor Konstantinos Varotsos

September 2020

Περίληψη

Η νανοτεχνολογία στον κατασκευαστικό τομέα προσφέρει ενδιαφέρουσες, νέες ευκαιρίες όσον αφορά την ανάπτυξη σύγχρονων κατασκευαστικών συστημάτων, δομικών υλικών και μεθόδων σχεδιασμού. Αυτές οι εφαρμογές συναντώνται σε οικοδομικές μήτρες, επιστρώσεις ή σε μονωτικά υλικά. Στον κατασκευαστικό τομέα, η νανοτεχνολογία διαθέτει ήδη στην αγορά αυτοκαθαριζόμενα παράθυρα, φωτοκαταλυτικό σκυρόδεμα, αντιμικροβιακές επιστρώσεις και πολλές άλλες καινοτομίες. Επιπλέον, η ενσωμάτωση των ανακυκλωμένων δομικών υλικών και της 3-Δ εκτύπωσης στον κατασκευαστικό τομέα αποτελεί ένα ακόμη βήμα προς την βιωσιμότητα. Τα φωτοκαταλυτικά νανοϋλικά με ιδιότητες αυτοκαθαρισμού μπορούν να χρησιμοποιηθούν ως επιστρώσεις σε δομικά στοιχεία ή πεζοδρόμια αλλά και σε διακοσμητικά αντικείμενα όπως πάνελ οροφής, κουρτίνες και ταπετσαρίες, προκειμένου να αποφευχθεί η αφαίρεση του στρώματος προστασίας των επιφανειών, η αλλαγή χρώματος των βαφών και η ρύπανση από τις χημικές ουσίες των καθαριστικών. Νανοδομές διοξειδίου του τιτανίου (TiO_2) αλλά και άλλων οξειδίων, μπορούν να χρησιμοποιηθούν ως φωτοκαταλυτικά προϊόντα με αυτοκαθαριζόμενες ιδιότητες. Το νανοϋλικό TiO_2 μελετάται σε αυτήν τη διπλωματική εργασία, λόγω της υψηλής φωτοκαταλυτικής του δραστηριότητας, της υψηλής σταθερότητας και του χαμηλού του κόστους. Το ντόπινγκ με μέταλλα έχει αποδειχθεί επιτυχής προσέγγιση για την ενίσχυση της φωτοκαταλυτικής απόδοσης των φωτοκαταλυτών. Νανοδομές TiO_2 χωρίς ντόπινγκ αλλά και με In-Ni-, Mn-In, Mn-Cu-, Mn-Ni- διμεταλλικό ντόπινγκ συντέθηκαν με την υδροθερμική μέθοδο υποβοηθούμενης από μικροκύματα. Μελετήθηκε ο αποχρωματισμός των νανοεπιστρώσεων που εφαρμόστηκαν σε 3-Δ τυπωμένα πλακίδια και υφάσματα, χρησιμοποιώντας ένα τεστ αυτοκαθαρισμού και απορρύπανσης, τον αποχρωματισμό του Methylene Blue (MB). Τα πλακίδια που επιστρώθηκαν με τα νανοϋλικά TiO_2 με Mn-In- και In-Ni- ντόπινγκ έδειξαν τον υψηλότερο καθαρό (net) αποχρωματισμό του MB, 25.1 και 22.6 % αντίστοιχα, μετά από 2 ώρες έκθεσης σε υπεριώδες φως. Ενώ τρία δείγματα υφάσματος (TiO_2 με Mn-In-, In-Ni- και Mn-Cu- ντόπινγκ) παρουσίασαν μεγάλο αποχρωματισμό του MB (58.1, 52.7 και 47.6% αντίστοιχα) κάτω από το έμμεσο ηλιακό φως. Ως εκ τούτου, τα νανοεπιστρωμένα δείγματα έδειξαν υψηλό αποχρωματισμό του MB και μεγάλες δυνατότητες σε εφαρμογές αυτοκαθαρισμού.

Abstract

Nanotechnology in the construction industry offers interesting new opportunities for advancing construction systems, building materials, and design methods. These applications can be found in building matrices, coatings or insulating applications. In the construction industry, nanotechnology has already brought to market self-cleaning windows, smog-eating concrete, antimicrobial coatings and many other advances. Moreover, the incorporation of recycled construction materials and 3-D printing in construction industry is a further step towards sustainability. Photocatalytic nanomaterials with self-cleaning properties can be used as coatings on building blocks or pavements, but also on interior decorative items such as ceiling panels, curtains and wallpapers, in order to avoid the removal of the protection layer of the surfaces, the color change of pigmented elements, and the chemical contaminants from cleaning. Nanostructured titanium dioxide (TiO_2) and other oxides can be used as photocatalytic products with self-cleaning properties. The nanomaterial TiO_2 is studied in this Master thesis, because of its high photocatalytic activity, the high stability and the low cost. Metal doping has proved to be a successful approach for enhancing the photocatalytic efficiency of photocatalysts. Undoped and In-Ni-, Mn-In, Mn-Cu-, Mn-Ni- bimetallic doped TiO_2 nanostructures were synthesized using the microwave-assisted hydrothermal method. Decolorization of applied nanocoatings on 3-D printed panels and fabrics was studied, using a self-cleaning and a de-pollution test, Methylene Blue (MB) decolorization. The panel coated with Mn-In- and In-Ni- doped TiO_2 showed the highest net MB decolorization, 25.1 and 22.6 %, respectively, after 2 hours of UV light exposure. While three fabric samples (Mn-In-, In-Ni- and Mn-Cu-doped TiO_2) showed great MB decolorization (58.1, 52.7 and 47,6 % respectively) under indirect sunlight. Therefore, nanocoated samples showed high MB decolorization and great potential in self-cleaning applications.

Acknowledgements

I would like to express my deep and sincere gratitude to my thesis supervisor, Associate Professor Margarita Niki Assimakopoulos at Physics Department, Applied Physics and Meteorology sector of the National and Kapodistrian University of Athens, head of the Group of Building Environmental Studies, for giving me the opportunity to do research and providing invaluable guidance throughout this research.

I would like to thank Senior Researcher Dimitra Papadaki for sharing expertise, and sincere and valuable guidance and encouragement extended to me. I would also like to express my gratitude for the X-Ray Diffraction experiments carried out at the Laboratory of X-Ray Diffraction, Section of Condensed Matter Physics, Department of Physics, National and Kapodistrian University of Athens under the supervision of Late Associate Professor Emmanouel Syskakis.

Finally, i must express my very profound gratitude to my parents for their love, prayers and sacrifices for educating and preparing me for my future, my sister and Ioanna for their valuable support and continuous encouragement throughout my years of study and through the process of researching and writing this thesis. This accomplishment would not have been possible without them. Thank you all.

Evangelos Karagiannis

September 2020

Table of Contents

List of Figures

List of Tables

Introduction

Nanotechnology, is bringing new materials and new possibilities to industries contributing to an improved living environment and comfort on a daily base. One of these is the construction industry, where nanotechnology can generate products with many unique characteristics that can improve the current construction materials. New materials and products based on nanotechnology can be found in building matrices, coatings or insulating applications. Specifically, lighter and stronger structural composites, low maintenance coatings, better cementitious materials, lower thermal transfer rate of fire retardant and insulation, self-cleaning windows, smog-eating concrete, antimicrobial coatings and many other advances.

The incorporation of recycled construction materials and 3-D printing in construction industry is a further step towards sustainability. The use of recycled materials in the construction industry totally changes the value chain linked to all stages of intervention in existing buildings, making the operations sustainable in social, environmental and economic terms [Cheshire et al., 2017; Mangialardo & Micelli et al., 2018]. The use of advanced materials and technologies such as 3-D printing are examples of new methods and products to improve the quality by minimizing the chance of errors by highly precise material deposition, reduce on-site construction time by operating at a constant rate and reduce the costs connected to the design and management of buildings and infrastructures by reducing the labor requirements, saving of materials and, consequently, sustainability [W. Gao et al., 2015; R.A. Buswell et al., 2007; X. Ming & S. Jay et al., 2016; W. Timothy et al., 2016].

Cleaning of surfaces may be disadvantageous involving the removal of the protection layer, changing the color of pigmented elements, leaving behind chemical contaminants and increasing the risk of rain penetration [Flores e Colen et al., 2008; Mansour et al., 2018]. Moreover, the pollutants have a major effect on building structures and interior decorative items. For example, black particles and tobacco smoke cause soiling of light-colored surfaces and sulfates/nitrates because of the acid rains enhancing the surface recession [Mansour et al., 2018]. A solution to this is the use of photocatalytic nanomaterials. Photocatalytic titanium dioxide nanoparticles with self-cleaning properties can be used as coatings on building blocks or pavements, but also on interior decorative items such as ceiling panels, curtains and wallpapers. Also nanostructured titanium dioxide (TiO_2) can be used as photocatalytic products with antimicrobial properties, or air purifier, waste water treatment cleaning and water disinfection [Gnanaprakasam & Sivakumar et al., 2015; D. Colangiuli et al., 2015; Matoh et al., 2019; Janjua et al., 2019].

In this Master thesis, synthesis and characterization of photocatalytic titanium dioxide nanoparticles took place, followed by the assessment of their decolorization effectiveness as coatings on fabrics and 3-D printed panels made of recycled materials. The synthesis of TiO_2 nanoparticles was conducted with the microwave-assisted hydrothermal method at Group Building Environmental Studies (GRBES) lab at NKUA. The characterization techniques used were, X-Ray Diffraction (XRD) and for the investigation of the specific surface area the BET (Brunauer, Emmett and Teller) analysis at Section of Condensed Matter Physics (CMP) Laboratory of X-Ray Diffraction and GRBES lab, at NKUA, respectively. Decolorization of applied coatings was evaluated by the use of a self-cleaning and a de-pollution test, of Methylene Blue decolorization, inside a self-made photocatalytic apparatus, also at GRBES lab.

This Master thesis consists of six chapters. Initially, in the first chapter, a theoretical background of nanotechnology is being presented. In this chapter, nanotechnology is defined, as well as the nanomaterials used in the construction industry are analyzed through applications, innovations and future trends. The mechanism of photocatalysis and the antimicrobial function are explained, and the basic information about TiO_2 photocatalyst is given. In the end of that chapter limitations, challenges and drawbacks of nanotechnology are being analyzed.

In the second chapter, additive manufacturing (AM) technology or 3-D printing is being presented. Types of small and large scale 3-D printing processes are being analyzed in the construction industry through innovative applications. Furthermore, the limitations and challenges of 3-D printing processes in the construction industry are being analyzed.

In the third chapter, the need for sustainable construction practices following the principles of circular economy is being explained. In addition, recycled and waste materials are being analyzed with special reference to concrete aggregate recycling.

Next, the experimental procedure is presented. In this chapter, the experimental methodology is explained, together with the synthesis and characterization methods of materials, techniques and instrumentations.

In the fourth chapter, the results from the characterization of TiO_2 photocatalyst are presented and analyzed. In this chapter the lattice parameters, interplanar spacing, the crystallite size, the micro strain and the surface area of undoped and doped TiO_2 were calculated. The crystallite size was calculated by two methods, the modified Scherrer equation and the Halder-Wagner method.

In the fifth chapter, decolorization of the nanocoatings on 3-D printed panels and fabrics was studied. Decolorization of applied coatings was evaluated by the decolorization of Methylene Blue. For decolorization of Methylene Blue under UV light irradiation the samples were placed inside a handmade photocatalytic apparatus.

Finally, conclusion remarks and recommendations are presented.

Chapter I

Theoretical Background of Nanotechnology

1.1 Nanotechnology definitions

Nanotechnology is not considered a modern science or a new technology; it is rather an extension of the sciences and technologies that have already been in development for many years. The National Nanotechnology Initiative defines nanotechnology as "the understanding and control of matter at the nanoscale, at dimensions between approximately 1 and 100 nanometers, where unique phenomena enable novel applications" [NNI et al.]. In other words, it is the use of very small particles of materials to create new large-scale materials [Mann et al., 2006]. The prefix "nano" means 10^{-9} or one billionth; hence, one nanometer is one billionth of a meter (International System of Units) that is, about 1/80,000 of the diameter of a human hair. To put the scale in another context, the comparative size of nanometer to meter is the same as that of a marble to the size of the earth or another way of putting it; a nanometer is the amount an average man's beard grows in the time it takes him to rise the razor to his face [S. Patel Abhiyan et al., 2013].

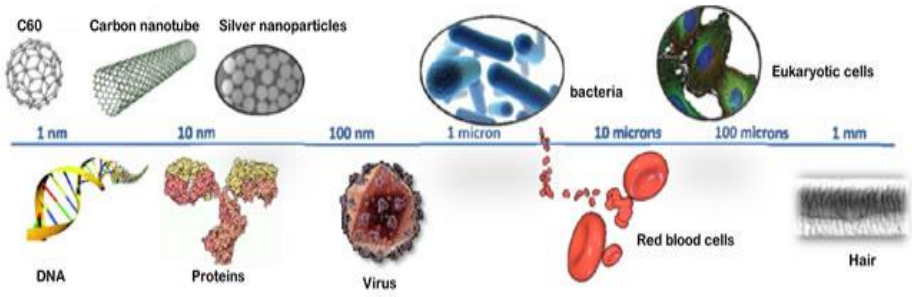

Fig. 1 Size comparison: nanoparticles and biological systems. [Contera Sonia et al., 2019]

The key in nanotechnology is the size of particles because the properties of materials are dramatically affected under a scale of nanometer. Because the size of the particles is a significant factor, the materials properties differ at the nanoscale from that at larger scale. Physical phenomena begin to happen below that: gravity becomes inconsequential, electrostatic force and quantum effect start to prevail. At the same time, the properties of atoms on the surface augment proportional to those inside creating the so-called "Nano-effect". All these nano-properties actually affect the materials behavior at macroscale and this is where the power of nanotechnology comes in. Traditional materials such as metals and ceramics show radically enhanced properties and new functionalities, the behavior of surfaces starts to dominate the behavior of bulk materials, and whole new realms open up for us [CMP et al., 2001].

There are two conventional approaches to designing materials with nanotechnology, the “top-down” and the “bottom-up.” These two models are fundamentally different, both in the approach to create structures and in the underlying science that will make them possible [Zhu et al., 2004]. The “bottom-up” approach, often referred to as molecular nanotechnology, focuses on producing complex structures through the build-up of atoms or molecules. The common processes of the bottom-up approach comprise imprinting, laser trapping/tweezers, contact printing, and spinodal wetting/de-wetting [Biscarini et al., 2002]. The “top-down” approach focuses on reducing the size of the smallest structures towards the nanoscale while maintaining their bulk-scale properties, so nanostructures are built from their macroscale counterparts without atomic level control. Common processes of the top-down approach include thin film deposition and growth, mechanical, electrochemical material removal, laser beam processing, and lithography processes [Biscarini et al., 2002].

Nanotechnology requires advanced imaging techniques for studying and improving the material behavior and for designing and producing very fine powders, liquids or solids of materials with particle size between 1 and 100 nm, known as nanoparticles [Gogotsi et al., 2006; Shaki et al., 2014]. More than anything else, nanotechnology is an enabling technology, allowing us to do new things in almost every conceivable technological discipline. At the same time, its applications will lead to better, cleaner, cheaper, faster and smarter products and production processes. The major application of nanotechnology is in the field of Nano-medicine, Environment, Energy, Nano-batteries, Information and communication, Heavy industry Civil Engineering and Construction.

1.1.1 Nanoparticles

The nanoparticles can be classified into different groups based on different criteria, like on the basis of their synthesis, the nanoparticles can be divided into three classes (i) engineered (ii) natural and (iii) Incidental [Mohajerani et al., 2019].

Engineered nanoparticles

Engineered nanoparticles are intentionally engineered through either bottom-up or top-down synthesis processes for application in a range of fields. These processes differ in approach, with the top-down synthesis gradually reducing larger structures in size to nanometer dimensions whilst the bottom-up synthesis involves constructing nanoparticles with individual atoms or molecules until the target size is achieved [Nowack et al., 2013]. The top-down approach allows for higher production volumes, but due to the production methodology involving mechanical stress, violent shocks, and deformation, the final nanoparticle product may lack homogeneity in size and formation. The bottom-up approach allows for greater accuracy in nanometric state, allowing a multiplicity of nanoparticle structures, greater precision in molecular positioning, uniformity in grain size, and homogeneity of the final product, albeit at the cost of reduced production quantities [Nowack et al., 2013].

The engineered nanoparticles on the basis of their composition can be further classified into different groups, which are illustrated in Table. 1 [Phogat et al., 2016].

Nanoparticles Composition	**Metal Based**	**Metal NPs**	**Au, Ag, Fe, Zn, Cu, Se, Sn, ..**
		Metal Oxide NPs	TiO_2, ZnO, MoO_3, ..
		Binary Oxide NPs	Bi_2O_3, CeO_2, CrO_2, ..
	Nanocomposites	Ceramic matrix NPs	Al_2O_3/TiO_2, Al_2O_3/SiO_2, Al_2O_3/CNT, ...
		Metal matrix NPs	Co/Cr, Fe-Cr/Al_2O_3, Fe-MgO, ..
		Polymer matrix NPs	Polymer/TiO_2, Polymer/CNT, ..
	C- Based	Fullerene	C_{60}, C_{70}, Fullerenol, ..
		Multiwalled Carbon Nanotube (MWCNT)	
		Single Walled Carbon Nanotubes (SWCNT)	
	Dendrimers	Nanosized Polymers	
	Quantum Dots	CdSe, CdTe, CdSeTe, ZnSe, Bi_2S_3, ..	

Table 1. Classification of engineered nanoparticles on the basis of their composition. [Phogat et al., 2016]

Natural nanoparticles

Nanoparticles occur naturally through a range of mechanisms commonly seen and can have a range of effects. Major producers of nanoparticle materials include volcanic eruptions, desert surfaces, and dust from cosmic bodies [Strambeanu et al., 2015]. Volcanic eruptions produce solid, liquid, and gas by-products, with a large portion of particulate matter being suspended by escaping gas. As the gas cools, the particulate matter is suspended within accumulates and deposits. Deserts produce nanoparticles on mass, with an estimated 50% of all aerosols occurring in the troposphere originating from deserts, comprising a variety of materials represented in mass distributions. Nanoparticles can also occur in food products naturally, with a prime example being casein micelle, which is found within the milk of mammals. The process of milk generation involves the development of casein molecules. During this process, the casein protein assumes the micelle structure at a nanometer scale, existing within milk as a colloidal suspension [Rogers et al., 2016]. Nanoparticles have also been found in foods that contain solid fats, with food items including chocolate, margarine, and lard demonstrating nanoscale platelets. These nanoscale platelets are generally 200 nm long, 80 nm wide and 20 nm thick, and act as the smallest microstructural elements of the colloidal fat crystal network [Rogers et al., 2016].

Incidental nanoparticles

The generation of incidental nanoparticles occurs through a variety of channels that are not immediately obvious in day to day life but can become apparent when identified and addressed. A clear example of incidental nanoparticles that occur in the built environment are those generated by cars through tyre material loss, brake pad material loss, exhaust emissions, and paint deterioration. Addressing the potential for negative health and environmental effects due to exposure to incidental nanoparticles is important to gauge the outcome of the interactions involving nanoparticles that are not immediately obvious. By identifying incidental nanoparticle and microparticle generation mechanisms, solutions can be proposed to address the issue. To highlight the oversight that may occur on a larger scale, tyre emissions can be assessed.

It is generally assumed that fine particulate matter results from exhaust fumes and any larger particle emissions are due to tyre or brake pad erosion; however, it has been seen that exhaust and non-exhaust related by-products contribute near equally to Particulate Matter 10 micrometers (PM10) emissions, with non-exhaust contributions predicted to increase [Grigoratos et al., 2014].

Based on the dimensions of the nanomaterials, they can be divided into four groups: zero-dimensional (0D), one-dimensional (1D), two-dimensional (2D), and three-dimensional (3D) nanoparticles [Pokropivny & Skorokhod et al., 2007; Pokropivny & Skorokhod et al., 2008]. A 0D nanoparticle is defined as a particle with all its dimensions subjected to nanoscale. This group includes nanoparticles, nanoclusters, and nanocrystals. SiO_2, TiO_2, ZnO, and $CaCO_3$ nanoparticles are categorized as 0D. A 1D nanoparticle can be described as having two dimensions in nanoscale, with the other dimension reaching above the nanoscale. Nanotubes, nanofibers, nanorods, and nanowires belong to this category. A 2D nanoparticle is originally a sheet with its thickness in the nanoscale and its sides spreading beyond the “nano” criterion. This group covers nanofilms, nanolayers, and nanocoatings. 3D nanomaterials include powders, fibrous, multilayer, and polycrystalline materials in which the 0D, 1D, and 2D structural elements are in close contact [Korayem et al., 2017].

1.1.2 History of Nanotechnology

Nature has been manufacturing nanosized objects for billions of years, such as cells in plants and animals, but we do not call that nanotechnology. Also, nanoparticles can be found in Ming-dynasty pottery and stained-glass windows in medieval churches, as well as in ancient Greece in the famous black-figure pottery, which is an alkalic aluminosilicate glass which is colored by magnetite nanocrystals. But then people were not aware of the nanoparticles involved, and as they had no control over particle size or knowledge of structures at the nanoscale, they were not using nanotechnology as currently defined.

Fig. 2 Black-figure calyx krater. One side shows a Homeric battle around the dead body probably of Patroclus. The rear has a quadriga (four-horse chariot). From Farsala. In the style of Exixia. Around 530 BC. [Collection of National Archaeological Museum, Athens]

The concept of nanotechnology was originally introduced by the famous physicist Richard Feynman in 1959, through his talk “There’s Plenty of Room at the Bottom”, which he delivered to an American Physical Society meeting at the California Institute of Technology. In his lecture, he discussed the possibility of using atoms as building particles to create nanosized products [Feynman et al., 1959]. The ideas put forward by Feynman passed unnoticed until 1974 when Norio Taniguchi introduced the word “nanotechnology” at the International Conference on Production Engineering [Taniguchi et al.,1974]. Taniguchi described the processes of creating semiconductor structures using various methods with nanometer precision. He introduced the “top-down” approach, which refers to the successive cutting or slicing of a bulk material to create nanosized particles.

Kim Eric Drexler envisioned tiny self-replicating molecular assemblers that could build everything from chairs to rocket engines and machines that turn domestic waste into foods and toys at a touch of a button, and nano submarines voyaging through our bloodstream zapping cancer cells. He presented the “bottom-up” approach; the creation of material from molecular and atomic components, molecule by molecule, atom by atom [Drexler et al., 1981]. In 1986 Kim Eric Drexler developed the idea of nanotechnology and published a book titled “Engines of Creation: The Coming Era of Nanotechnology”. In the book, he proposed the idea of a nanoscale assembler, which would have the capacity and ability to build copies of itself and other things of distinctive complexity, known as molecular nanotechnology [Drexler et al., 1986].

Around the same time, Binnig and Rohrer at IBM invented the scanning tunneling microscope (STM) which allowed scientists for the first time to view things (e.g. nanoparticles) at atomic resolution. Soon afterwards the atomic force microscope (AFM) for working with non-conductive materials was also developed. Since then, a raft of related instruments now known collectively as scanning probe microscopes (SPMs) have been developed to analyze properties of nanostructures, molecules and atoms on the surfaces. The capability to manipulate and positionally control matter on a nanoscale was demonstrated, for the first time, in 1989 when Eigler used a SPM to slowly arrange 35 xenon atoms to spell out the letters IBM (spanning less than 3 nm) on top of a crystal of nickel.

In 1999, nanotechnology received a major boost when the USA government created the National Nanotechnology Initiative (NNI) and started to pour huge amounts of funding into research areas related to nanotechnology. This was soon followed by unprecedented investment provided by many other governments, businesses and venture capitalists.

1.2 Nanotechnology in the construction industry

Nanotechnology has been introduced in several industries, contributing to an improved living environment and comfort on a daily base. Nanotechnology is bringing new materials and new possibilities to industries as diverse as electronics, medicine, energy and aeronautics. Our ability to design new materials from the bottom up is impacting the building industry as well. New materials and products based on nanotechnology can be found in building insulation, coatings, and solar technologies. This area is perhaps the most commercially developed and the use of these nanoscale materials has been the basis for many current and potential applications in various industrial sectors. In the building industry, nanotechnology has already brought to market self-cleaning windows, smog-eating concrete, and many other advances.

Nanotechnology can generate products with many unique characteristics that can improve the current construction materials. Specifically, lighter and stronger structural composites, low maintenance coatings, better cementitious materials, lower thermal transfer rate of fire retardant and insulation, better sound absorption of acoustic absorbers and better reflectivity of glass [Lee et al., 2010].

The slab of the structure with still reduced thickness, and hence the reduced weight of structure with benefits of reduced sections of beams, columns and foundation footings, which may result to faster construction and reduced overall life time cost because of such enhanced property of concrete [S. Patel Abhiyan et al., 2013]. More functionally operated green buildings with glass facade, as the light can enter but not the heat and also the self-cleaning properties, hence the operating cost of maintaining the temperature within the building and extra effort, risk and cost for maintaining and cleansing the glass facade at greater height for sky scrapers reduces [S. Patel Abhiyan et al., 2013]. The improved coatings can result to more durable structure requiring less maintenance cost, along with the view point of creating better environment as some of the nanoparticles such as TiO2 and silver nanoparticles has sterilizing and anti-fouling properties, the particles catalyze powerful reactions that break down organic pollutants, volatile organic compounds and bacterial membranes [S. Patel Abhiyan et al., 2013].

Nanotechnology, promises to heighten building security and homeland security through the introduction of stronger materials and more powerful sensors. Many of the nanotech innovations now available or in development will have applications for building security. The primary areas of application will be in the strengthening of materials, the advent of nano-sensors, and improved air and water filtration [G. Elvin et al., 2004]. Nanotechnology has the potential to transform the construction sector into a period focused on environmental protection and innovation competitiveness, and, moreover, it has the capability to radically change our built environment by promising “more for less” [Mohamed et al., 2015].

1.2.1 Nanomaterials in building matrices

The most studied materials so far are cementitious materials, and knowledge on the nanoscale level of cement materials is available by several studies bringing light to basic knowledge and understanding of structural and mechanical properties [Kurapati et al., 2014]. Much analysis of concrete is being done at the nano-level in order to understand its structure. Such analysis uses various techniques developed for study at that scale such as Atomic Force Microscopy (AFM), Scanning Electron Microscopy (SEM) and Focused Ion Beam (FIB). This has come about as a side benefit of the development of these instruments to study the nanoscale in general, but the understanding of the structure and behavior of concrete at the fundamental level is an important and very appropriate use of nanotechnology [S. Patel Abhiyan et al.].

From a bottom-up perspective, concrete is a composite material in which molecular surfaces and chemical bonds interact with chemical reactions, intermolecular forces, and intraphase diffusion [Sanchez & Sobolev et al., 2010]. Concrete consists of nano to macro sized particles suspended in a calcium-silicate-hydrate (C-S-H) matrix [Wong Shane et al.].

At the nanoscale, processes within the material are defined by the interactions between particles and phases, while at a macroscale the effects of working loads and the surrounding environment are dominating [Sanchez & Sobolev et al., 2010]. Nanoparticles such as SiO_2, Al_2O_3, TiO_2, Fe_2O_3, ZnO, nanoclay, carbon nanotubes and carbon nanofibers can be used in concrete binders to enhance performance [Sanchez & Sobolev et al., 2010]. The particle size and specific surface area scale related to concrete materials reflect the general trend to use finer materials [Sobolev & Ferrada-Gutiérrez et al., 2005]. Nanomaterials are characterized by a high surface area to volume ratio, making them suitable for chemical reactions [Sanchez & Sobolev et al., 2010].

A variety of nanoparticles have been studied for use in chemical processing to improve mechanical and electrochemical properties (strength, ductility, electrical conductivity, corrosion inhibition), durability, workability, surface protection of the reinforcement through application of surface coatings (nanomodified reinforcement), reduce waste or replace toxic materials and for treatment or remediation of pollutants in the environment. Hereby several additional nanomaterials commonly induced in cementitious matrices and concrete, are presented. The addition of nano-silica (SiO_2) to cement based materials can control the degradation of the calcium-silicate-hydrate reaction caused by calcium leaching in water, blocking water penetration and leading to improvements in durability [Mann et al., 2006]. Tests have shown that nano-silica SiO_2 can increase concrete's workability (its ability to fill the desired mold/form) and strength. Adding 10 % nano-silica increased the compressive strength of cement mortar (the basic ingredient in concrete) by up to 26 %. Whereas adding 15 % of the larger silica fume only strengthened it by 10 %. This is the same as 0.25 % nano-silica, which also increased flexural strength by 25 % [Sanchez & Sobolev et al., 2010]. These increased compressive strengths have the potential to be useful in the foundations of large buildings.

Nanoclay materials are also promising additives for enhancing the mechanical performance, the resistance to chloride penetration and reducing permeability and shrinkage. Clay particles are hydrophilic therefore attention should be given to the control of water requirements in clay-cement composites [Sanchez & Sobolev et al., 2010]. On the other hand, carbon nanostructures (CNS) such as nanotubes (CNT), nanofibers (CNF) and graphene addition to concrete can give the benefits to strengthen and monitor concrete.

CNS exhibit extraordinary strength with moduli of elasticity on the order of TPa and tensile strength in the range of GPa, and they have unique electronic and chemical properties [Sanchez & Sobolev et al., 2010]. Compared to CNT, vapor grown CNF have a lower production cost and are suitable for mass production. While CNT/CNF has been extensively studied in polymeric composites, their use in cement composites has remained limited. Most research efforts have focused on CNT rather than CNF and have been performed on cement pastes and mortars [Sanchez & Sobolev et al., 2010; Makar et al., 2005; Sanchez et al., 2009; Shah et al., 2009].

CNT have 5 times the Young's modulus and 8 times (theoretically 100 times) the strength of steel while being 1/6th the density. Oxidized multi-walled nanotubes (MWNT's) show the best improvements both in compressive strength (+ 25 N/mm2) and flexural strength (+ 8 N/mm) compared to the reference samples without the reinforcement. It is theorized the high defect concentration on the surface of the oxidized MWNTs could lead to a better linkage between the nanostructures and the binder thus improving the mechanical properties of the composite rather like the deformations on reinforcing bars [Saurav et al., 2012].

Moreover, the role of Alumina (Al_2O_3) induced cementitious materials, is mainly on increasing the mechanical properties of cement. Zirconium dioxide (ZrO_2) has also been studied in building matrices as it forms more hydrated products and improves the pore structure.

The addition of the nanoparticles decreased also the fluidity and increased the water demand for normal consistency [Kurapati et al., 2014]. There has been limited study on using nano Iron (III) Oxide (Fe_2O_3) in concrete mixtures. Like nano-silica, nano Fe_2O_3 increases the flexural and compressive strengths of concrete. But it also provides a novel self-sensing property to the concrete. The Fe_2O_3 causes concrete's electrical resistance to change depending on the load being applied to it [Sanchez & Sobolev et al., 2010]. This property could be used as a replacement for, or in conjunction with, instruments like inclination sensors and GPS units to develop dynamic structure monitoring systems similar to that in use at the Rixos Hotel [Ozer Cemal et al., 2014]

Self-healing process and Acid resistance

When a micro crack forms in the self-healing concrete, it will spread through the material. By doing so, this crack will rupture the microcapsules and release the healing agent. This healing agent will flow down through the crack and will inevitably come into contact with the catalyst, which initiates the polymerization process that bonds the crack closed. In fracture tests, self-healed composites recovered as much as 75 % of their original strength. They could increase the life of structural components by as much as two or three times [J. Saurav et al., 2012]. In the case of acid attack on cement, the consequences can be minimized by investigating into the concrete's porosity. The smaller the porosity, the smaller the chances of an acid attack on concrete are. High-performance concrete, with the use of nanomaterials, is effective in this category. Nonetheless, materials with high strength are associated with high density and lead to increased weight of the structure [Kurapati et al., 2014].

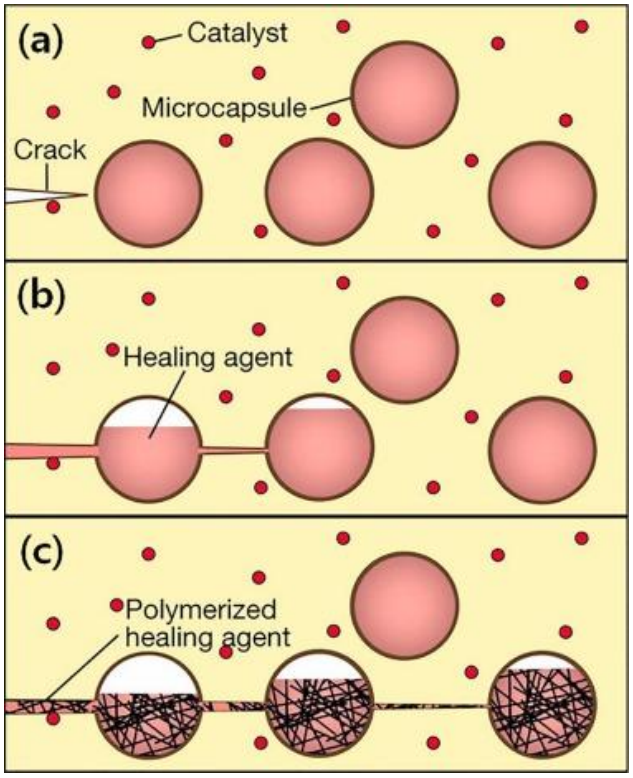

Fig. 3 Schematic of the self-healing process using embedded microcapsules. (a) A crack forms in the matrix due to damage; (b) the growing crack ruptures microcapsules in its path, thereby releasing the healing agent into the crack plane; (c) polymerization occurs and the crack faces are bonded closed. [A. Seongpil et al., 2018]

Self-Consolidated Concrete (SCC)

Self-Consolidated Concrete (SCC) is one that does not need vibration in order to level off and achieve consolidation [Dresselhaus et al., 2004]. This represents a significant advance in the reduction of the energy needed to build concrete structures and is therefore a sustainability issue. In addition, SCC can offer benefits of up to 50% in labor costs [Makar & Beaudoin et al., 2003], due to it being poured up to 80 % faster and having reduced wear and tear on formwork. The material behaves like a thick fluid and is made possible by the use of poly carboxylates (a material similar to plastic developed using nanotechnology). SCC initial development was in Japan by Okamurain the late 1980s in order to reach durable concrete structures. The advantages of SCC offer many benefits to the construction practice, for example the elimination of the compaction work results in reduced costs of placement, equipment needed on construction, shortening of the construction time and improved quality control [Maraveas et al., 2012].

Fiber wrapping of concrete

Fiber wrapping of concrete is quite common today for increasing the strength of preexisting concrete structural elements. Advancement in the procedure involves the use of a fiber sheet (matrix) containing nano-silica particles and hardeners.

These nanoparticles penetrate and close small cracks on the concrete surface and in strengthening applications, the matrices form a strong bond between the surface of the concrete and the fiber reinforcement [Radu Olar et al., 2011].

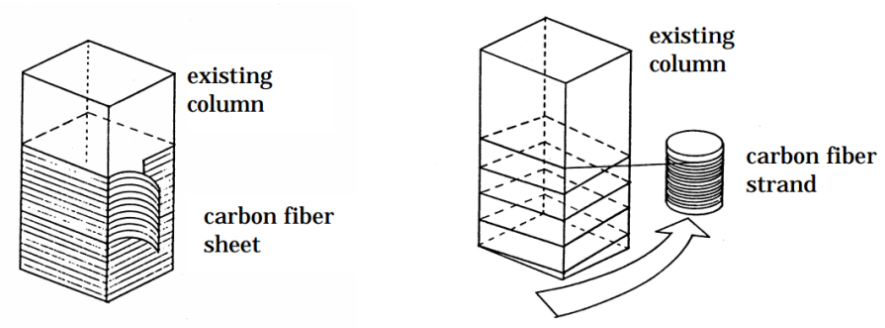

Fig. 4 Two methods for providing CFRP. Wrapping CF sheet (Sheet Method) and winding CF strand (Strand Method). [Toshimi Kabeyasawa et al., 2005]

Conductive concrete

Conductive concrete may be defined as a cementitious composite which contains a certain amount of electronically conductive components to attain stable and relatively high electrical conductivity. It has the potential to address a wide variety of applications, including grounding, heating, cathodic protection of reinforcing steel in concrete structures such as bridges and parking garages, and electromagnetic shielding for protection of critical infrastructure, such as power grids and data centers [K. Venkatraman et al., 2015]. There is great interest in making the top surface of concrete conductive, allowing the surface to be warmed slightly to prevent freezing in winter. This would have enormous cost savings from the point of spreading of natural rock salt onto ways and bridges, and the point of reduced deterioration of bridges and abutments regularly doused in salt and reduced contamination of water courses. Less than 1 % of carbon fibers in the concrete volume have big effect in improving the electrical concrete conductivity. Conductive concrete shows interesting and different properties with regard to ordinary concrete as follow: Ability to monitor itself for cracks because of the fibers' ability to conduct electricity [Abulmagd S. et al., 2018], monitor and weigh passing traffic ability to heat a road, a bridge, or a runway through electric current leading to snow and ice-free surfaces and ability to control heating and lighting systems [Saptarshi Sasmal et al., 2013].

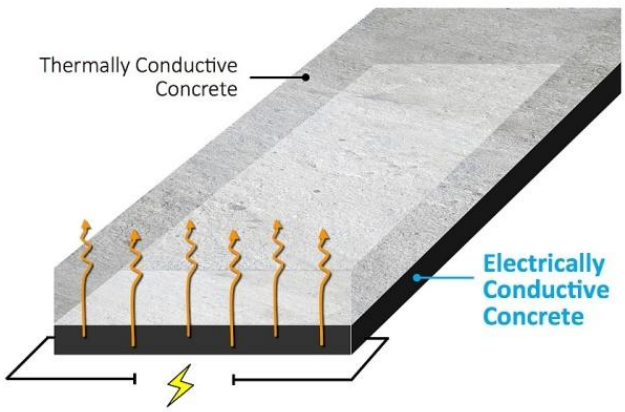

Fig. 5 Conceptual underfloor heating. [TalgaResources]

Nanoclay-modified asphalt materials

Increasing traffic loads and traffic volume, combined with the rising cost of asphalt, have led to an urgent need to improve the durability, safety and efficiency of asphalt pavements through asphalt modification. Ideal asphalt it should possess high relative stiffness at high service temperatures (summer) to reduce rutting and shoving and increased adhesion between asphalt and aggregate in the presence of moisture to reduce stripping. Blending small percentages of nanoclay-composites into virgin asphalt appear to have beneficial impact on the high-temperature properties of asphalt binders modified with these materials. The motivation is to significantly reduce the temperature sensitivity of the binder at service temperatures while maintaining workability at construction temperatures [Kibayah et al., 2014]. Nano-modified asphalt may potentially improve the rutting, crack and fatigue resistance of asphalt mixtures. So nanoclays can be effectively used as a modifier to improve the mechanical properties of asphalt binders [Dhir et al., 2009; Whitby & Busquets et al., 2013].

Bricks

Bricks have been used as a construction material for many years. The current composition of bricks consists of 50 % clay but no greater than 80 % clay, with the remainder of the earth brick made up of sand and other granular materials. With these materials bound together under high temperatures, a good compressive strength material is formed which makes the earth brick an exceptional domestic construction material [Mohajerani et al., 2016; Mohajerani et al., 2019]. However, existing earth bricks do not demonstrate good compressive strength.

Nanoclays are considered to be layered mineral silicates of nanoparticles and the use of varying nanoparticles in bricks is dependent on the chemical makeup of the brick. A 5% inclusion of nanoclay can develop a compressive strength 4.8 times that of normal clay bricks [Niroumand et al., 2013]. Over the life of the brick material, the nanoclay modifier prevails as the more sustainable material when compared against normal clay bricks. Alkosiloxane and silica nanoparticles prove to be the most effective way to protect bricks [Stefanidou & Karozou et al., 2016]. The treated bricks show high resistance to water uptake and a significant improvement in terms of durability.

1.2.2 Energy saving nanomaterials in the building sector

Buildings are a central part of our daily lives, and we spend a large part of our days in them - at home, at work, or during our spare time. However, the building sector is the largest energy consumer in the EU and one of the largest carbon dioxide emitters. Collectively, buildings in the EU are responsible for 40 % of our energy consumption and 36 % of greenhouse gas emissions, which mainly stem from construction, usage, renovation and demolition. Improving energy efficiency in buildings therefore has a key role to play in achieving the ambitious goal of carbon-neutrality by 2050, set out in the European Green Deal [European Commission et al., 2020].

Urban heat island and global warming increase the urban ambient temperature, leading to tremendously higher energy demand for cooling, and total energy demand [Kolokotsa et al., 2017; IPCC et al., 2018], Taking into account building and district level, energy efficient technologies the zero energy buildings are a necessity while climate change is putting pressure in the urban thermal environment [Kolokotsa et al., 2011; Kolokotsa et al., 2012]. Today, roughly 75 % of the EU building stock is energy inefficient. This means that a large part of the energy used goes to waste. Such energy loss can be minimized by improving existing buildings and striving for smart solutions and energy efficient materials when constructing new houses. Renovating existing buildings could reduce the EU's total energy consumption by 5-6 % and lower carbon dioxide emissions by about 5%. Yet, on average, less than 1 % of the national building stock is renovated each year. (Member State rates vary from 0.4 % to 1.2 %.) In order to meet our climate and energy objectives, the current rates of renovations should at least double. The EU recently introduced new ambitious policies to help steer member states towards better energy efficiency in buildings. Knowing that cost is often the major hurdle to renovation, the new rules also ease access to financing for improving the building stock. The Energy Performance of Buildings Directive (EPBD) 2010/31/EU and the Energy Efficiency Directive (EED) 2012/27/EU were revised in 2018, as part of the Clean energy for all Europeans package, to better reflect the EU's aim of driving the clean energy transition [European Commission et al., 2020].

Thermochromic windows

Energy-efficient glass windows have been steadily developed over the years and as a result there has been rapid development of thermochromic glazing techniques that promise next-generation architectural windows with energy saving characteristics [Cui et al., 2018]. A thermochromic coating can regulate the internal temperature of the building via the variation of solar IR transmittance thus contributing to energy efficient buildings and indoor comfort. Vanadium dioxide (VO_2) is an inorganic compound, its thermochromism was first reported in 1959 [Morin et al., 1959].

It belongs to the general family of "photochromic" materials which may undergo changes in their transmission under a stimulus such as temperature, light or current [Gagaoudakis et al., 2016]. VO_2 undergoes a structural transformation from a semiconducting to a metallic state when heated over the critical temperature of 68°C. These states are referred to as "light" and "dark" states, respectively, since the former is relatively transparent to infrared radiation while the latter is absorptive (or opaque) to such radiation [Morin et al., 1959]. What makes this material a promising oxide for smart windows applications is that this process is highly reversible [Blaauw et al., 1975].

FIg. 6 Thermochromic glass windows installed at an educational facility in Keller, Texas, USA. [Source: Pleotint, LLC]

Self -powered smart window system

Min-Hsin Yeh and his team established a fully integrated self-powered smart window system by integrating an electrochromic device with a dual-mode triboelectric nanogenerator. The entire device was a transparent, multilayered structure, which was compatible with the smart window structure [Min-Hsin Yeh et al., 2015].

Electrochromic devices (ECDs) are developed to provide reversible changes of their optical properties via the electrochemical redox reactions corresponding to an external electric field [Beaujuge & Reynolds et al., 2010; Rosseinsky & Mortimer et al., 2001; De Longchamp et al., 2003]. The ECD was composed of Prussian blue (PB) nanoparticles and zinc hexacyanoferrate (Zn-HCF) nanocubes as the electrochromic material and the ion storage layer, respectively. The triboelectric nanogenerator (TENG) was recently invented to convert mechanical energy into electricity, based on the coupling effect of contact electrification and electrostatic induction [Fan et al., 2012; Wang et al., 2013]. The TENG can take advantage of environmental oscillations such as blowing wind and raindrops to deliver an output current. Reversible electrochromic reactions can be driven directly by the TENG.

The TENG consisted of a multi-layered structure with micropatterned polydimethylsiloxane (PDMS) thin films and transparent electrodes, which could be employed for harvesting the kinetic energy from wind impact and water droplets. The multilayer structure of the self-powered smart window is schematically illustrated in Fig. 7 [Min-Hsin Yeh et al., 2015].

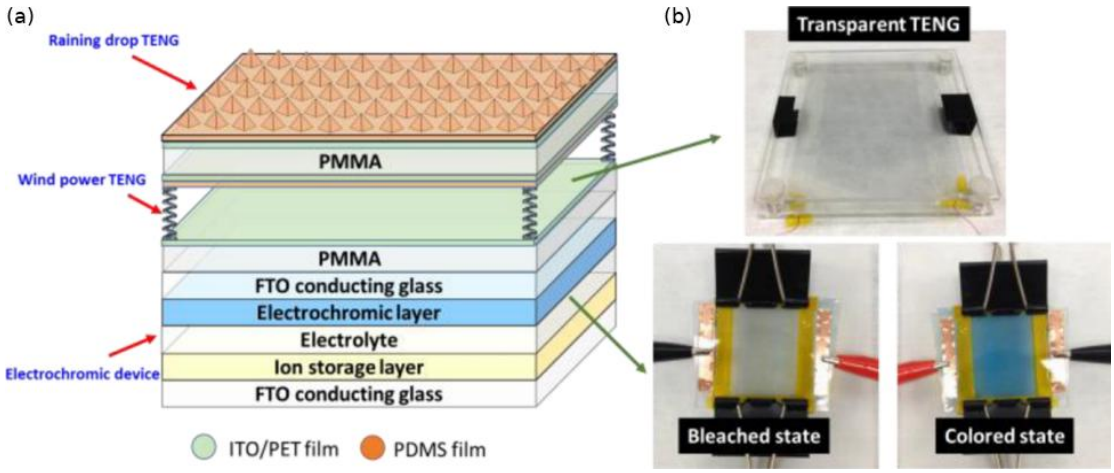

Fig. 7 (a) Schematic diagram of the detailed structure of the self-powered smart window integrated with a raindrop-TENG, a wind-powered-TENG, and an ECD from top to bottom. (b) Photographs of the PB/Zn-HCF ECD in bleached and colored states, depicting the color change of the ECD from colorless to dark blue at an applied potential from -2.0 to 2.0 V, respectively. [Min-Hsin Yeh et al., 2015]

1.2.3 Photocatalytic nanomaterials

Urban air quality refers to how "clean" the ambient air is inside of cities with a density, population, and level of activity that generally are recognized as "urban." Urban air quality generally differs from rural air quality since there are more concentrated sources and the ability for the pollutants in the air to be dispersed are limited by the physical constraints of the urban environment [Goodsite & Hertel et al., 2012]. Although emissions of air pollutants have decreased substantially in Europe over recent decades, air quality problems in Europe persist. Air pollution harms human health and the environment (EEA et al., 2019a). Urban air pollution is mainly contributed by harmful inorganic and organic molecules (NOx, SOx, CO_2, and VOCs) and particulate matter [Cros et al., 2015; Guo et al., 2015; Gnanaprakasam et al.], with nitrogen oxides (NOx) representing some of the largest air polluting agents, which are produced mostly by combustion (Table 2).

COUNTRIES	PM_{10} (daily limit value)	O_3 (target value)	NO_2 (annual limit value)
Austria	2	14	2
Belgium	0	0	3
Bulgaria	87	0	7
Croatia	99	81	3
Cyprus	6	0	0
Czech Republic	12	44	1
Denmark	0	0	2
Estonia	0	NA	0
Finland	0	0	< 1
France	< 1	10	2
Germany	< 1	3	5
Greece	29	73	2
Hungary	2	0	2
Ireland	0	0	0
Italy	44	61	30
Latvia	4	0	0
Lithuania	2	0	0
Luxembourg	0	0	5
Malta	NR	0	0
Netherlands	0	0	2
Poland	59	2	1
Portugal	0	0	< 1
Romania	0	0	0
Slovakia	1	0	0
Slovenia	100	0	0
Spain	2	17	6
Sweden	0	0	< 1
United Kingdom	0	0	14
EU-28	13	12	7

The colour coding of exposure estimates refers to the fraction of urban population exposed to concentrations above the reference level:

0%	< 5%	5-50%	50-75%	> 75%

Table 2. Percentage of urban population exposed to concentrations of air pollutants above selected air quality standards. [EEA et al., 2018b]

However, indoor pollution involves both chemical agents and pathogenic microorganisms [Chen & Poon et al., 2009; Nath et al., 2016; Saeli et al., 2017] as illustrated in Fig. 8 [EEA et al., 2013].

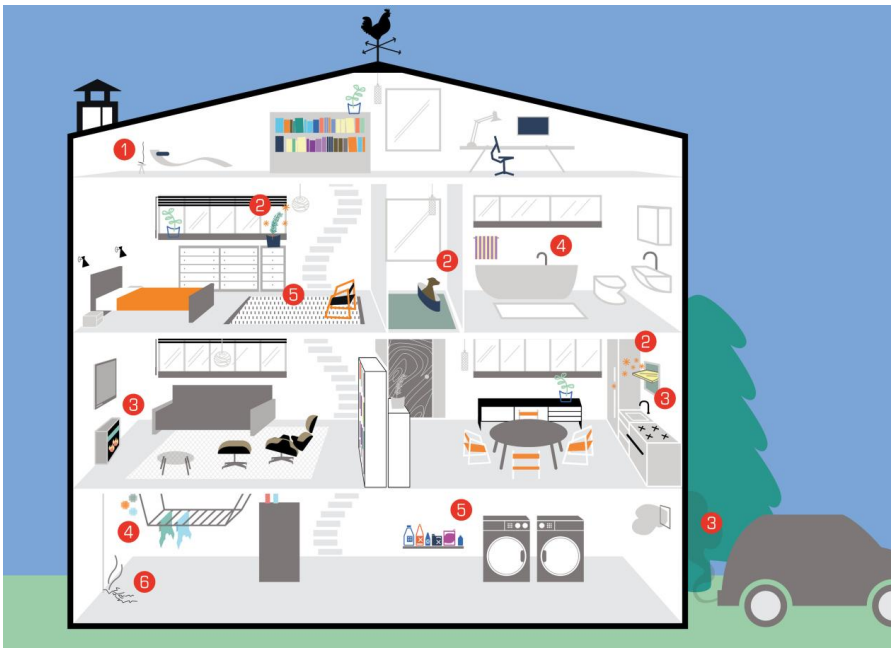

Fig. 8 Indoor air pollution. We spend a large part of our time indoors, in our homes, workplaces, schools, or shops. Certain air pollutants can exist in high concentrations in indoor spaces and can trigger health problems. (1) Tobacco smoke: exposure can exacerbate respiratory problems (e.g., asthma), irritate eyes, and cause lung cancer, headaches, coughs, and sore throats. (2) Allergens (including pollens): can exacerbate respiratory problems and cause coughing, chest tightness, breathing problems, eye irritation, and skin rashes. (3) Carbon monoxide (CO) and nitrogen dioxide (NO2): CO can be fatal in high doses and causes headaches, dizziness, and nausea. NO2 can cause eye and throat irritation, shortness of breath, and respiratory infection. (4) Moisture: hundreds of species of bacteria, fungi, and molds can grow indoors when sufficient moisture is available. Exposure can cause respiratory problems, allergies, and asthma, and affect the immune system. (5) Chemicals: some harmful and synthetic chemicals used in cleaning products, carpets, and furnishings can damage the liver, kidneys, and nervous system, cause cancer, headaches, and nausea, and irritate the eyes, nose, and throat. (6) Radon: inhalation of this radioactive gas can damage the lungs and cause lung cancer. [EEA et al., 2013]

Advanced Oxidation Processes

One alternative to lower the levels of air pollutants in the atmosphere is the use of Advanced Oxidation Processes (AOPs), those processes are based on formation and reaction of reactive oxygen species (ROS), reactive nitrogen species (RNS), oxygen radicals ($^{\cdot}O_2^-$) and hydroxyl radicals ($^{\cdot}OH$) [Waiskopf et al., 2016; Nosaka Y. & Nosaka A. Y. et al., 2017]. AOPs can be divided into homogeneous (ozone, Fenton and photo-Fenton systems, H_2O_2/UV) and heterogeneous systems (semiconductor photocatalysis). In homogenous AOP systems a continuous input of chemical reagents is required as a source of the reactive species and catalysts to maintain operation of the system. On the other hand, semiconductor photocatalysis is generally thought of as the catalysis of a photochemical reaction at a solid surface of a semiconductor with the help of an energy source for the reaction, which can be in the form of artificial or natural light [Matoh et al., 2019]. This implies that there must be at least two reactions occurring simultaneously, the first involving oxidation, from photogenerated holes, and the second involving reduction, from photogenerated electrons. Both processes must be balanced precisely in order to conserve the charge neutrality and for the photocatalyst itself not to undergo change (which is one of the basic requirements for a catalyst).

In other words, photocatalysis is based on short-circuited photoelectrochemical reactions, balancing electrons and holes [Fujishima et al., 2008].

Photocatalysis mechanism

Upon irradiation of the light with the energy equal or more than the bandgap of the semiconductor photocatalyst, the electrons are excited from the valance band of the catalyst to the conduction band, leaving the holes behind in the valance band. Then the electron-hole pair separates by the transfer of these charges to the surface. Consequently, these photogenerated charge carriers then react with water or dissolved oxygen to produce reactive oxidizing species such as $^{\cdot}O_2^-$ and $^{\cdot}OH$, that decompose pollutants into smaller molecules as well as inactivate microorganisms, through oxidation and reduction reactions [Regmi et al., 2018]. Finally, the electronic semiconductor system recovers its ground state. The mechanism of photocatalysis is described in Fig. 9 [Regmi et al., 2018].

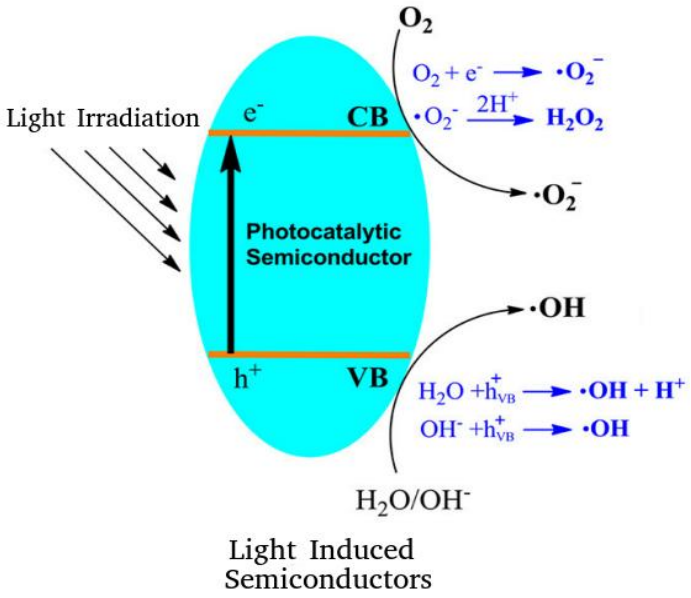

Fig. 9 Mechanism for the photocatalytic activity on the surface of the semiconductor under the irradiation of light. [Regmi et al., 2018]

$$\text{Photocatalyst} + hv \rightarrow e^- + h^+$$

$$h^+ + H_2O\ (ads) \rightarrow {}^{\cdot}OH + H^+$$

$$h^+ + OH^- \rightarrow {}^{\cdot}OH\ (ads)$$

$$e^- + O_2 \rightarrow {}^{\cdot}O_2^-$$

$$2H + {}^{\cdot}O_2^- \rightarrow H_2O_2$$

$$e^- + H_2O_2 \rightarrow {}^{\cdot}OH + OH^-$$

$${}^{\cdot}OH + \text{pollutants/micro-organisms} + O_2 \rightarrow \text{simpler products (salts, } CO_2, H_2O, ..)$$

$${}^{\cdot}OH\ (ads) \rightarrow {}^{\cdot}OH_{free} + \text{pollutants} \rightarrow \text{simpler oxidation products}$$

It has been generally noticed that the degradation rate of the dyes and pollutants on the surface of the catalyst increases with an increase in the loading of the catalyst [Vinu & Madras et al., 2011]. This is mainly due to increase of hydroxyl radical produced from irradiated photocatalyst [Liu et al., 2010; Zhang et al., 2008]. The photocatalytic activity of semiconductor catalyst also decidedly confides on surface and structural properties, such as surface area, crystal composition, distribution, porosity, bandgap, particle size, and surface hydroxyl group density [Kruefu et al., 2012]. Furthermore, the photocatalytic degradation rate increased with increasing intensity of radiation [Gaoa et al., 2011] and decreased with the increased initial organic compound concentration [Mai et al., 2008]. When investigating photocatalytic performances, the source of the irradiation provided to the catalyst must be further analyzed due to the fact that in real-time outdoor applications, the nanomaterials might appear to have a lower performance, due to uncontrollable environmental parameters.

Historical hints

In 1835 Berzelius coined the word catalysis. In 1911, 76 years after Berzelius, the term photocatalysis appeared in several scientific communications [Coronado et al., 2013]. In 1972, the pioneers of photocatalysis, Fujishima and Honda, achieved an electrochemical photolysis of water using a rutile electrode exposed to near-UV light and connected to a platinum counter electrode through an electrical load [Fujishima & Honda et al. 1972]. The influence of Fujishima's work was also important to consolidate the preponderance of TiO_2 among photoactive materials because its stability in aqueous solution was established under a wide range of pH and external potentials [Coronado et al., 2013]. Therefore, the relevance of this semiconductor progressively increased. In 1973 Bickley et al. tested the photooxidation of isopropanol on rutile TiO_2 [Bickley et al., 1973]. Since 1977, when Frank and Bard showed that cyanide (CN^-) could be efficiently photo-oxidized to cyanate (CNO^-) in alkaline conditions and in the presence of TiO_2 and oxygen [Frank & Bard et al., 1977], there has been increasing interest in environmental applications [Fujishima et al., 1999]. According to the historical background it seems clear that photocatalysis has acquired knowledge from very different fields. Nowadays, nanotechnology provides new opportunities for the development of more efficient and advanced photocatalytic materials.

1.2.4 Antimicrobial function

Photocatalytic nanomaterials when come in contact with microorganisms via different energy such as electrostatic attraction, hydrophobic interactions, van der Waals forces and receptor-ligand interactions, they exert their effect on the microorganism's cell membrane. Various reactive radicals generated by photocatalytic nanoparticles on receiving the photon energy higher than the band gap energy enters to the cells and brings different stresses such as oxidative stresses, membrane permeability imbalance, changes in cell shape, protein inhibition and alteration in metabolism and DNA damages [Wang et al., 2015]. Nanoparticles affect most of the cell at a time, thus microorganisms could not make such big changes in metabolism by making mutational changes in the genomes and bringing changes in the metabolism in short period of time. This eliminates the concern of pathogens getting resistance to such treatment systems [Regmi et al., 2018]. The possible mechanisms of antimicrobial activities exhibited by different photocatalytic semiconductors are described below (Fig. 10).

Oxidative stress induction

The excess ROS ($^{\cdot}O_2^-$, $^{\cdot}OH$, H_2O_2), generated as a result of redox (reduction–oxidation) process, favors the oxidation process in the cells that leads to the peroxidation of lipid membrane and eventually attack proteins, depress the activity of certain periplasmic enzyme, and eventually interact with DNA and damage it [Ansari et al., 2015; Padmavathy et al., 2011].

Metal ion release

The metal ions released from metal oxide semiconductors are percolated through the cell membrane and directly interact with the –SH, -NH and –COOH group of nucleic acid and protein and finally damaging them. However, this method is less lethal than the other, so is not considered as the major cause of cell death [Hussein-Al-Ali et al., 2014].

The non-oxidative mechanism

This mechanism involves the inactivation of microorganisms by decreasing the critical cellular metabolism such as protein, amino acid, nucleotide, energy, and carbohydrate metabolism without oxidative stress induction. The mechanism of non-oxidative stress cell death of Escherichia coli is poorly understood according to Leung et al. using MgO nanoparticles [Leung et al., 2014].

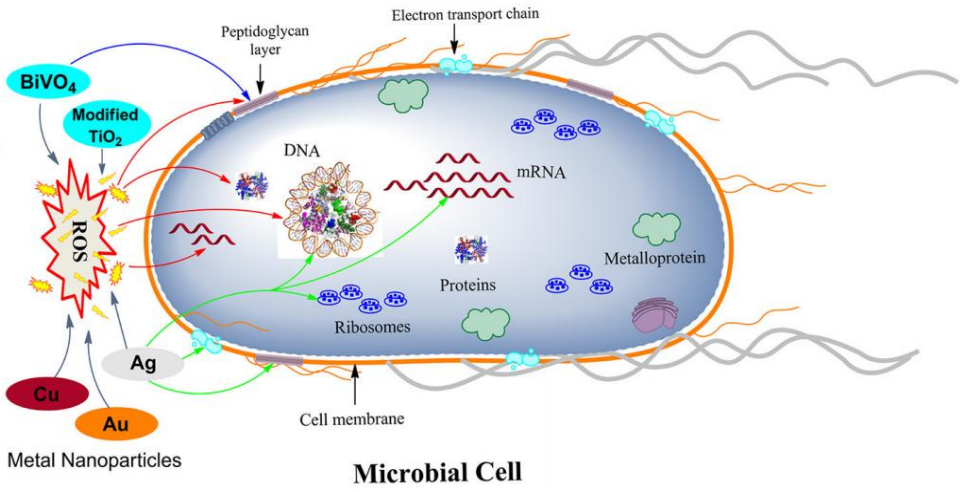

Fig. 10 The possible mechanisms of antimicrobial activities exhibited by different photocatalytic semiconductors. Red colored arrows point the targets of reactive oxygen species (ROS) generated by various semiconductors. The blue color arrow represents the target of BiVO4. Ag, Cu, and Au metal nanoparticles are also known to generate ROS and targets different parts in the cell. The green color arrow represents targets of Ag nanoparticle. Different targets in the microbial cells are labeled within the cell. [Regmi et al., 2018]

Among these three possible mechanisms of antibacterial activities of NPs, the first mechanism has attracted the most attention of the researchers. The exact mechanism of the antimicrobial mechanism of NPs is not understood yet and warrants further research.

1.2.5 Self-cleaning applications

Photocatalysis can be successfully used for real condition application in order to decompose air or liquid pollutants [Matoh et al., 2019 & Fujishima et al., 2000], enhance the quality of atmospheric air [Janus & Zając et al., 2019] and hinder the biodeterioration of inorganic materials [Goffredo Giovanni Battista et al., 2019].

Photocatalytic air cleaning and self-cleaning coatings

Coating is one of the important areas in construction. Coatings are extensively use to the walls, doors, and windows. Nanoparticles are being applied to paints to obtain the coatings having self-cleaning capabilities and remediate pollution.

The pollutants have a major effect on building structures. Additionally, particulates as dirt, dust, and fumes can cause damage to exposed surfaces [Mansour et al., 2018]. Gases from the atmosphere induce increasing corrosion. For example, black particles cause soiling of light-colored surfaces and sulfates/nitrates as a consequence of the acid rains enhance surface recession. Blackening of light-colored surfaces eventually reaches a point where it becomes aesthetically unacceptable. However, cleaning of surfaces may also be disadvantageous involving the removal of the protection layer, changing the color of pigmented elements, leaving behind chemical contaminants and increasing the risk of rain penetration [Flores e Colen et al., 2008; Mansour et al., 2018]. Therefore, it is necessary to use modern materials and technologies that can guarantee durability and good exterior condition of building and architectural elements, reducing the high cost of their conservation-restoration.

Titanium dioxide (TiO_2) nanoparticles are added to paints, cements and windows for its self-cleaning properties since TiO_2 breaks down organic pollutants and volatile organic compounds (VOCs) through powerful catalytic reactions. It can therefore reduce airborne pollutants when applied to outdoor surfaces. TiO_2 nanoparticles in the coating react with ultra-violet rays from natural daylight to break down and disintegrate pollutants. Additionally, the surface coating is hydrophilic, which lets rainwater spread evenly over the surface and 'sheet' down the surface to wash out the intermediates from the photocatalytic process and dust from the surfaces. The superhydrophilicity feature makes the surface dry faster and prevents the undesirable water streaking or spotting on the surface [Lee et al., 2003]. Therefore, TiO_2 nanoparticles give self-cleaning properties to surfaces to which it is applied.

For example, in 2001 Pilkington St announced the development of the first self-cleaning windows [Pilkington et al., 2001]. In 2019 Macoma Environmental Technologies applied FN NANO® coating on the ceiling of the terminal's second floor of North Las Vegas Airport with overwhelmingly positive results in the reduction of the toxic compounds that make up pollution and harmful micro particles in the environment from the jets engine fumes [Fn Nano Inc. et al., 2019].

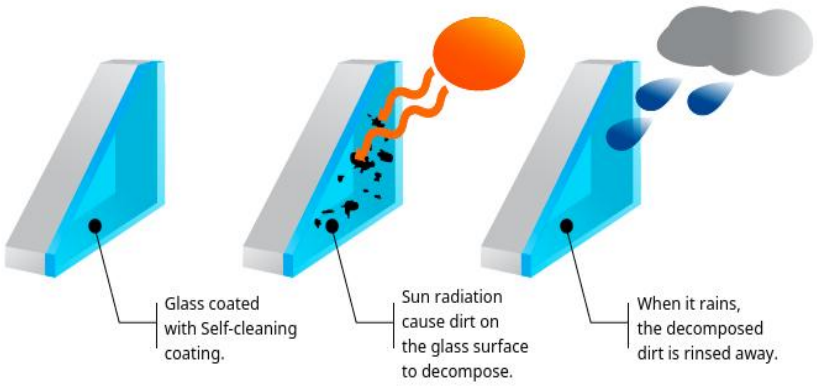

Fig. 11 A Self-cleaning Glass System Based on Titanium Oxide (TiO2) Thin Film Coating.

Anti-graffiti coatings

Another reason that affects the facades' appearance is painting or other surface signs on the walls due to various paints or markers is absorbed by the porous materials. Graffiti attacks and associated cleaning procedures cost Europe approximately 90 million € per year [Effaceur et al., 2012] and in the United States, the cost is estimated 12 billion $ per year [MacDonald et al., 2017]. Special coatings developed can also make the applied surface both hydrophobic and oleophobic at the same time. These could be used for anti-graffiti surfaces [Pratik Dewan et al., 2009]. Researchers in Mexico has successfully developed a new type of anti-graffiti paint DELETUM, by functionalizing nanoparticles (silica) and polymers to form a coating repellent to water and oil at the same time. As a result, the coated surface is non-stick or very easy to clean, and able to withstand repeated graffiti attacks [Rawat Parul et al., 2015].

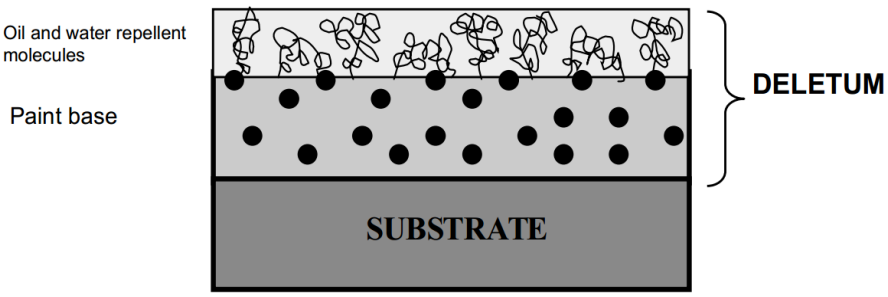

Fig. 12 Stratigraphy of the coating DELETUM 3000^{TM}. [Castaño & Rodriguez et al., 2004]

Fig. 13 Antigraffiti effect of DELETUM 3000^{TM}. [Castaño & Rodriguez et al., 2004]

Self-cleaning applications in interior design

The application of nanotechnology in interior decoration items such as furniture, floor, sofas, curtains, wallpapers, ceiling panels and carpets will bring changes to interior decoration and improvement in the comfort of the living environment. It includes finishing materials and environmental materials such as wood and fabric coatings.

Nanocoating for wood provides protection against sunlight and moisture. It preserves the natural look of the wood and is resistant to extreme environmental conditions such as very cold weather and snow [Anous et al., 2014]. Nanocoated wood can be water-repellent, self-cleaning and antimicrobial. It is suitable for all types of wood and ideal for wooden furniture and floor.

Nanocoated fabric repels any liquid or dirt that comes in contact with the surface without affecting the feel of the material. It is suitable for all types of fabrics and ideal for sofas, chairs, carpets, curtains and more [Anous et al., 2014]. Nanocoated fabric can be self-cleaning, antimicrobial, oil-water repellent, flame and chemical resistant without changing the original look. For example, nanocoated carpets and curtains are capable of freeing interior spaces from odours and interior pollutants, such as cigarette smoke and formaldehydes [Anous et al., 2014].

1.2.6 Antimicrobial applications

Nanotechnology can be used in the building industry for the degradation of microorganisms such as fungi, bacteria and viruses [Regmi et al., 2018]. Another application of antimicrobial coatings can be for the reduction of hospital acquired infections [Reid Matthew et al., 2018]. A dual-functional coating was successfully synthesized via UV curing, showing both thermochromic and antimicrobial properties. This work offers an inspiration of dual-functional coating production for many applications such as windows [Y. Liu et al., 2020]. In indoor environments, biodeterioration is the main cause for the degradation of building materials and also for many health-related issues [Pacheco-Torgal & Jalali, 2011]. Additional microorganisms may cause both aesthetic changes, such as the appearance of stains [Urosevic et al., 2012] and structural damages to stone [Doehne & Price et al., 2010]. The use of a photocatalyst based coating on stones exposed to marine underwater environment, would be able to stop or slow down the bio-colonization (antifouling effect), which are often related to the stone degradation [Aloise et al., 2014].

TiO_2 nanoparticles have been used to limit the growth of a wide spectrum of organisms such as cancer cells, viruses, bacteria, fungi, algae. Bio-receptivity of treated surfaces, environmental conditions and the characteristics of a so extensive range of microorganism especially the complexity and the thickness of cell envelope greatly influence the resistance to the photokilling action of TiO_2 [Chen et al., 2009; Seven et al., 2004]. In the field of construction technology, TiO_2 nanoparticles have been applied as a surface treatment or additive together with concrete, stones, glass, bricks turning them to self-sterilization surfaces [Maury-Ramirez et al., 2013; Guo et al., 2015; Fonseca et al., 2010] both for new and preexisting buildings, as well as for the preservation of stone works of art and surfaces of monuments [Baglioni et al., 2015; Gherardi et al., 2016; Pino et al., 2016].

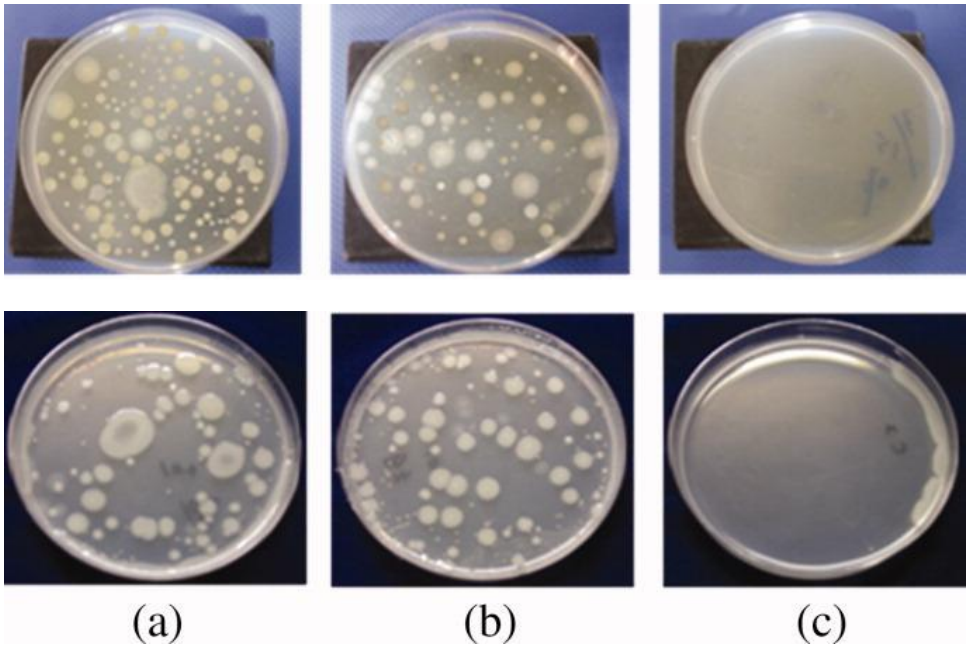

Fig. 14 S. aureus and E. coli colonies formed on petri dishes after 24 h on the (a) group A stainless steel specimens, (b) group B stainless steel specimens, and (c) TiO2-coated stainless-steel specimens. [Chung et al., 2008]

Water purification

Enabling water purification for human consumption from alternative sources such as rivers, oceans and sewage is a necessity of high priority. The variety of contaminants present in these water sources is vast. Photocatalytic properties of nanomaterials such as metal oxides have long been utilized for providing clean water resources free of microbial and chemical contaminants. Consequently, nanomaterials have great impact in water purification. However, combination of these nanomaterials with other purification techniques (ozonation, sonolysis, the Fenton process, etc.) synergistically improves these processes [Fadlalla et al., 2019].

During the last decade, titanium dioxide nanoparticles have emerged as promising photocatalysts for water purification [Rakkesh & Balakumar et al., 2013]. The use of immobilized TiO_2 for the photodegradation of 15 selected CECs in a simulated and real effluent wastewater under solar irradiation was studied by Miranda-Garcia et al. [Miranda-García et al., 2011]. Moreover, Salam et al. synthesized CNT/polypyrrole hybrids via oxidative polymerization of pyrrole with silver nitrate, leading to nanocomposites loaded with 80 wt. % AgNPs, which were further used for water disinfection in a column filter test. The CNT/polypyrrole/AgNP nanocomposites effectively inactivated the Escherichia coli and Staphylococcus aureus cells by nearly 100 wt. % [Salam et al., 2017]. In Figure 15 a schematic representation of a water purification system with a multilayered nanomaterial-based matrix is shown, which could remove organic, inorganic, and microbial contamination [Fadlalla et al., 2019].

Fig. 15 Nanomaterial-packed layer for purification of water contaminants. [Fadlalla et al., 2019]

Applications in air cleaners

Another important application of photocatalytic nanomaterials is in the purification of indoor air. A photocatalyst-type air cleaner is typically composed of TiO_2-based filters, UV lamps, and a fan for air circulation. The filters feature honeycomb-type construction or three-dimensional porous structure for minimum pressure drop (Fig. 16). The photocatalyst-type air cleaner can kill the bacteria floating in indoor air, which is very important for the applications in hospitals, institutions for the elderly, offices and schools [Fujishima & Zhang et al., 2006]. These air cleaners may be readily applied into new and existing heating, ventilation, and air conditioning systems.

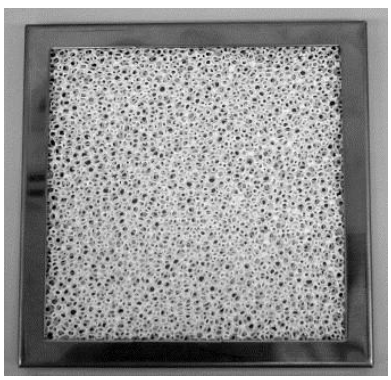

Fig. 16 TiO_2 coated porous ceramics filters for air cleaner uses. [Fujishima & Zhang et al., 2006]

In contrast to the conventional filters in air cleaners, the TiO_2-based photocatalyst filter can decompose the adsorbed pollutants instead of accumulating them, and thus it exhibits better air-cleaning performance [Fujishima & Zhang et al., 2006].

Antimicrobial coatings in interior design

TiO_2 coated ceramic tiles are considered to be very effective against organic and inorganic materials, as well as against bacteria. For example, Hydrotect® tiles can kill bacteria at an extremely high rate of speed [Hydrotect1]. Hydrotect® exerts various effects, including anti-dirt and anti-odor effects, by decomposing and reducing bacteria. It reduces the production of dirt and odors and facilitates the cleaning of interior spaces that need to be kept hygienically clean, such as toilets, kitchens and bathrooms [Hydrotect2]. The application of these tiles in hospitals, care facilities, schools and other public and commercial facilities can reduce the spread of infections and the threat to people whose immune system have been weakened, while reducing the use of cleaning products, that can harm the environment and cause health problems.

It is also advantageous to formulate paints with antimicrobial nanomaterials. The largest amounts of antimicrobial coatings are consumed in building industry, particularly for producing interior coatings that are designed for providing protection against growth of moulds, mildews and generally for achieving high standard of hygiene in hospitals, nursing homes, daycares and medical applications [K. Davidson et al., 2007; C. Vielkanowitz et al., 2008; J. Baghdachi & D. Clemans et al., 2006]. For example, masonry coatings based on photocatalytic TiO_2 pigments are proposed by E. Bagda for producing clean surfaces, air purifying and antibacterial effects [E. Bagda et al., 2006]. The antimicrobial properties of coatings are influenced by the type of acrylic dispersion, the morphology of surfaces, the type and the pigment volume concentration of the photocatalytic nanomaterials [E. Bagda et al., 2006].

Applications in textiles and fabrics

Textile materials can provide favorable media for the growth of pathogenic microorganisms due to moisture, sweat contaminants, and sometimes the nature of bulk material. Nowadays the need to protect users against pathogenic or odor-generating microorganisms that cause health problems is high, so the demand for textiles with antimicrobial properties has been on the rise. Additionally, antimicrobial fabrics are protected from undesirable discoloration or damage caused by microorganisms. The main reasons for the wide acceptance of TiO_2 nanoparticles as a coating material its safety and non-toxicity to the fabrics as well as to the skin, durability, stability, high compatibility with fabrics, no degradation on repetitive wash cycles, low cost of production and the scope for manipulations in its photocatalytic properties by modifying reaction conditions [Pakdel, et al., 2013; Zhang, et al., 2014; Behzadnia, et al., 2015; Kim, et al., 2016; Gupta, M. et al., 2017]. For instance, antimicrobial cotton fabrics were fabricated by M. Zahid et al. using manganese doped TiO_2 nanoparticles immobilized into polydimethylsiloxane matrix and tested against Staphylococcus aureus and Klebsiells pneumoniae. Nanocoated cotton fabrics revealed a 100% reduction in bacteria within 120 min of sunlight exposure [M. Zahid et al., 2018].

Wu Deyong et al. successfully developed cotton fabrics coated with TiO_2 nanoparticles. TiO_2 coated fabrics with self-cleaning and antibacterial performance, were practically promising in the textile industry, environmental cleanup and hospital sterilization [Wu Deyong et al. 2009]. Results show that TiO_2 coating not only prevented the formation of a biofilm of adsorbed bacteria but also destroyed the bacteria cell (Fig.17).

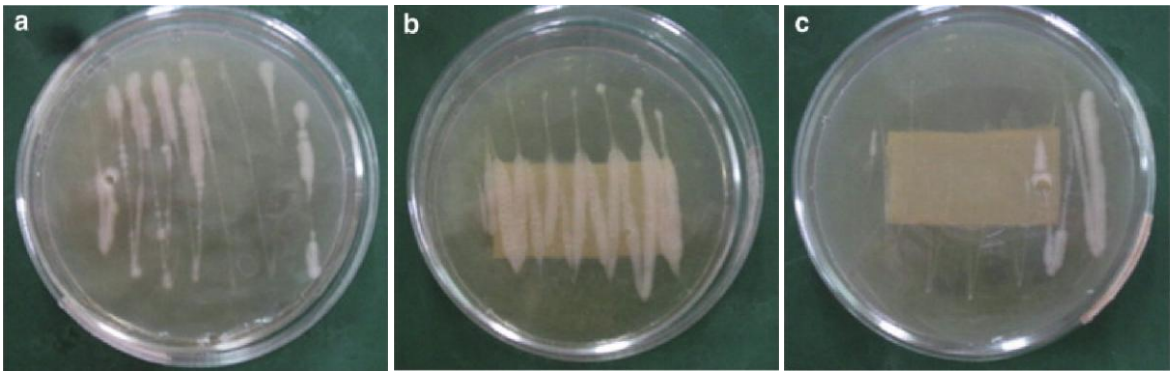

Fig. 17 Bacterial growth on the solid Luria–Bertani Medium (LBM) comparison between with (a) no other things, (b) pristine cotton fabric and (c) TiO_2 coated cotton fabric. [Wu Deyong et al. 2009]

Healthcare applications

One of the greatest concerns in the health sector (hospitals, laboratories or pharmaceutical industries) is the possibility of contamination or disease transmission from pathogens especially from bacteria and viruses. Healthcare acquired infections (HCAI) are of major concern across the globe, especially nowadays. It is likely that objects that can harbour and serve in transmitting bacteria and viruses, such as door handles, table tops and any other contactable surfaces held microorganism reservoirs for transfer. For example, Clostridium difficile and Methicillin Resistant Staphylococcus aureus are the two most common nosocomial pathogens and have been shown to survive on such surfaces for months [Magill SS et al., 2014; Leyland & Carroll et al., 2016].

Clostridium difficile spores in particular are highly resistant to alcohol-based cleaning and disinfection solutions [Rutala et al., 2006]. Moreover, in the Health sector clinicians and patients are exposed to bodily fluids, microscopic deposits are sometimes inevitable and gone unnoticed. Clinicians' lab coats, patient robes, bed linens and curtains are all potential carriers of microorganisms [Ogunsona et al., 2019]. These fabrics are excellent environment for harboring and growing microbes as they present large surface areas, which can hold oxygen and moisture [V.R.G. Dev et al., 2009; Ogunsona et al., 2019]. Hence, it is necessary to develop antimicrobial technologies to reduce the growth and spread of diseases directly at the source in the healthcare sector. Chung et al. attempted to use an arc ion plating (AIP) method to deposit TiO_2 nanoparticles by using this optimized deposition condition on common medical grade AISI 304 (austenitic chromium-nickel) stainless steel [Chung et al., 2008]. The TiO_2 coating exhibits excellent antimicrobial efficacy against Staphylococcus aureus and Escherichia coli and could possibly serve as a new antimicrobial treatment for medical implements to reduce the risk of HCAI [Chung et al., 2008].

Applications in medical devices and consumables

A complication from which patients undergoing mechanical ventilation in the intensive care unit (ICU) are at risk is ventilator-associated pneumonia (VAP) [Klompas M. et al., 2015]. VAP can affect as many as a quarter of all mechanically ventilated patients and has the potential to double the risk of mortality, increasing the duration of hospitalization, mechanical ventilation and causing the increase in the costs of care [Dalmora et al., 2014; Rello et al., 2002; Safdar et al., 2005]. One of the factors contributing to the pathogenesis of VAP is believed to be the rapid colonization of biofilm-forming pathogens, such as Pseudomonas aeruginosa and Staphylococcus aureus, on the surface of endotracheal tubes (ETT) [Adair CG. et al., 1999; Caratto et al., 2017]. Nanomaterials could be used to prevent or reduce bacterial colonization of medical devices as well as furniture and working surfaces, especially in environments like the ICU, where the high prevalence of multi-resistant strains of bacteria requires non-pharmaceutical measures to control the spread of infection [Caratto et al., 2017]. Caratto et al. showed that nanosized N-TiO2 can effectively prevent the growth of a small bacterial inoculum when exposed to conventional fluorescent light, widely available in hospital environments, avoiding the use of potentially harmful UV light.

Significant amounts of medical personal protective equipment (PPE) such as masks, overall gowns and hair covers are heavily consumed globally and disposed of after a very short period of use, in order to minimize exposure and transport of bacteria and viruses from one individual to another due to airborne bacteria as well as bacteria in liquid transport media such as bodily fluids [C.B. Hiragond et al., 2018]. However, changing of masks and gowns might not be done immediately. Incorporation of antimicrobial nanoparticles into PPE such as masks, can reduce the microorganisms' activities. As a result, nanocoated PPE can be used for prolonged periods of time and reused when laundered, while providing added protection to the wearer by eliminating these microbes upon contact. For example, Y. Li et al. investigated the efficacy of a combination of silver nitrate and titanium dioxide as antimicrobial agents against E. coli and S. aureus on coated facemasks [Y. Li et al., 2006]. Results showed that there was a 100% reduction in the viable count of bacteria growth after 48 h of incubation for masks coated with the antimicrobial particles, whereas, the uncoated masks revealed a 25 and 50% increase in the viable count of E. coli and S. aureus, respectively [Y. Li et al., 2006].

1.3 Semiconductor TiO_2

Titanium dioxide (TiO_2 or Titania) is one of the most used nanoparticles and the most common among titanium minerals. It is extensively used in everyday life, especially as white pigment in painting, food, and cosmetic industries, thanks to its high refractive index. TiO_2 is a white pigment and can be used as an excellent reflective coating [Saurav et al., 2012]. It exists in three main crystallographic structures, anatase, which presents a distorted tetragonal crystal structure, rutile, tetragonal as well, and brookite, with orthorhombic crystal structure (Fig. 18). The most interesting phases for practical applications are anatase and rutile, which are wide bandgap semiconductors. Anatase has more photocatalytic activity than rutile.

The E_g value for anatase is 3.20 eV, which corresponds to a wavelength absorption threshold of 384 nm. The narrow band-gap in the UVA region reduces the harvesting of solar radiation (at ground level with the sun at zenith, sunlight consists of 44 % visible light and of a mere 3 % UV light) [Faraldos & Bahamonde et al., 2019]. This means that its activation requires an irradiating source with wavelength lower than that indicated, that is, in the near-UV region, while visible light is not sufficiently energetic to induce photoactivity in this material, unless it is doped or combined with other elements to form heterojunctions [Diamanti & Pedeferri et al., 2019].

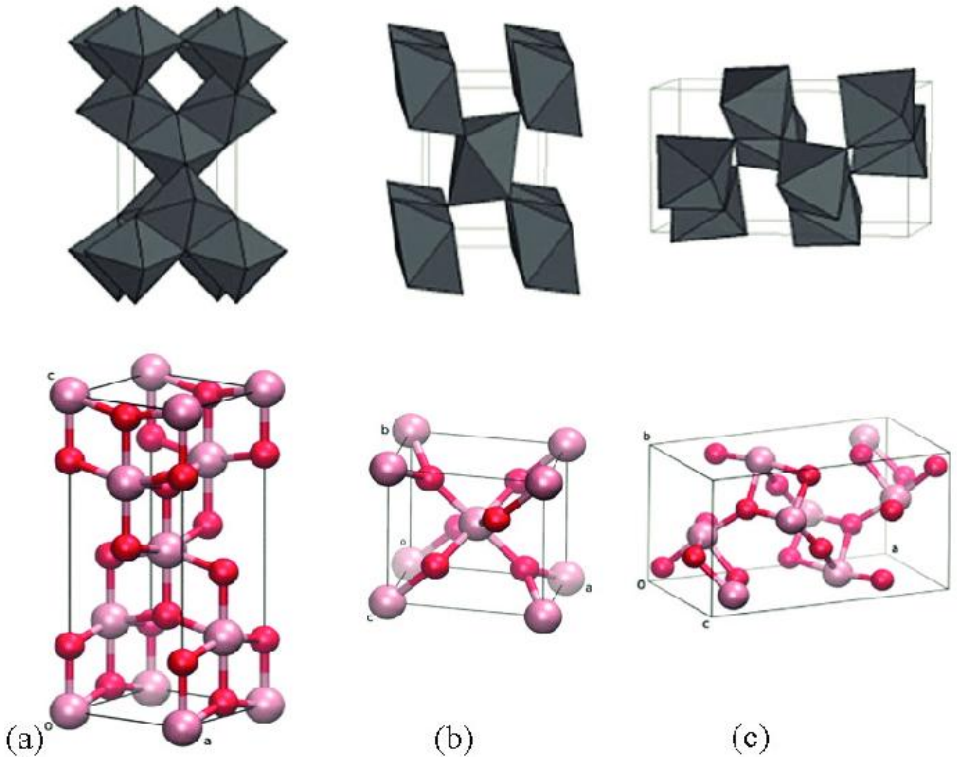

Fig. 18 Crystal structures of TiO_2: (a) anatase, (b) rutile, and (c) brookite. [Moellman et al., 2012; Godbert et al., 2018]

Property	TiO_2		
Molecular weight (g mol^{-1})	79.88		
Melting point (°C)	1825		
Boiling point (°C)	2500–3000		
Phase	**Anatase**	**Rutile**	**Brookite**
Refractive index	2.52	2.72	2.63
Dielectric constant	31	114	
Crystal structure	Tetragonal	Tetragonal	Orthorhombic
Space group	I41/amd	P42/mnm	Pbca
Lattice constant (Å)	a = b = 3784 c = 9515	a = b = 4593 c = 2959	a = 9184 b = 5447 c = 5145
Molecule/cell	4	2	8
Volume ($Å^3$)	136.25	62.07	257.38
Density (g cm^3)	3.79	4.13	3.99

Table 3. Compared intrinsic properties of main TiO_2 phases. [Godbert et al., 2018]

TiO_2 is proposed for several environmental applications such as air purifier, waste water treatment cleaning, water disinfection and photo-induced hydrophilic coating with self-cleaning and icephobic properties [Gnanaprakasam & Sivakumar et al., 2015; D. Colangiuli et al., 2015; Matoh et al., 2019; Janjua et al., 2019]. As expected, this highly used nanomaterial is also used often by the building industry. It can be embedded in bulk concrete, mortars, ceramic or as a coating on glass and stone [Janus & Zając et al., 2019; Chi Sun & Ming-Zhi et al. 2015; Diamanti & Pedeferri et al., 2019; S. Patel Abhiyan et al., 2013].

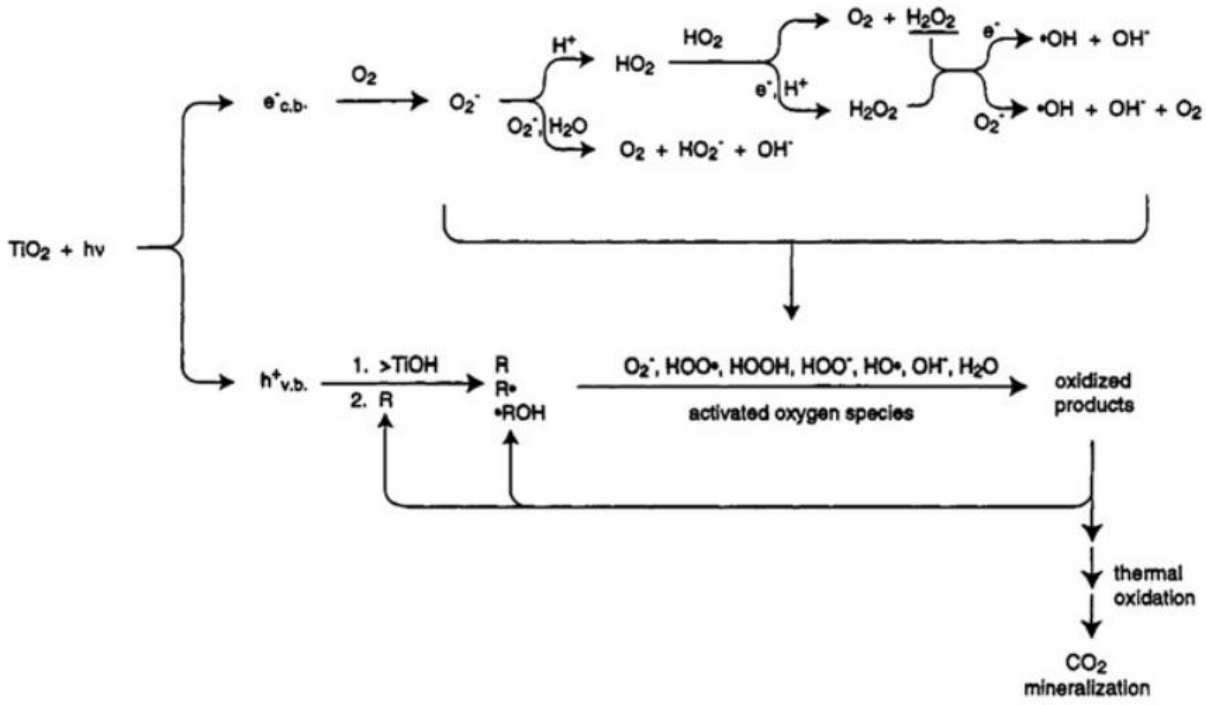

Fig. 19 Active oxygen species produced as a result of the irradiation of TiO_2. [Hoffmann et al., 1995]

TiO_2 nanoparticles gives concrete the ability to photo catalytically break down pollutants like carbon monoxide and volatile organic compounds (VOCs). That makes this type of concrete useful for things like facades and sidewalks in dense urban areas. However, this effect becomes less efficient with aging due to carbonation. In addition to the novel effects of TiO_2 it also gives concrete increased flexural strength, compressive strength, and abrasion resistance, which could also make it a viable structural material [Sanchez & Sobolev et al., 2010]. A photocatalytic cement technology has been used for a number of construction projects including the "Dives in Misericordia" Church (architect Richard Meier) located in Rome, Italy [Pacheco-Torgal & Jalali, 2011]. White surfaces with TiO_2 nanoparticles, remain white as a result of the self-cleaning property [Greßler & Gazso et al., 2012] and there is some evidence of improved air quality through its use on pavements, tunnels and walls, provided suitable light is available [Allen et al., 2008; Guerrini et al., 2012; Shen et al., 2012]. For example, TiO_2 nanoparticle-based coatings can capture and absorb organic and inorganic air pollutants by a photocatalytic process. Coating of 7000 m² of road surface with such a material in Milan in 2002 has led to a 60% reduction in nitrogen oxides concentration at street level [Edie News et al., 2004]. Furthermore, TiO_2 can be successfully used to degrade deleterious microorganisms, improving the conservation of historical surfaces and artifacts [Doehne & Price et al., 2010; Munafo et al., 2015; Cho et al., 2004; Seven et al., 2004; Goffredo Giovanni Battista et al., 2019; Maury-Ramirez et al., 2013; Baglioni et al., 2015; Gherardi et al., 2016; Pino et al., 2016]. For example, Fonseca et al. [Fonseca et al., 2010] tested the efficacy of TiO_2 (anatase) on the "Palacio Nacional da Pena in Sintra, Portugal", and showed that it was more effective than two conventional biocides.

1.4 Limitations, Challenges and Drawbacks

Nanotechnology contributes significantly to the construction sector. However, many challenges and drawbacks need to be overcome. A major challenge of nanomaterials in the construction industry is the problem of dispersion. The lack of homogeneous dispersion negatively affects the quality of the final product [Li et al., 2004; Nazari & Riahi et al., 2011]. Cement is chosen, as the most important construction material. In a cement matrix, the nanomaterials tend to agglomerate and therefore cannot be homogeneously dispersed by a simple mixing procedure [Mudimela et al., 2009]. Poor dispersion of nanoparticles could create weak zones and form voids [Li et al., 2004]. Particles of nanosilica with bigger primary particle sizes such as 40 nm are better dispersed in cement mortars [Haruehansapong et al., 2014]. Heterogeneous dispersion, particularly in carbon nano-reinforcements, due to their inherent self-attraction and hydrophobicity, can cause many drawbacks. Mudimela et al., 2009 introduced a simple method for the creation of good dispersion of carbon nanomaterials. Specifically, CNTs and CNFs were grown on the surface of model object, such as silica fume and cement particles. The produced carbon nanomaterials were homogenously dispersed in the matrix materials and the bonding between carbon and matrix materials was good. This way the growth of the nanomaterials inside the building materials solves the dispersion problems of CNTs and CNFs in a matrix [Mudimela et al., 2009].

Attention should be also paid on the light source when using photocatalytic nanomaterials. For example, anatase TiO_2 has an energy band gap of 3.2 eV and can be activated by UV radiation with a wavelength up to 387 nm thus limiting its application as a photocatalyst under visible light illumination. To extend the photocatalytic activity of TiO_2 into the visible spectral range, doping of TiO_2 by nonmetal elements such as N, C, F, and S has been reported [Bergamonti et al., 2017]. Choi et al. performed a systematic study of TiO_2 nanoparticles doped with 21 metal ions by the sol–gel method and found that the presence of metal ion dopants significantly influenced the photo reactivity, charge carrier recombination rates, and inter facial electron-transfer rates [W. Choi et al., 1994]. Binas et al. prepared TiO_2 nanomaterials doped with manganese by a modified sol–gel method, capable to absorb and activate under visible light irradiation [Binas et al. ,2012]. On the influence of the pH on photocatalytic cement, it was found that high pH values (pH > 10) could reduce the photocatalytic degradation rate i.e. of reactive yellow dye [Wang et al., 2015].

A separate note should be dedicated to pigmented materials, due to the interactions that may take place between TiO_2 and other inorganic substances, typically iron oxides and hydroxides, used to impart color to finishing mortars [Diamanti et al. ,2019]. Especially in the case of dark colors, the evaluation of the self-cleaning property is more difficult and self-cleaning seems to play a less relevant role. In addition, the photocatalytic activity is often reduced, in terms both of dye degradation and gaseous pollutants removal. An explanation to this could be the fact that pigments interact with TiO_2 and physically occupy its active sites, altering or hindering its photoactivation, or they may block concrete pores reducing the diffusion of pollutants into the material; or they may act as recombination centers for photogenerated species [Diamanti et al., 2013b; Guo & Poon et al., 2013; Rioult et al., 2016; Laplaza et al., 2017]. So, when producing a colored photocatalytic mortar, the type of pigments used may reduce or less frequently enhance the material functionalities, thus requiring different formulation compared with white mortars.

In the construction industry the large volumes of materials employed and the actual availability of sunlight make the use of nanomaterials less appealing. This limitation is due to the fact that the cost as nanomaterials and the tools required to use them are often quite expensive. However, costs have been shown to decrease over time and as manufacturing technologies improve, these costs may further decrease. Moreover, it is expected that these nanomaterials will enable unique solutions to complicated problems leading to large scale applications, therefore, making the cost effective [Rana et al., 2009]. For the use of specifically CNTs and graphene the high cost and energy consuming synthesis prevent the scale-up of their use in the nearest future [Pacheco-Torgal & Jalali, 2011; Hu et al., 2013]. Their high cost contributes to the difficulty of massive production of these materials in order to be incorporated in the building industry.

Except all these, some basic drawbacks of the use of nanomaterials involve health and environmental issues. Nanotechnology products could be harmful to health. There are major potential risks that need to be considered at all stages of nanotechnology [Mohajerani et al., 2019]. The extremely small size of nanomaterials means that they are much more easily taken up by the human body than the corresponding larger sized particles. A major concern is related to the accumulation of non-degradable or slowly degradable nanoparticles in organs and how these nanomaterials behave inside the body. Some investigations showed that nanoparticles can cause symptoms like the ones caused by asbestos fibers. The extremely small size of nanomaterials also means that they are much more readily taken up by the human body than the corresponding larger sized particles. How these nanoparticles behave inside the body is one of the issues that need to be resolved. Research has shown that some nanoparticles such as titanium oxide and iron nanoparticles can cause lung damage in rats [Fraser et al., 2010; Gonzalez L. et al., 2008].

However, it is still unknown, how much exposure to “nanolitter” may affect living organisms and the specific mechanisms of toxicity. Dhawan and Sharma studied the toxicological effects on biological systems with metal and metal oxide nanoparticles, fullerenes and carbon nanotubes [Dhawan A. & Sharma V. et al., 2010]. They concluded that there is still a need for further studies that conclusively establish the toxicity of nanomaterials, due to the many experimental challenges and issues encountered [Dhawan A. & Sharma V. et al., 2010].

The behavior of nanoparticles is a function of their size, shape and surface reactivity with the surrounding tissues [Thomas Selvin et al., 2013]. The deposition of nanoparticles in the respiratory tract is determined by their aerodynamic or thermodynamic diameter (i.e. particle shape and size). Agglomerates of nanoparticles deposit according to the diameter of the agglomerate, not constituent nanoparticles. Evidence indicates that agglomeration can affect the toxicity of inhaled nanoparticles [Shvedova et al., 2007].

More research is needed to determine the physical factors that contribute to the agglomeration and de-agglomeration of nanoparticles in air, suspended in aqueous media, or once in contact with cells and biological proteins. Regarding toxicity, no conclusive statement regarding the effect of agglomeration can be made, either for in vitro or in vivo. The currently available in vitro literature is controversial, and literature regarding the effect of agglomeration in vivo is nearly nonexistent [Bruinink Arie et al., 2015]. Bruinink Arie et al. recommended the selection of in vitro systems that mimic more precisely the in vivo situation, thus enabling a more correct prognosis to be made. Regarding in vivo effects, a possible step in improving predictions of hazard is to use computer modelling to simulate the whole pathway from human exposure to exposure of single cells within the body, which should help identify critical knowledge gaps in making a comprehensive assessment of the effects of nanomaterials on human health [Bruinink Arie et al., 2015; Albanese Alexandre et al., 2012].

Moreover, an environmental and health issue is the appearance of nanowastes. Nanowastes are the release of nanomaterials via dust into airways, materials entering into water, and exposure to potentially harmful materials during construction and maintenance procedures. Bystrzejewska-Piotrowska et al. suggest that products containing nanoparticles should be labeled in order to facilitate future separation and recycling procedures [Bystrzejewska-Piotrowska et al., 2009]. The release/leaching of nanoparticles into the water system poses serious risk. Hence, tremendous efforts are required in the synthesis of cost-effective nanomaterials and restriction of leaching of nanoparticles into aqueous environments [Fadlalla et al., 2019]. The use of filters or other methods to remove nanoparticles (e.g. TiO_2) has been proved to be inefficient and cost-effective. Benedix et al. studied water purification using photocatalytic TiO_2 nanoparticles. They designed reactors where the titanium dioxide is fixed on a glass, ceramics or metal surface. In this reactor type industrial waste water is passing a TiO2 coated material (glass, polystyrene, methacrylate) without the risk of leaching of nanoparticles [Benedix et al., 2000]. In a same way Vignesh and Somasundaram used a borosilicate glass support to immobillize TiO_2 nanoparticles, to overcome the recovery of nanoparticles for recycling. The efficiency of TiO_2 was still maintained after five recycles for the simulated water system [Vignesh & Somasundaram et al., 2019].

Another important segment of the application of nanotechnologies is resolving the problem of binding nanoparticles to the surface. For example, in the textile industry the main problem is to assure tight binding of nanoparticles to the surface of textiles in order to increase the durability of the desired properties [Senić et al., 2011]. This also ensures that nanoparticles are not released in the environment, fulfilling also the health and environmental requirements [GOWRI et al., 2010]. The literature stated several methods used for this purpose. Some of these methods uses covalent linking agents a layer by layer method (using electrostatic interactions), while other methods use the introduction of reactive functional groups onto textile surface which applies radio-frequency (RF) or microwave (MW) or UV plasma or hydrolytic enzymes [Senić et al., 2011]. Kale Ravindra and Meena Drchet applied titanium dioxide nanoparticles by layer by layer (LBL) technique on Nylon 6,6 fabric for imparting antimicrobial activity. In their study Polymer thin film deposited directly onto textile fabrics by following LBL deposition technique to produce Polyelectrolytes Multilayers (PEM). The PEM method has opened the way for easy preparation of truly nano-composite textiles containing a wide range of molecules and nanoparticles allowing the preparation of new technical fibers [Dubas et al., 2006]. The effectiveness of the treatment was assessed after washing treatment to check its durability [Kale Ravindra & Meena Drchet et al., 2012].

For clinical applications, the development of a method to apply the nanoparticles on the surfaces is necessary. Nanocoated fabrics can be used as wound dressings. However different techniques such as Sol-Gel casting has been tried, but the resulting coatings have all been too thick and brittle, causing the coating to flake off when the dressing is manipulated [Haugen, Håvard & Lyngstadaas, Staale et al., 2016]. So, microparticles can released into the wound causing foreign body reactions that hamper a proper healing process. Haugen Håvard and Lyngstadaas Staale suggested a new technique using Atomic layer deposition (ALD), which would provide a thin, nano-coating that allow manipulation of the wound dressing without damaging the nanomaterial layer [Haugen, Håvard & Lyngstadaas, Staale et al., 2016].

Chapter II

3-D Printing in the Construction Industry

2.1 Additive Manufacturing technology.

Additive manufacturing (AM) technology or 3-D printing was introduced first in 1986 by Charles Hull in the stereolithography (SLA) process. The first stereolithography machine was introduced in 1987 by 3-D Systems, Inc., a company founded by the inventor Charles Hull in 1986 that gave start to the industrial exploitation of this technology [Charles Hull et al., 1986]. Additive manufacturing has been defined as ‘‘the process of joining materials to make objects from 3-D model data, usually layer upon layer, as opposed to subtractive manufacturing methodologies, such as traditional machining” [ASTM et al., 2010]. According to Bogue, 3-D printing is an automated, additive manufacturing process for producing 3-D solid objects from a digital model [R. Bogue et al., 2013]. In other words, in a 3-D printing process, the 3-D digital model will be sliced into a series of 2-D layers, which will later be deposited by the printer to construct the model.

AM is unlike traditional manufacturing processes, such as formative processes that require the production of a mold to manufacture a product in mass quantities or subtractive processes that produce significant amounts of waste material as a solid piece of material is cut into the desired shape [Delgado Camacho et al., 2017]. AM can advantageously fabricate complex geometries with no part-specific tooling, significantly reduce the waste material and enables the mass customization of industrial production, where small quantities of customized products can be built affordably, filling a gap left by the other manufacturing processes [Berman et al., 2012; Campbell et al., 2011]. Due to its potential for freeform design, manufacturing of complex geometries, minimizing waste materials, mass-customization and speeding up the fabrication process [B. Panda et al., 2016], additive manufacturing has captured the imagination of everyone from industrial experts to at-home hobbyists [S. Tibbits et al., 2014].

AM technologies are increasingly having an impact on industrial processes in many fields and numerous applications have been developed so far, ranging from aerospace to security, automotive to medical and prototyping extensively [B. Panda et al., 2016; T. Wohlers et al., 2014; B. Berman et al., 2012; H. Lipson & M. Kurman et al., 2013; F. Rengier et al., 2010]. Initial applications of AM technology focused on rapid prototyping by artists and designers to reduce the time required to produce prototypes with complex geometries [ISO/ASTM et al., 2015] and to verify the concepts of their work (conceptual modelling) before production [B. Panda et al., 2016].

Different materials including polymers [J.A. Inzana et al., 2014], metals [C. Ladd et al., 2013], ceramics [U. Scheithauer et al., 2015] and concrete (cement-based material) [Khan et al., 2020] have been applied in different AM techniques. Nowadays, 3-D printers are able to achieve dimensional accuracy, surface roughness and improved mechanical properties for the end-user products. In addition, major advancements in materials have transformed 3-D printing technology to a platform for material science which allows scientists and researchers to customize material deposition, anisotropic behavior and active sensing based on surrounding environments [S. Tibbits et al., 2017; Z. Ding et al., 2017]. These achievements would pave the way for more innovations in 3D printing technology.

2.2 Types of 3-D printing processes.

The American Society for Testing and Materials (ASTM) published a document in collaboration with the International Organization for Standardization (ISO) to define standard terminology for AM. Depending on the technologies used in the 3-D printing process, there are seven types of 3-D printing processes [ISO/ASTM et al., 2015]. These AM processes are categorized into vat photopolymerization, material extrusion, binder jetting, powder bed fusion, material jetting, sheet lamination and directed energy deposition, as shown in Figure 20 [ISO/ASTM et al., 2015; Yusuf et al., 2019].

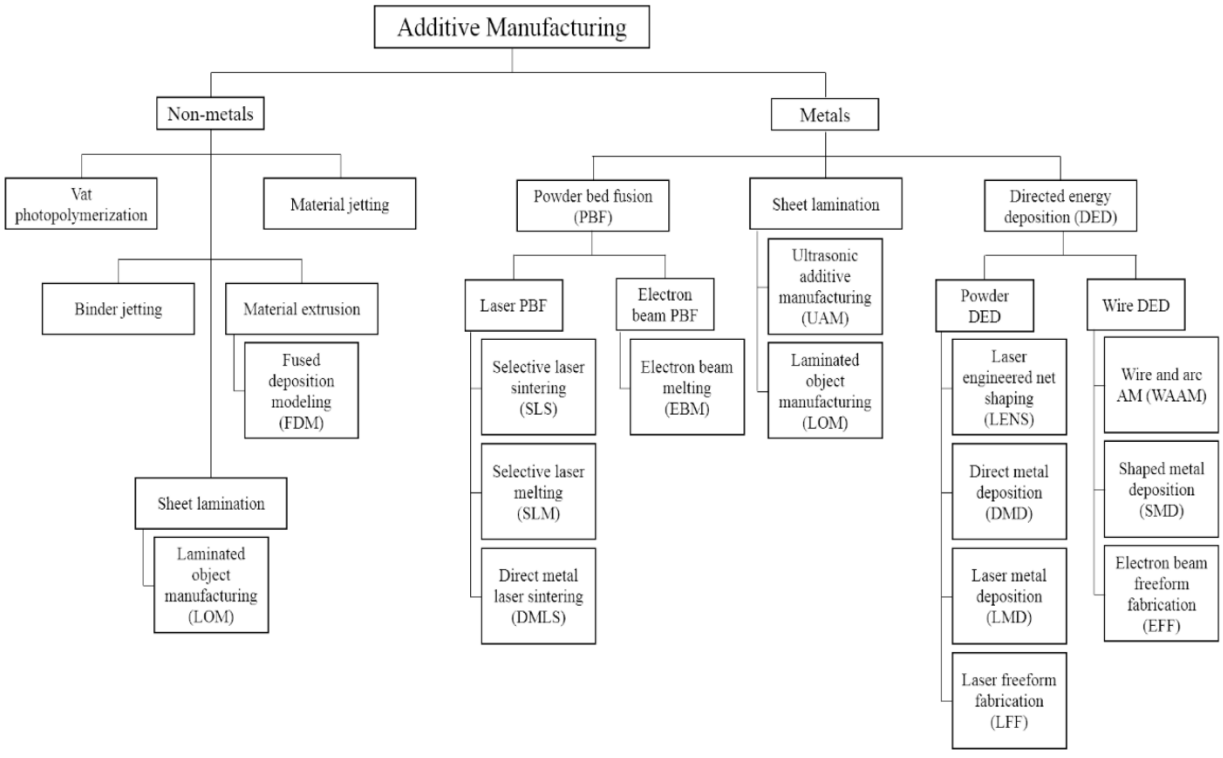

Fig. 20 Hierarchical breakdown of all additive manufacturing (AM) categories. [ISO/ASTM et al., 2015; Yusuf et al., 2019]

2.2.1 Vat Photopolymerization

A process of selectively curing a liquid light-activated polymer with a laser. An example of this process is stereolithography apparatus (SLA), a technique developed by Hull in the 1980's and commercialized first by 3-D Systems [M. Yossef & A. Chen et al., 2015; P. Wu et al., 2016; Gibson et al., 2010]. Stereolithography usually includes a perforated platform, a container of a liquid UV-curable polymer, and a UV laser [F.P.W. Melchels et al., 2010]. Based on the layers extracted from the CAD model, a beam of laser is used to trace the bottom layer of the model on the surface of the liquid UV-curable polymer, which cause the polymer to harden. The perforated platform will then be lowered and the second layer will be traced and hardened by another beam of laser. The process will be repeated until the 3-D model is created [Wu Peng et al., 2016]. An example of these type of 3-D printer is Formlabs' high-resolution desktop 3-D printer (Fig.21). The main barrier to implementing this technology is the development of suitable and affordable resin materials for stereolithography as the current photo-curable resin cost is high [H.W. Kang & D.W. Cho et al., 2012].

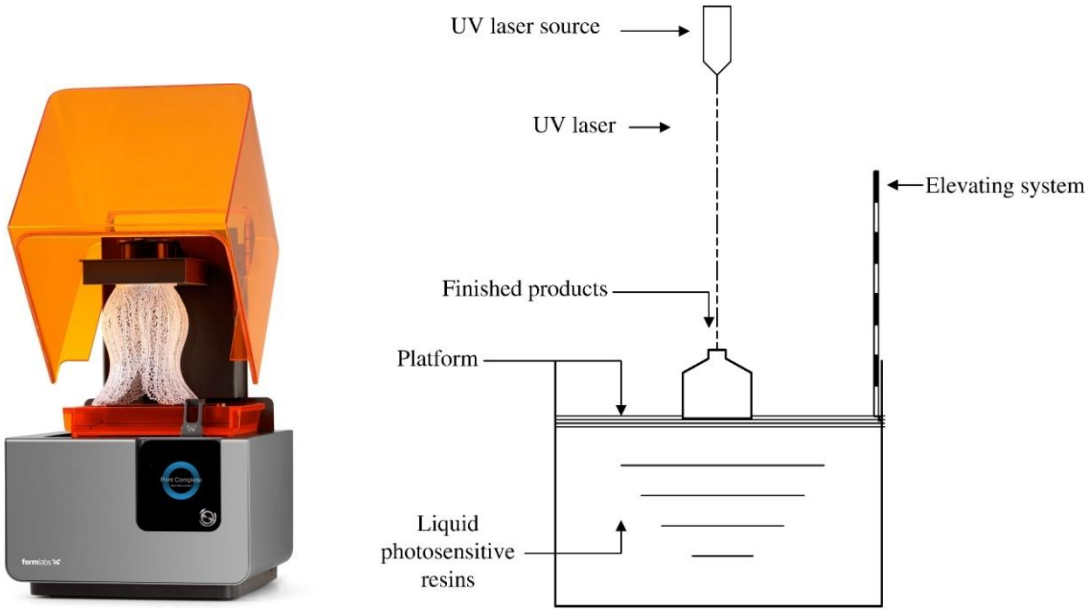

Fig. 21 An illustration of the components and processes in stereolithography (SLA). [Formlabs; Wu Peng et al., 2016]

2.2.2 Material Extrusion

A process of extruding material through a nozzle and depositing it layer-by-layer onto a substrate. The most common process was invented by Crump and commercialized by Stratasys as Fused Deposition Modelling (FDM) [Gibson et al., 2010]. FDM consists of a printer head, a printing material (e.g. polymers and synthetic stone) and support material. Printing material is firstly fed to the printing head, which later moves in X- and Y-coordinates to deposit the material to print the first layer of model extracted from the CAD model. Then the base moves down for the printer head to work on the second and other layers. The process is repeated until the 3-D model is created. Once completed, support material is removed. An example of these type of 3-D printer is Alfawise' FDM 3-D printer (Fig.22). The main disadvantages of FDM are the limitation of the material to low-temperature and low-strength alloy as well as the possibility for oxidation during the printing process due to the lack of a controlled environment [J. Mireles et al., 2012].

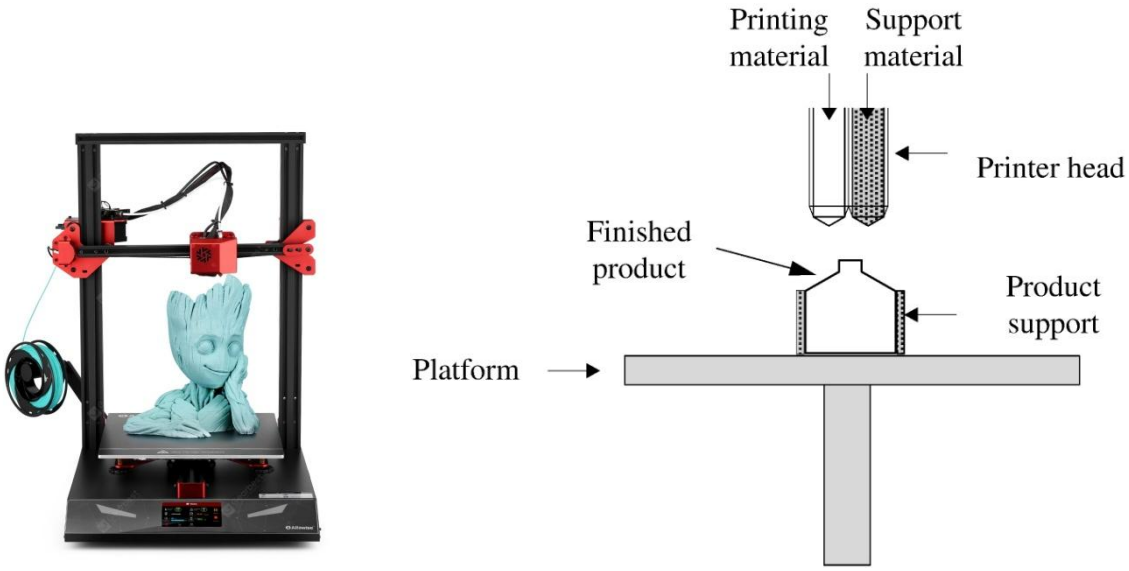

Fig. 22 An illustration of the components and processes in FDM. [Alfawise; Wu Peng et al., 2016]

2.2.3 Binder Jetting

A process of depositing a powdered material layer upon layer and selectively dropping a liquid binding agent onto each layer to bind the powders together. Binder jetting was primarily developed at MIT in a process called 3D printing (3DP) [Gibson et al., 2010]. It is usually referred to as inkjet powder printing process which uses glue or binder to bond successive powder layers together. Inkjet powder printing can use metal as the printing material. Metal (e.g. steel or bronze) in the powder form is deposited in the first layer. The printer head sprays binder material which is heated and dried by a lamp [B.-J. De Gans et al., 2004]. Powdered material is spread over the build platform using a roller, next the print head deposits the binder adhesive on top of the powder where required.

The build platform is lowered and another layer of powder is spread over the previous layer. The object is formed where the powder is bound to the liquid. Unbound powder remains in position surrounding the object. The process is repeated until the entire object has been made. When all layers are printed, the product is cleaned from unbound powder and cured in an oven (Fig. 23).

The main barrier to implementing inkjet method is the requirement for the printing material that is safe to ingest, has no odour, low migration of monomers and other components, satisfactory abrasion resistance for the packaging and distribution process, ability to heat seal, pierce, and die-cut without chipping, while still providing the intense colors and high definition needed for primary retail packaging on a supermarket shelf [Castrejon-Pita et al., 2013]. Due to the use of binder material this process is not always suitable for structural parts.

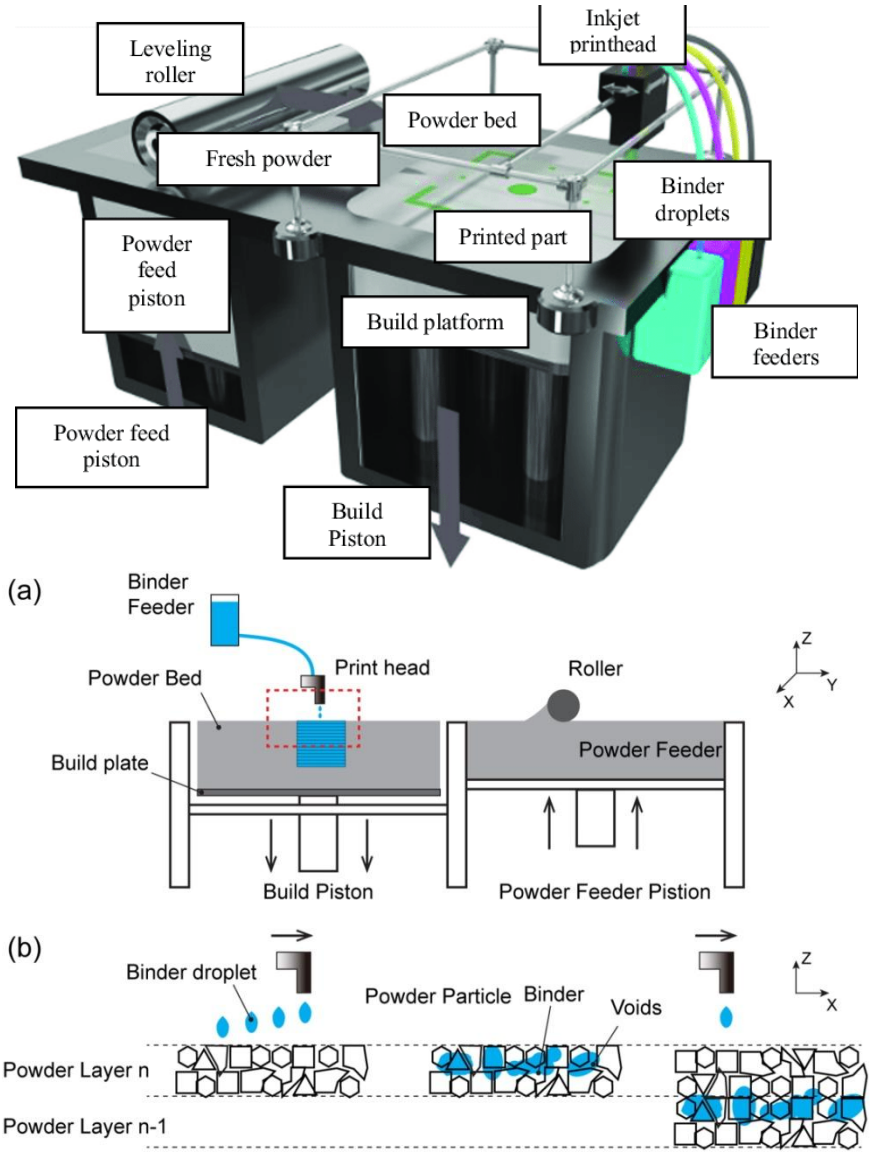

Fig. 23 An illustration of the components and processes in inkjet powder printing. (a) 3DP inkjet printing system, (b) Enlargement of the area in red rectangle: powder/binder interaction between adjacent layers. [Galeta Tomislav et al., 2016; Xia & Sanjayan et al., 2016]

2.2.4 Powder Bed Fusion

A process of selectively fusing a powder bed using thermal energy, typically in the form of a laser or electron beam. A layer of material is spread over the build platform. Then a laser fuses the first layer and a new layer of powder is spread across the previous layer using a roller. The process repeats until the entire model is created. Unfused powder is removed during post processing. The most common powder bed fusion process is selective laser sintering (SLS). SLS is a layer manufacturing process that allows generating complex 3-D parts by consolidating successive layers of powder material on top of each other [J.-P. Kruth et al., 2005]. The consolidation process is conducted using a focused laser beam. SLS was developed at the University of Texas at Austin for polymer materials and commercialized by DTM and 3D Systems [Gibson et al., 2010].

When SLS is used to produce metal products, the process is usually referred to as selective laser melting (SLM) or direct metal laser sintering (DMLS) [J.-P. Kruth et al., 2004]. In the SLM process, the metal powders are completed molten by the laser beam. As a result, the printed products have much higher density than the products printed by SLS. Although SLS and SLM are able to print high-strength product, these technologies face challenges include temperature sensitivity and print size. To avoid oxidation of materials during the printing process, the material fusing temperature should be hold to just below its melting point [A.K. Kamrani & E.A. Nasr et al., 2010]. Other disadvantages of power bed fusion are the high-power usage and the size limitation.

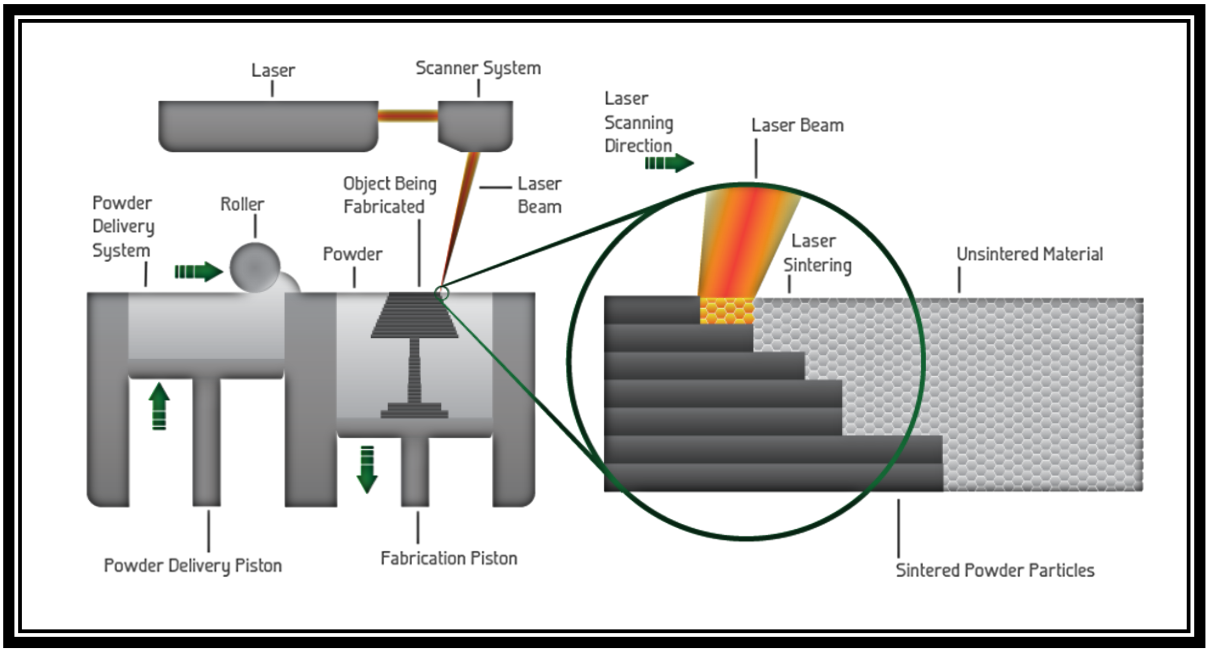

Fig. 24 An illustration of the components and processes in SLS. [Rapidprototyping Services Canada]

2.2.5 Material Jetting

A process of selectively depositing drops of material in a layer wise fashion. Material jetting creates objects in a similar method to a two-dimensional ink jet printer. Material is jetted onto a build platform using either a Continuous Inkjet Printing (CIJ) or Drop on Demand (DOD) approach. The unique difference between CIJ and DOD is the timing of droplet generation. In DOD, droplets are generated when required, whereas in CIJ, the droplets are generated by breaking up the continuous stream of droplets through an ejection nozzle [Sireesha et al.,2018]. Material is jetted onto the build surface or platform using either thermal or piezoelectric method, where it solidifies and the model is built layer by layer. Material is deposited from a nozzle which moves horizontally across the build platform. Machines vary in complexity and in their methods of controlling the deposition of material. The material layers are then cured or hardened using ultraviolet (UV) light. An example of this process is PolyJet technology from Stratasys (Fig. 25b) [Gibson et al., 2010]. The process benefits from a high accuracy of deposition of droplets and therefore low waste. Some of the disadvantages of material jetting are the fact that often requires support material and despite the high accuracy, materials are limited and only polymers and waxes can be used.

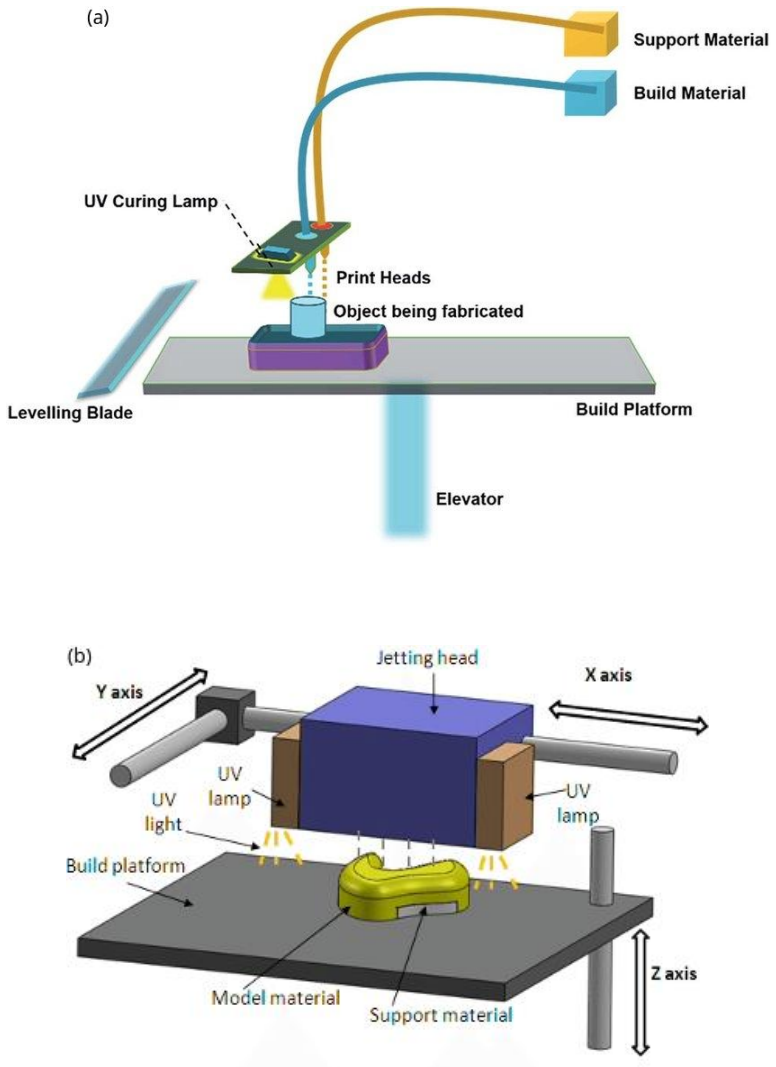

Fig. 25 Schematic representation of the (a) material jetting process and (b) PolyJet technology. [Udroiu & Braga et al.,2017; S. Merum et al.,2018]

2.2.6 Sheet Lamination

A process of successively shaping and bonding sheets of material to form an object. In sheet lamination layers of paper, plastic, or metal laminates are successively bonded together using ultrasonic welding or adhesive, followed by modeling using a blade or laser cutter (Fig. 26). The material is positioned on the platform. Then the material is bonded in place, over the previous layer, by the heated roller. The required shape is then cut from the layer, by laser or knife. Alternatively, the material can be cut before being positioned and bonded. The process repeats until the entire model is created. Depending on the materials and binding method used, sheet lamination can be subdivided into Ultrasonic Additive Manufacturing (UAM) focusing on metals and Laminated Object Manufacturing (LOM) based on adhesive and paper. The UAM process uses sheets or ribbons of metal, which are bound together using ultrasonic welding. The process does require additional computer numerical control (cnc) machining and removal of the unbound metal, often during the welding process. UAM uses metals and includes aluminium, copper, stainless steel and titanium [R. Friel & R. Harris et al., 2013]. The LOM uses a similar layer by layer approach but uses paper, plastic or less commonly metal as material and adhesive instead of welding. Since the sheet lamination process involves solid state bonding and additional adhesives are used, the material is not required to reach its melting point for the bonding to occur, as a result the energy demand is low. A variety of materials can be manufactured using sheet lamination which includes paper, ceramics, metals (e.g. aluminum, stainless steel, copper and titanium), plastics, fabrics, synthetic materials and composites [I. Gibson et al., 2014]. Laminated objects are often used for aesthetic and visual models and are not suitable for structural use. An example of sheet lamination process is Laminated Object Manufacturing (LOM) developed by Helisys Inc., in which paper sheets were trimmed to size and glued together [Gibson et al., 2010]. Another example is Ultrasonic Additive Manufacturing (UAM) commercialized by Solidica Inc. fabricates metal objects using ultrasonic welding [Gibson et al., 2010]. Benefits include speed, low cost, ease of material handling, but the strength and integrity of models is reliant on the adhesive used. Other disadvantages are the high requirement of material and the high production of waste.

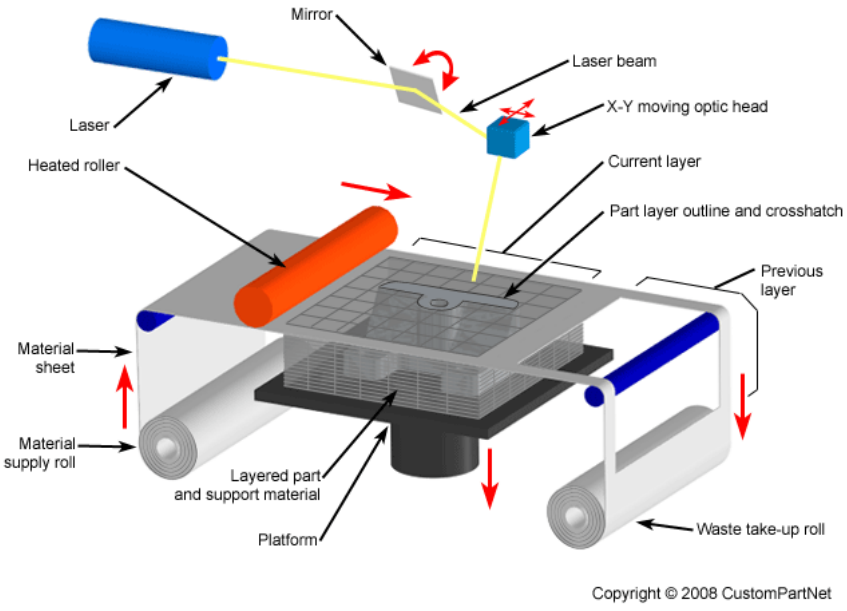

Fig. 26 Schematic diagram showing the sheet lamination process. [CustomPartNet]

2.2.7 Direct Energy Deposition

A process of fusing materials with focused thermal energy that melts the material as it is being deposited. Directed Energy Deposition (DED) is often referred to by other names such as Laser Engineered Net Shaping (LENS), Directed Light Fabrication (DLF), Direct Metal Deposition (DMD) and Electron Beam Additive Manufacturing (EBAM), depending on the specific application or method. Although the general approach is the same, differences between these techniques commonly include changes in laser power, laser spot size, laser type, powder delivery method, inert gas delivery method, feedback control scheme, and/or the type of motion control utilized [Gibson et al., 2015]. DED is a more complex printing process commonly used to repair or add additional material to existing components (Gibson et al., 2010). An example of this process is laser engineered net shaping (LENS), developed at Sandia National Laboratories [Y. Huang et al., 2015; Gibson et al., 2010], which is particularly useful for repair of damaged metal parts [R.P. Mudge & N.R. Wald et al., 2007]. A typical DED consists of a nozzle mounted on a multi axis arm, which deposits melted material onto the specified surface, where it solidifies. The process is similar in principle to material extrusion, but the nozzle can move in multiple directions and is not fixed to a specific axis. DED processes direct energy (typically a laser or electron beam) into a narrow, focused region to heat a substrate, melting the substrate (wire or powder form) and simultaneously melting material that is being deposited into the substrate's melt pool. Unlike powder bed fusion techniques DED processes are not used to melt a material that is pre-laid in a powder bed but are used to melt materials as they are being deposited. Each pass of the DED head creates a track of solidified material, and adjacent lines of material make up layers [Gibson et al., 2015]. Complex three-dimensional geometry requires either support material or a multi-axis deposition head [Gibson et al., 2015]. Although this process can work for polymers, ceramics, and metal matrix composites, it is mainly used for metal powders (e.g. Cobalt, Chrome and Titanium). A balance is needed between surface quality and speed, although with repair applications, speed can often be sacrificed for a high accuracy and a pre- determined microstructure [Gibson et al., 2010]. Some disadvantages are the limited material use and the fact that finishes can vary depending on paper or plastic material and may require post processing to achieve desired effect.

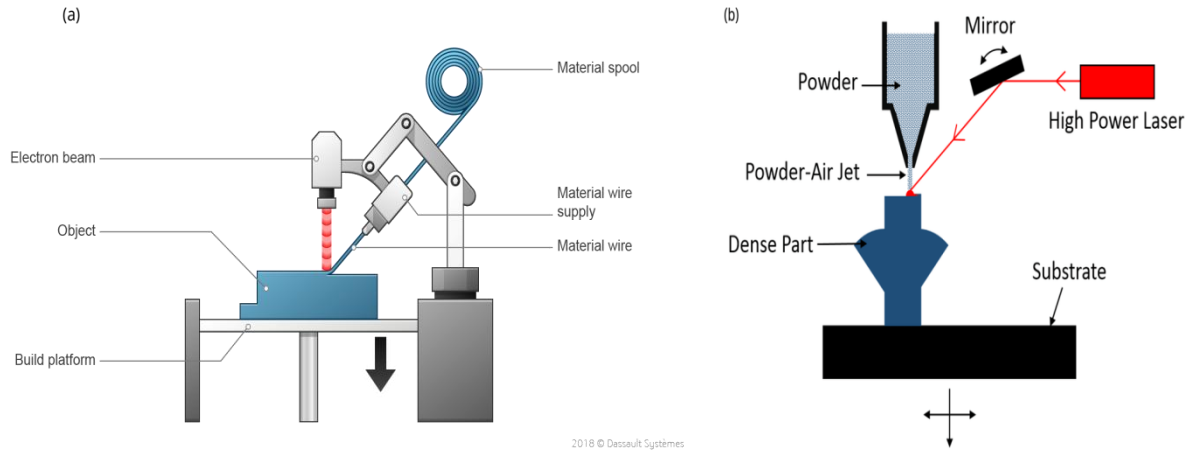

Fig. 27 An illustration of the components and processes in DED (a) using wire and (b) powder. [Dassault Systèmes; Feilden et al., 2017]

2.3 Construction industry and potential for AM technologies

The main emphasis for innovation strategy in the construction industry is to use technology from elsewhere to reinforce other competitive advantages [J. Tidd et al., 1997]. This is one of the reasons why the construction industry is viewed as a low-tech industry with low levels of innovation [C. Harty et al., 2008]. With evolution in time, the construction designs are becoming more complicated and the workers involved in this process are increasingly exposed to unhealthy environments [Kittusamy & Buchholz, 2004]. Experimental applications of AM in the construction industry started appearing in the late 1990's [J. Pegna et al., 1997]. These initial proof-of-concept applications helped identify potential benefits and challenges for AM technologies in construction. Recently, AM technologies are attracting a growing interest in construction industry as well, especially in the concrete technology [D. Asprone et al., 2018]. Many researchers and industry experts began to explore technologies like large scale additive manufacturing or 3-D printing to bring automated solutions in the construction process. The interest in exploiting AM technologies in construction industry is mainly the result of the expectation of new freedom in terms of the design of shapes, elements and structures, enabling at the same time new aesthetic and functional features (often referred to as freeform constructions) [D. Asprone et al., 2018]. In comparison to conventional construction processes, the application of AM technologies in construction industry may reduce the labor requirements which would result in a decreased construction cost and an increased level of safety, reduce on-site construction time by operating at a constant rate, minimize the chance of errors by highly precise material deposition, saving of materials and, consequently, sustainability and increase architectural freedom which would enable more sophisticated designs for structural and aesthetic purposes [W. Gao et al., 2015; R.A. Buswell et al., 2007; X. Ming & S. Jay et al., 2016; W. Timothy et al., 2016].

Conventional construction processes require pieces to be cut through subtractive technologies, in which the material is machined out to produce the final object (e.g. natural stone, ceramic pavements) or proper moulds to be created. The moulds are used in combination with formative technologies, where the fresh material (e.g. reinforced concrete elements) is cast in a mould to achieve the final shape of the object [R.A. Buswell et al., 2007]. Architectural designers are often forced to use multiple identical elements in a project to save materials and reduce costs of labour and moulds. Recently the 3-D printing construction has started to move from usage of an architect’s designing aide to produce a full-size complete construction module namely walls, ceilings and external façade systems, by changing the approach in the way that components are produced, without incurring prohibitive costs [S. Lim et al., 2012]. For example, major contractors, such as Foster and Partners in London, now have a suite of modeling equipment and 3-D printing process to print 3-D architectural models [R.A. Buswell et al., 2007].

Notably, with regard the saving of materials and, consequently, sustainability, a recent study has demonstrated that digital fabrication is able to provide environmental benefits when applied to complex structures, for which additional complexity can be achieved without additional environmental costs [Agustí-Juan, Isolda et al., 2017]. As moulds make up approximately 60% of the materials which assist in the conventional construction processes, 3-D printing has been proven to save up to 60% of construction waste, 70% of production time and 80% of labour costs [El Sakka & Hamzeh et al., 2017]. Thus, 3-D printers provide promisingly lower energy consumption, as well as reduced emissions & materials.

However, numerous processing challenges still remain in construction and manufacturing processes including void formation, anisotropic behavior, design software constraints, and low resolution of printed parts. Additionally, AM technology still suffers from rigid and static parts as well. Therefore, there are many ongoing researches towards eliminating present challenges such as coupling smart materials with AM techniques [A. Bandyopadhyay & B. Heer et al., 2018; J.-Y. Lee et al., 2017].

2.3.1 Largescale AM processes in construction industry

In recent years, the development of largescale AM processes has been developed to accommodate the need of architecture and construction. Currently there are three large-scale AM processes targeted at construction and architecture in the public domain. The three main categories of large-scale 3-D printing are Contour Crafting (CC) [B. Khoshnevis et al., 2004; B. Khoshnevis et al., 2006], D-Shape [V. Colla & E. Dini et al., 2013] and Concrete Printing [S. Lim et al., 2009; S. Lim et al., 2011]. All three have proven the successful manufacture of components of significant size (Fig. 28) and are suitable for construction and/or architectural applications [S. Lim et al., 2012].

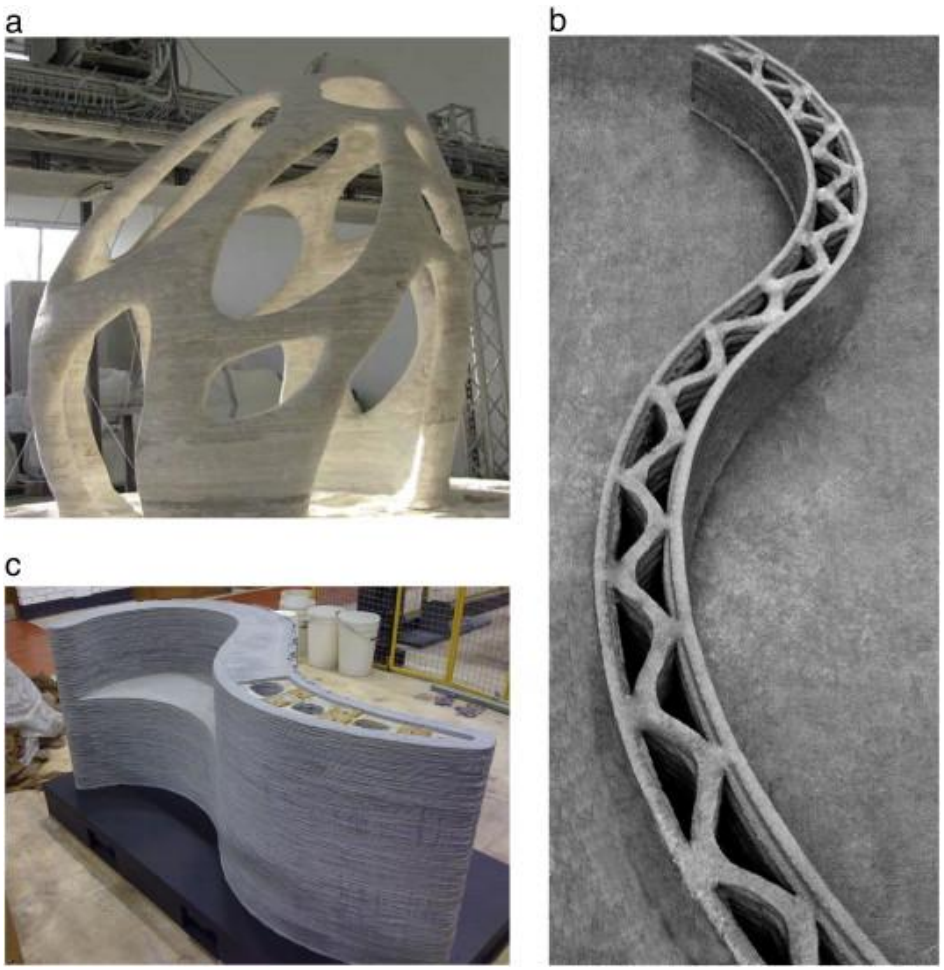

Fig. 28 Examples of full-scale constructions from (a) D-Shape, (b) Contour Crafting and (c) Concrete Printing. [S.Lim et al., 2012]

Contour Crafting

Contour crafting (CC) is an extrusion-based technology which has been developed by B. Khoshnevis for the automated construction of buildings and infrastructure on earth and other planets [B. Khoshnevis et al., 2004]. For printing bigger structures, complex structure needs bigger printers and CC solved this problem. CC improves surface quality, fabrication speed and material input choices [B. Khoshnevis & Dutton R. et al., 1998; B. Khoshnevis et al., 2006; B. Khoshnevis et al., 2004]. The CC makes it possible to complete an entire house in the duration of a few hours instead of a few months [B. Khoshnevis et al., 2004; Zhang J. & Khoshnevis B. et al., 2013]. For example (Fig. 29), Winsun Decoration Design Engineering Co., build 10 houses in one day with the help of contour crafting [Levy Karyne et al., 2014].

Fig. 29 3-D printed house by Winsun Decoration Design Engineering Co. with the help of contour crafting. [Levy Karyne et al., 2014]

A complete contour crafting system includes a crane (sliding mechanism), a material storage, a gantry system and a nozzle (Fig. 30). This method uses high pressure in order to extrude the material (e.g. concrete, clay, cement, plaster, ceramics, thermoplastics) through a large nozzle of the printhead attached to automatic cranes. The gantry system can carry the printing nozzle move along X axis and Z axis and two parallel sliding structures (crane) carry the nozzle moving along Y axis. The gantry system used in CC is very similar to the gantry system used in precast concrete fabrication. When the printing material is extruded from the nozzle, it is troweled using a set of actuated and computer-controlled trowels. One layer at a time, the extructed material is placed in his particular position through the nozzle movement. After being partially cured, the hardened lower layers are able to support the fresh cement layer [D. Smith et al., 2012]. Using materials with rapid curing properties and low shrinkage characteristics, the structural components can be built up rapidly with consecutively deposited layers [Ma GuoWei et al., 2017].

The layer-by-layer construction technique in CC, render its ability to build utility conduits within walls. This capability also makes it possible to mechanize the installation of plumbing, and electrical services. Only installation of doors and windows will need human intervention, therefore, CC is a completely automated fabrication process [B. Khoshnevis et al., 2003]. Hence, due to the superior characteristics of CC, it has potential to be used for construction of not expensive houses, emergency sheltered housing, and complex architectural structures which their fabrication through conventional approaches are expensive [B. Khoshnevis et al., 2003].

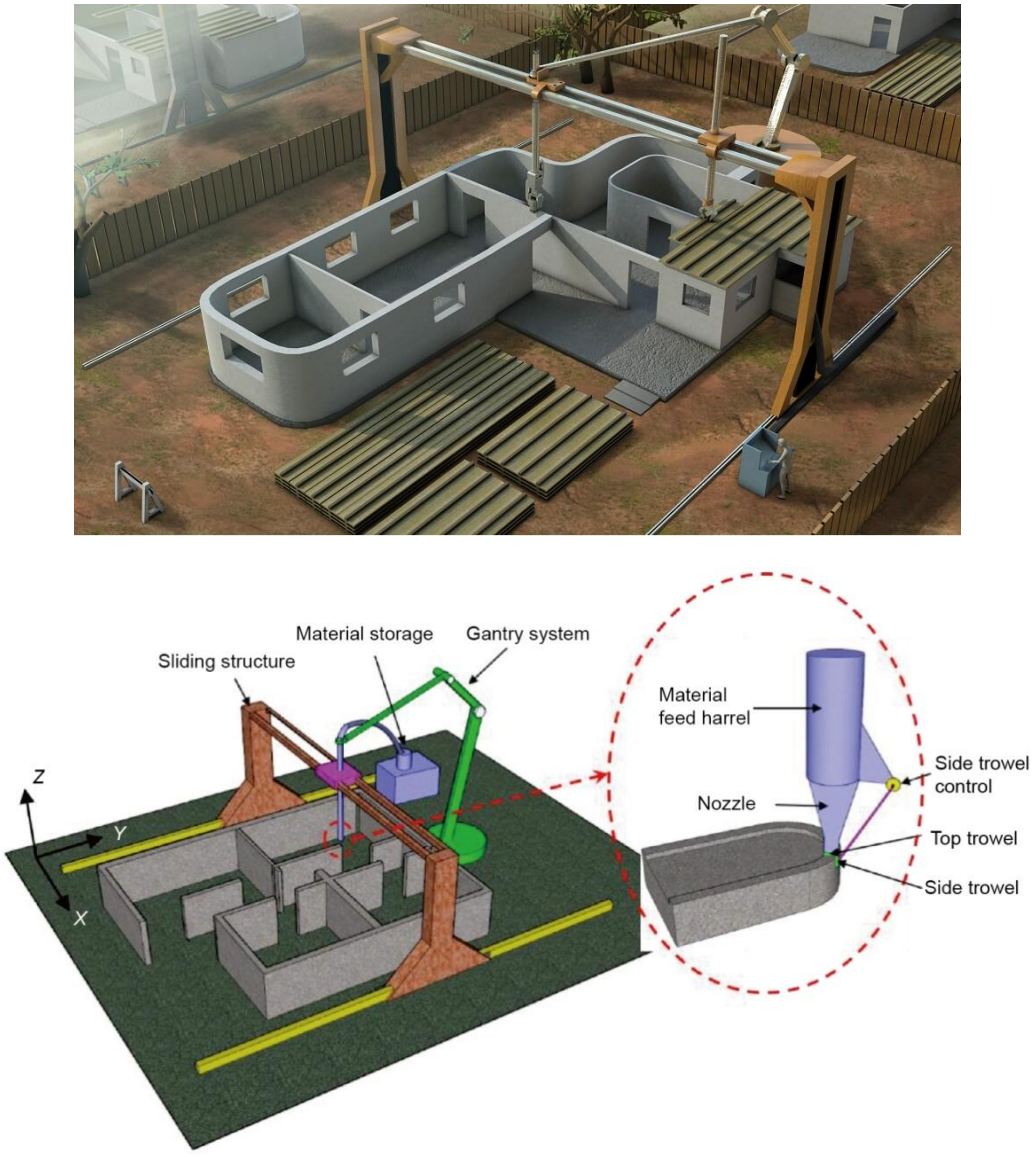

Fig. 30 Construction of building using contour crafting printing. [Contour Crafting CORP.; Ma GuoWei et al., 2017]

A simple illustration of the nozzle and trowels used in contour crafting is shown in Fig. 31 [Wu Peng et al., 2016]. CC has been successfully applied in construction applications. Existing example is Andrey Rudenko's 3D printed castle [Rudenko A. et al., 2014]. Material used in the printer was a mix of cement and sand. Whole building was printed on a single run, except of towers, that were printed separately and assembled to the building.

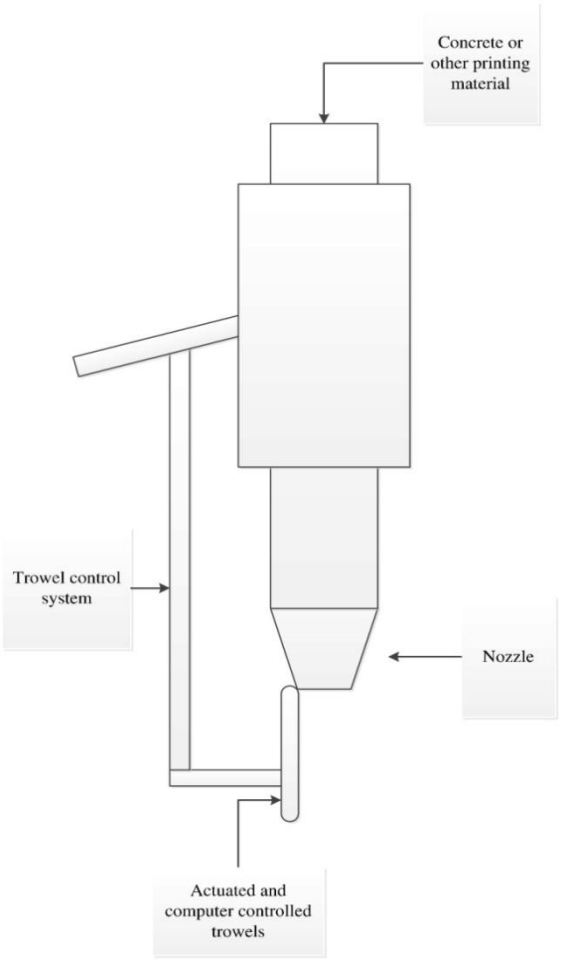

Fig. 31 A simple illustration of the nozzle and trowels used in Contour Crafting printing. [Wu Peng et al., 2016]

CC has certain limitations arising from the use of the side trowel. For example, very small hollow volumes, such as small holes, can't be made because they cannot accommodate the side trowel. Also, it is not possible to use the side trowel to create features that are relatively thin (e.g., a vertical blade). In such cases, the extrusion deposition thickness may exceed the feature thickness. The extent of this limitation, however, depends on the size of the side trowel, which could be 3 mm x 3 mm for fabricating small objects and 2 cm x 2 cm for large objects [B. Khoshnevis et al., 1999].

D-Shape

D-Shape is a method of digital construction that uses a binder jetting 3-D printer for architecture. D-Shape method adopted by Enrico Dini [V. Colla & E. Dini et al., 2013; G. Cesaretti et al., 2014]. His first patent was published in 2006 accompanied with subsequent development [Enrico Dini et al., 2006; Enrico Dini et al., 2008]. D-Shape materializes buildings or building blocks directly from a CAD (Computer-Aided Design) via a process of alternating layers of granular material and writing on them with an appropriate 'Ink Binder' that turns the granular material into a shape. The granular material may be of almost any nature, while the binder may be an aqueous solution of different additives [Dini Engineering S.R.L.]. The D-shape printer consists of a stationary horizontal frame (the base) with four perpendicular beams at each corner.

The printer head is attached to the square base by a horizontal beam, which can freely move along X axis (vertical direction). The square base moves upwards (z-axis) along vertical beams through four stepper motors. The printer head has approximately 300 spraying nozzles (20 mm apart) spanning the entire base and utilizes a magnesium-based binder to fuse sand or stone dust particles in a process of additive manufacturing [Kashani & Ngo et al., 2018].

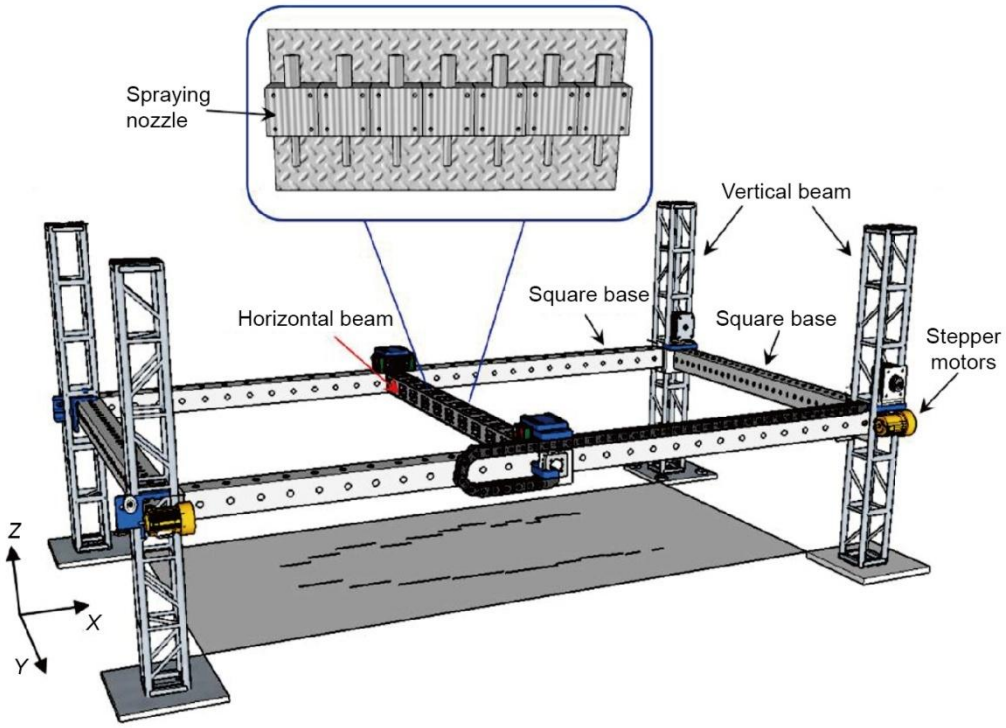

Fig. 32 Schematic view of the D-shape printer. [Ma GuoWei et al., 2017]

Inlet materials ('ink'&'paper')					
Inert granular materials				**Reactive granular materials (only for indoor production)**	
Layering Materials	A cat.	Fines		Portland cement's premixed mortars	
	B cat.	Sand		Sorel cement's premixed mortars	
	C cat.	Gravel		Sorel cements + A,,C,D,E,F cat.	
	D cat.	Mixes of A + B + C Materials		Portland cement's + A,,C,D,E,F cat. Premixed mortars	
	E cat	Expanded Clay aggregates, ceramics			
	F cat	Recycled crushed materials (chipped wood, chipped plastics, demolition rejects, glass, rubber, gypsum)			
	G cat.	A, B,C,D,E,F cat +	Natural Fibers	A, B,C,D cat + :	Natural Fibers
			Glass fibers		Glass fibers
			Basaltic Fibers		Basaltic Fibers
			Polymeric Fibers		Polymeric Fibers
			Steel Fibers		Steel Fibers
Liquid Binders /Reagents	Portland cement based slurries (v ≤ 3°E)			Water	
	Sorel cement based Slurries (v≤ 3°E)			Water + additives	
	Geolpolymer slurries (v≤ 3°E)			Salt solutions	
	Polymeric primers (urethanic, silossanic,vinylic, except Fenolic and PPBs,PPCs binders) (v≤ 3°E)			Solvents	
	Other dispersions having viscosity (v≤ 3°E = 22 cSt.				

Table 4. Inlet granular materials used for D-shape printer. [Dini Engineering S.R.L., Materials]

During printing process, nozzles sprays the binding liquid on predefined areas of the powder layer to selectively bind the powder together according to the digital prototypes. Once a layer has been printed, a horizontal beam also acts as powder material spreader prior to subsequent layer manufacturing [G. Cesaretti et al., 2014]. Meanwhile, the remaining powder serves to support the structure. Heat treatment or infiltration can be conducted as post-processing step in order to improve the strength and durability of the printed component [Lowke Dirk et al., 2018]. This is done in a layer-by-layer manner. Once completed, the printed part can be taken out of unconsolidated material and remaining powder can be reused in another fabrication process [S. Lim et al., 2012; Tibaut et al., 2016]. With this method we can control the accumulated waste by recycling the waste sand materials. D-Shape process has been used to create 1.6 m high architectural pieces called “Radiolaria” (Fig.33).

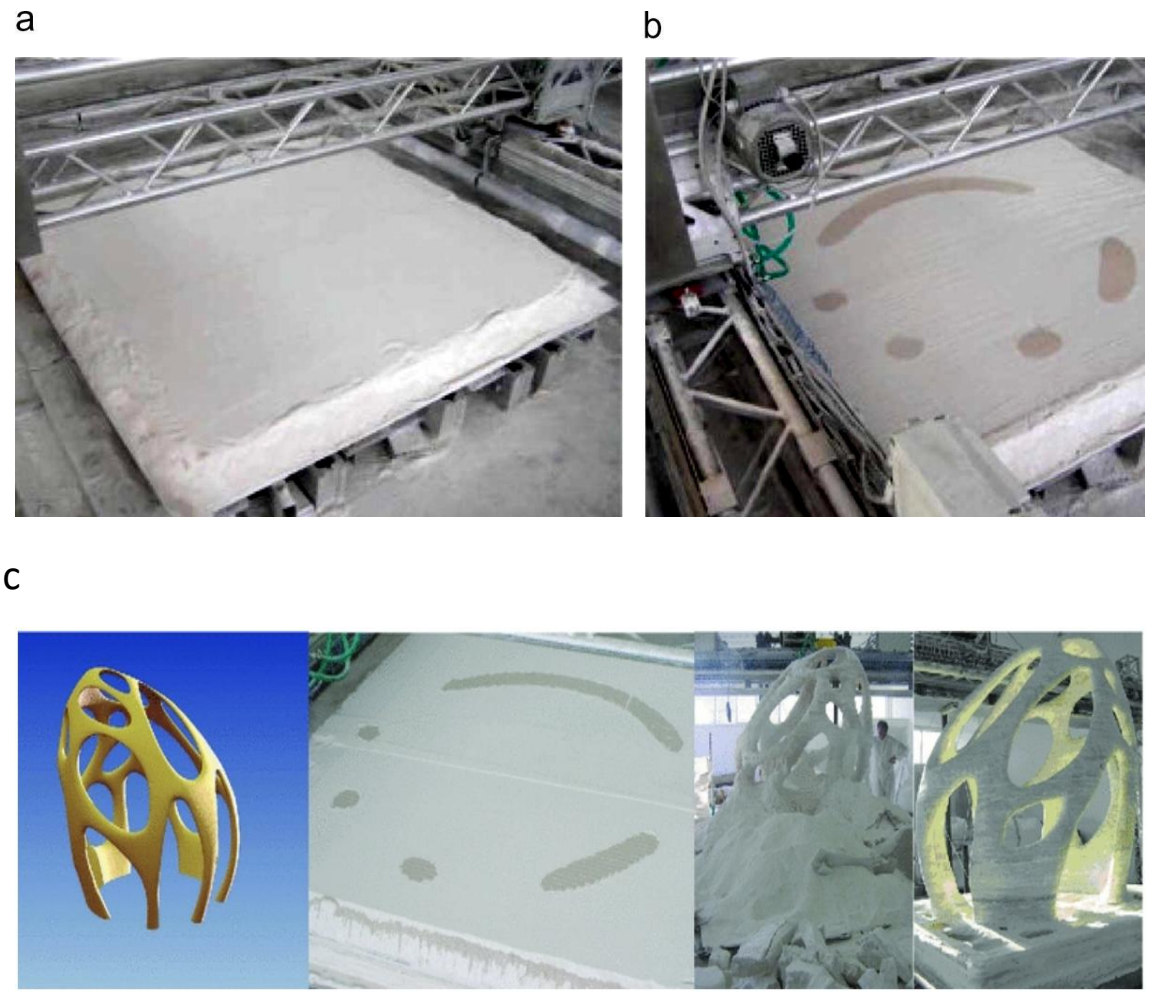

Fig. 33 (a) A layer of deposited material ready for binder, (b) a cross section of the printed model and (c) D-Shape process phases: digital model, 3-D printing, cleaning, and polishing final product. [G. Cesaretti et al., 2014]

D-shape proved to be very effective in printing very large-scale objects. For instance, D-Shape is the only large-scale 3-D printer that can build up entire conglomerate building structures in one go, from the basement to the roof, including ceilings, stairs, base- and high-reliefs, and partitioning walls [V. Colla & E. Dini et al., 2013; Dini Engineering S.R.L.]. Enrico Dini and a collaborator Louisa Vittadello intended to print out many different structural blocks using the D-shape technique. The material was a mixture of sand, salt and an inorganic binding agent.

The blocks were assembled by machines to create a futuristic looking structure [Krassenstein E. et al., 2015]. It is claimed that D-shape will allow military to construct infrastructure such as bunkers, hospitals and bases, much faster than it would take with more traditional methods [Krassenstein E. et al., 2014].

Concrete Printing

Concrete Printing is another largescale construction process [S. Lim et al., 2011; S. Lim et al., 2012; Le Thanh et al., 2012a; Le Thanh et al., 2012b]. Specifically, Concrete Printing is an extrusion-based method to fabricate cementitious components in a layer-by-layer process. Similar to CC the print head used for the extrusion of cementitious material is also mounted on an overhead crane. Printing nozzle moves along a pre-programmed path and continually extrudes concrete materials [S. Lim et al., 2012]. Concrete Printing uses no trowels, therefore its printing resolution is lower than CC. Notwithstanding the lower resolution, better control of internal and external geometries is accessible through Concrete Printing [S. Lim et al., 2009; S. Lim et al., 2012]. The printing head is installed in a tubular steel beam, which can freely move in X, Y and Z directions. Fresh concrete is firstly delivered to a pump through the delivery pipe, then concrete material is delivered smoothly to the printing nozzle with the help of the pump. Finally, concrete filaments are extruded out from the nozzle to continually trace out the cross section of structural components [Ma GuoWei et al., 2017]. This print process has the potential of incorporating functional voids into the structure [S. Lim et al., 2012].

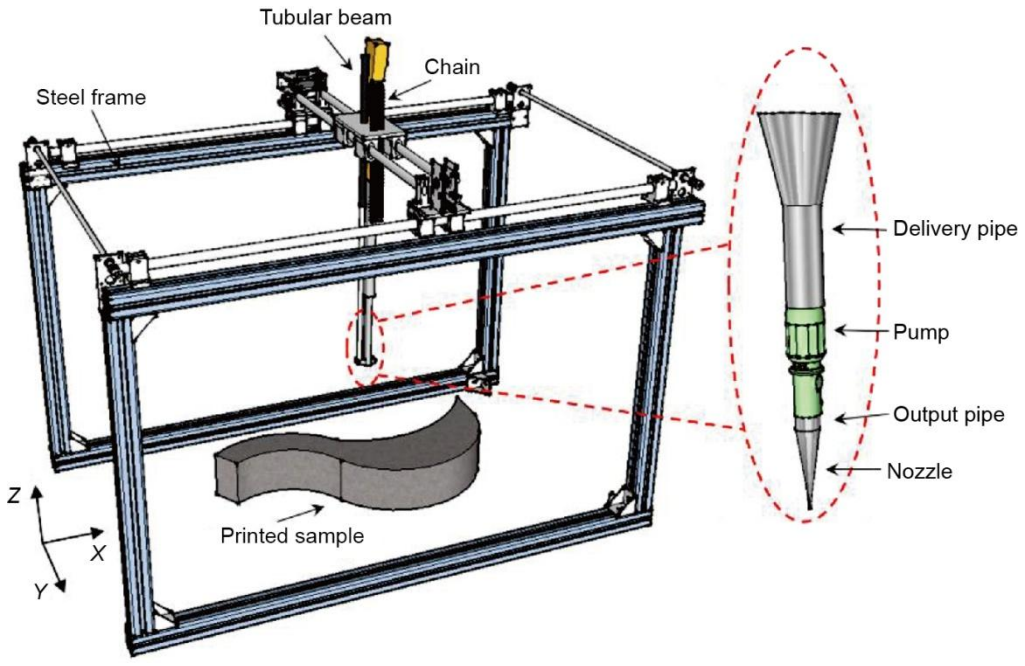

Fig. 34 Schematic view of Concrete Printing, magnified region is the concrete deposition system. [Ma GuoWei et al., 2017]

Concrete Printing has the potential to produce highly customized building components [S. Lim et al., 2011; S. Lim et al., 2009]. For example, S. Lim et al. at Loughborough University (UK) developed a novel Concrete Printing system within a 5.4 m×4.4 m×5.4 m steel frame. A named Wonder Bench (2 m×0.9 m×0.8 m) is manufactured by Concrete Printing (Fig. 35), which consists of 128 layers with an average printing speed of 20 min/layer [S. Lim et al., 2012]. The curved shapes and hollow interior channels would be impossible to make using traditional cement pouring techniques.

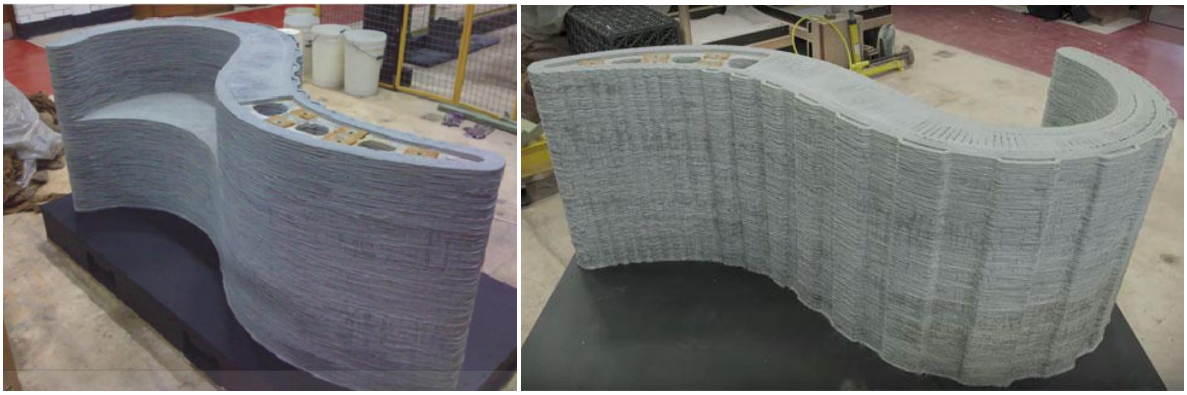

Fig. 35 Wonder bench constructed by Concrete Printing. [S. Lim et al., 2012]

Another example is the construction of a pavilion with modern design (Fig. 36) from a research team at Eindhoven University of Technology (TU/e) in the Netherlands with their massive concrete 3-D printer. The printer is made up of a four-axis gantry robot and features a print bed of 9.0 m×4.5 m×3 m. It also has its own mixing pump, with the entire printer controlled by a numeric controller [Bridget B M. et al., 2016].

Fig. 36 Pavilion constructed by Concrete Printing. [Bridget B M. et al., 2016]

It is important to mention that the layered structure is likely anisotropic due to the formation of voids among each single filaments or threads from the concrete paste (Fig. 37), deteriorating the constructed structure strength and durability more over hardened properties of the concrete parts impacted by the bond between each filament and each layer [Le Thanh et al., 2012a]. This problem can be minimized by reinforcing the structure layers with additional components/chemicals. The finishing and post-processing of Concrete Printing differ from CC due to the production of the characteristic ribbed finish (Fig. 37b). In the case if a smooth finish is required, shall be planned and execute more skill oriented to achieve the required end product. If smooth finishes are required due to not available automatic process, either the wet paste can be trowelled during printing, or the printed finish can be ground to a smooth surface, manually by post grinding/sanding [S. Lim et al., 2009].

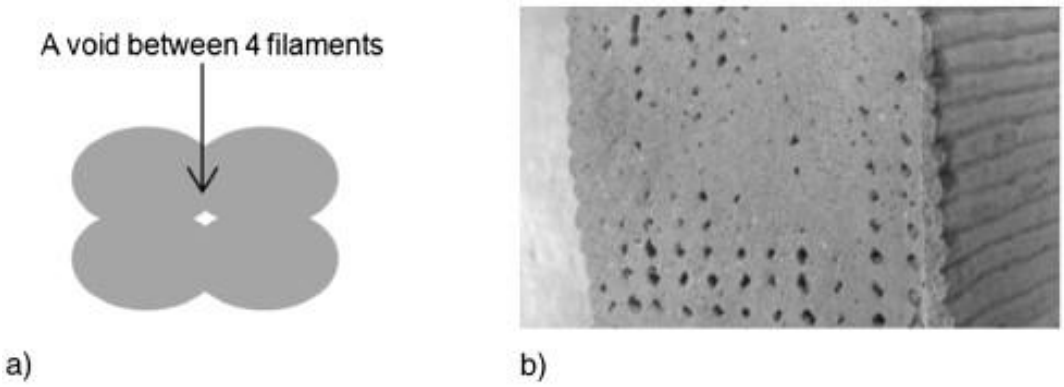

Fig. 37 (a) Four Filaments may form a void and (b) poor Concrete Printing with voids between filaments, showing layers and ribbed finish. [Le Thanh et al., 2012a]

Moreover, due to the fabrication of freeform components without formwork, low shrinkage is an essential element for Concrete Printing since the absence of formwork could accelerate water evaporation, and hence occurrence of cracks in the concrete which causes failure of the structure [Le Thanh et al., 2012a]. Considering this kind of risks, a high-performance cement has been developed with a high compressive strength, around 100–110 MPa, to neutralize the weaker structure of printed components through Concrete Printing [S. Lim et al., 2011].

2.3.2 A comparison of Contour Crafting, Concrete Printing and D-Shape printing

Concrete Crafting, Concrete Printing and D-Shape are all similar by using Additive Manufacturing process to produce the materials thru step by step process from 3-D model data to construction layers in an automotive manner, however each process keeps its own distinct features, resulting in different advantages when applied in engineering situations. The similarities and differences in respect to the characteristics (e.g. construction methods, processes and materials) of each largescale AM processes are summarized in Table 5.

Contour Crafting, Concrete Printing and D-Shape require additional support to create overhangs and other freeform features. Contour Crafting process needs a lintel to bridge the gap right above the windows, otherwise adopting self-supporting layers to form small curvature structures. It is beyond the capability of Contour Crafting to print an entire building including window and roof all at once [Ma GuoWei et al., 2017].

Concrete Printing uses a second material for support, in a similar manner to the Fused Deposition Modelling Process, while D-Shape is a powder-based process and uses the unconsolidated material [S. Lim et al., 2012]. The disadvantage of these types of process is an additional deposition device is requiring more maintenance, cleaning and control instructions and the secondary structure must be cleaned away in a post processing operation. As a result, D-Shape is the best solution to this problem and allows the entire building being printed within a single process once the dimension of the printer is larger than the house.

In terms of printing scale, Contour Crafting is a promising approach to realize real-life construction contributed by its multi-axis robotic arm. Compared with Contour Crafting, the manufacturing dimension of the other two processes is greatly restrained by their deposition method and in particular the mechanical frame [Ma GuoWei et al., 2017]. Print speed is also affected by the build material and/or binder deposition rate. In terms of printing speed, the Contour Crafting and Concrete Printing process are currently fixed with a single and large-diameter nozzle, resulting in a high layer build-up rate, minimizing the printing time. Contour Crafting and Concrete Printing process, while being quite fast, are limited to low printing resolution (i.e. the smallest detail that can be built) and large layer thickness. D-Shape possesses higher printing resolution, which precisely profit from the small-diameter nozzles. Specifically, D-Shape has a high printing resolution 0.15 mm while Contour Crafting and Concrete Printing a low printing resolution 15mm and 9-20 mm respectively. In terms of layer thickness, the print resolution varies from 5-25 mm in Concrete Printing, from 4-6 mm in D-Shape and to approximately 13 mm in Contour Crafting. Therefore, increasing printing precision will inevitably extend the printing time and require more layers to print [Ma GuoWei et al., 2017].

In terms of deposition path, Contour Crafting reduces cycle times between layers by printing an entire layer with two passes of the printing head. D-Shape uses a gantry with multiple nozzles mounted in series that requires a single traverse per layer, although the build material must be pushed over the entire build area, compressed and flattened. Concrete Printing also utilizes a single deposition nozzle, however, unlike D-Shape, it has to traverse the entire build area by lots of cycles [S. Lim et al., 2012; Ma GuoWei et al., 2017]. Contour Crafting and Concrete Printing are wet processes while D-Shape is predominantly a ‘dry’ process (Table 5). Materials in all three techniques harden through a curing process, which is inherently less controllable that the heat or UV based phase change methods of conventional additive methods. Hardened properties of the three techniques are described in Table 5. Contour Crafting and Concrete Printing are extremely impacted by mix design, and particle size while in D-Shape, binder penetration through layers and its flowability is a critical parameter [S. Lim et al., 2012]. Concrete Printing produces a characteristic ribbed finish, which can be controlled and designed to exploit the effect. If smooth finishes are required either the wet paste can be trowelled during the build process, or the printed finish can be ground to a smooth surface, manually by post grinding/sanding [S. Lim et al., 2009], or by adding conventional finishes such as plaster or concrete render onto the printed finish. The design of the Contour Crafting deposition head allows smoothing to be carried out during the build phase.

Similar to Concrete Printing, the D-Shape process produced a texture of finish, which requires grinding and polishing if such a surface is desired [S. Lim et al., 2012].

	Contour Crafting	D-Shape	Concrete Printing
Process	Extrusion based	Selective binding	Extrusion based
Use of mould	Yes (Becomes a part of component)	No	No
Support	Vertical: no Horizontal: lintel	Unused powder	A second material
Material	Cementitious material	Granular material (sand/stone powder)	High performance concrete
Binder	None (Wet material extrusion and backfilling)	Chlorine-based liquid	None (Wet material extrusion)
Printing resolution (Nozzle diameter)	Low (15 mm)	High (0.15 mm)	Low (9–20 mm)
Nozzle number	1	6-300	1
Layer thickness	13 mm	4–6 mm	5–25 mm
Printing speed	Fast	Slow	Slow
Printing dimension	Mega-scale	Limited by frame (6m×6 m×6 m)	Limited by frame
Reinforcement	Yes	No	Yes
Mechanical (Hardened) properties	Tested with zero degree (0°) of layer orientation, which means the force was given from the top of the printed surface.		
Compressive strength	unknown	235-242 MPa	100-110 MPa
Flexural strength	unknown	14—19 MPa	12—13 MPa
Print size	> 1 m dimension	> 1 m dimension	> 1 m dimension
Pre / Post processing	Reinforcements per 125mm vertically and back fill the mould with a cementitious per 125 mm height.	Reinforcement after printing.	Compression of the powder for the next layer with light pressure compaction.
Conclusion	Smooth surface by trowel. Extra moulding process. Weak bond between batches.	High strength. Minimum printing process and reinforcement. Limited printing dimensions 5.4m*4.4m*5.4m	High strength. Slow process. Rough surface. Printing limited to the frame. Massive materials placement. Removal of unused materials.

Table 5. Similarities and differences of largescale AM process in construction industry**.** [S. Lim et al., 2012; Ma GuoWei et al., 2017; Barnett & Gosselin et al.,2015]

2.3.3 The challenges and limitations of 3-D printing in the construction industry

3-D printing is not a perfect solution that can solve all the problems in the construction industry. There are several challenges, such as the scale of the project and printing materials, which should be achieved in order for the 3-D printing technology to perform at its maximum potential. These challenges limit the use of 3-D printing in the construction industry. However, the improvement of technology minimizes the limits and as a result the applicability of 3-D printing expands accordingly.

The implementation of 3-D printing in construction industry processes requires much larger printers than those used for metal or plastic objects, due to the dimensions of the final objects to be printed. The size of 3-D printer greatly restricts the scale of building and objects it could print. So, the primary limitation of 3D printing technology is the size of the printer necessary to print the item [B. Berman et al., 2012; T. Campbell et al., 2011]. The current application of 3-D printing technologies in the construction industry is limited to construct structural components and low-rise buildings [T. Campbell et al., 2011; I. Gibson et al., 2002]. However, it is possible to print structural components piece-by-piece and then assemble them together as a real-scale building [F. Liang & Y. Liang et al., 2014]. With the development of new and more advanced 3-D printers, there have been a lot of large-scale models or buildings that were printed using large-scale 3-D printers. For example, KarmerMaker in the canal house project was 6 m tall and the 3-D printer used by WinSun had a dimension of 150 × 10 × 6.6 m [F. Liang & Y. Liang et al., 2014]. The design of proper largescale 3-D printers for cementitious material would undoubtedly improve and expand the applicability of 3-D printing. However, D-Shape is the first available particle-bed 3D printer for production of large-sized elements with a wide range dimensions up to 12 × 12 × 10 m [Dini Engineering S.R.L., 3-D Printers] and the VX4000 printer from Voxeljet which is capable of making sand casts as large as 4 × 2 × 1 m [Voxeljet].

In addition to the 3-D printer size, printing speed is another important limitation. The printing speed is a critical parameter as well, and can have an impact on the mechanical properties of the printed elements. In powder-based 3-D printing process, several factors will affect printing speed, such as the movement of the gantry system, velocity of the binder jetting in the printhead and velocity of the powder spreading [X. Ming & S. Jay et al., 2016]. The binder jetting process and powder spreading process are not in parallel and this nonsynchronous process has become the most critical issue that affects the printing speed in powder-based 3DP process. Designing a system which can make these two processes operate in parallel will improve the printing speed [X. Ming & S. Jay et al., 2016]. Layer thickness also plays an important role in printing time, with higher resolution requiring thinner layers and more printing time [S. Lim et al., 2011]. Printing speed must be set based on the rheology of the printed mortar, the dimensions of the objects and the dimensions of the extrusion head. Moreover, the time elapsed between the deposition of two layers (open-time) must be long enough to let the first layer adequately harden and become capable of sustaining the weight of the second layer, but short enough to guarantee that the first layer is still fresh enough to develop a good bond with the second layer [W. Timothy et al., 2016; A. Perrot et al., 2015; Le Thanh et al., 2012b].

Except of the size and speed of the 3-D printing, materials play a very important role in 3-D printing. The material should have satisfactory mechanical properties, sufficient bonding between layers to ensure structural integrity while constructing a homogenous structure and possess stability since no form work is used [Zareiyan & Khoshnevis et al., 2017]. Various materials, such as plaster and clay that used as printing materials sometimes perform low strength, large shrinkage and poor dimension stability, which prevent the technology from being used in large-scale models or buildings. Although plaster has been frequently used as printing material because it was commercially available, cheap, light in weight, and quick hardening, the material demonstrated low wet-strength and a larger than 3% shrinkage [B. Khoshnevis et al., 2001; S. Khoshnevis et al., 2001]. Similarly, although clay demonstrated a better wet-strength compared with plaster, the stability of the printed products has only been tested in small object sizes [B. Khoshnevis et al., 2001; S. Khoshnevis et al., 2001]. Traditional types of concrete are not the most convenient material for 3-D printing as a result of aggregate jamming in the nozzle, compacting issues, and the consistency to be placed layer-by-layer [Allouzi et al., 2019]. The low availability of high-strength printing materials also led to the speculation that 3-D printing might not be used in large-scale structures. However, various materials have been modified and proven to be effective as high-strength printing materials recently. The printed material should be effective with acceptable degree of some specific rheological properties such as pumpability, extrudability, buildability and with satisfactory mechanical properties such as high strength. Pumpability is the capacity to be worked and moved to the printing head through a pumping system throughout a given time interval [D. Asprone et al., 2018].

Extrudability is the capability to be extruded properly through the printing head with a continuous material flow and buildability is the capacity to both remain stacked in layers after extrusion and sustain the weight of the subsequent layers that are deposited by the printing process [D. Asprone et al., 2018]. Cementitious materials have been modified and proved to be effective printing materials with acceptable degree of pumpability, extrudability, buildability and high strength. The change of cementitious materials can be obtained by modifying the nanostructure through inclusion of nanomaterials into the cement matrix. The use of nanomaterials in structural engineering can enhance the durability, the mechanical, electrical and rheological properties of printed materials [Krystek & Górski et al., 2018].

Nanomaterials such as Al_2O_3, TiO_2, SiO_2, MgO, ZnO, silver nanoparticles, carbon nanotubes, or graphene may have improved in terms of hydration and porosity which is reflected on improving their mechanical properties. Implementation of reinforcement is a further challenge for 3-D printing, for manufacturing load bearing structures. Steel reinforcement integration into 3-D printed concrete structures is characterized by lower technological progress. Conventional reinforced concrete structure cannot be achieved by extruded cementitious materials. 3-D printed structures are brittle and weak in tension. Although fiber reinforcement can enhance the ductility and improve the brittleness of concrete materials, tensile behavior and crack controlling of reinforced structures still cannot be reached by fiber reinforced composite [Ma GuoWei et al., 2017]. Existing largescale 3-D printers concerned this issue. For example, Contour Crafting uses extra robotic arms to imbed steel reinforcements in the construction process and Concrete Printing creates some voids in the printed structures for the post inserting of steel bars to improve tensile capacity [S. Lim et al., 2012; Leach et al., 2012]. Another solution to this problem is the Mesh Mould approach which consists in digitally fabricating metal wires formworks that act as permanent reinforcement during the concreting process [W. Timothy et al., 2016].

Another issue that affects the implementation of 3-D printing in the construction industry is whether it could lead to cost increase or cost reduction, as the industry remains cost sensitive [M. Rajeh et al., 2015]. 3-D printing process is an automated process that centrally operates by computer, so the requirement of manpower is greatly reduced [R.A. Buswell et al., 2007]. For structures such as walls with the installation of electrical conduits, using 3-D printing technology could bring cost reduction in terms of optimized material usage and site work, thus leading to reduced likelihood of costly remedial works [Le Thanh et al., 2012a; Le Thanh et al., 2012b]. However, there are cases where the construction of a wall structure using 3-D printing technology was prohibitively expensive due to the use of current printing materials which were usually more expensive [R.A. Buswell et al., 2007]. The cost of 3-D printing should also include the cost of 3-D printers. Over the years the price of 3-D printers has been reduced significantly [S. Bradshaw et al., 2010]. 3-D printer needs certain software packages to edit and compile the source code in order to print the architectural models or largescale constructions. These software packages would increase the cost of the 3-D printing, thus restricting the scaling of the 3-D printing technology [J.M. Pearce et al., 2010]. In conclusion, although a short-term cost reduction can be observed by 3-D printing, there is the need to investigate the financial performance of the printed construction product or project over its life cycle.

Chapter III

Recycled construction materials for sustainability

3.1 Need for sustainable construction practices

The concept of sustainability is composed of three pillars which are economic, environmental and social (Fig. 38). As economy and population continue to expand, designers and builders face a unique challenge to meet demands for new and renovated facilities that are accessible, secure, healthy, and productive while minimizing their impact on the environment. Sustainable development (Fig. 38) requires that improvements in economic and social living conditions accord with the long-term process of securing the natural foundations of life [Alnaser N.W. et al., 2008].

Fig. 38 Sustainable development elements. [Sustainable development]

Sustainability is defined as the physical development and institutional operating practices that meet the needs of the current generation without compromising the ability of future generation to meet their needs, which implies a precautionary approach to those activities that effect the environment to prevent irreparable damage [A. D. Basiago et al., 1995]. Sustainability in terms of the environment implies a natural resource balance [S.-s. Chung & C. W. H. Lo et al., 2003]. For this reason, various research is becoming apparent into sustainable construction practices [S.-s. Chung & C. W. H. Lo et al., 2003]. Construction and demolition waste (C&D) have a large impact on the environment [M. Yeheyis et al., 2013; M. d. R. Merino et al., 2010; F. Yuan et al., 2011].

C&D waste constitute a major portion of total waste production in the world. Most of C&D waste being disposed of landfill space is quickly being depleted [V. Tam et al., 2008]. Besides depleting landfill space, natural resources are being consumed at an alarming rate for the production of new construction materials, rather than recycling and reusing existing materials [M. Behera et al., 2014].

Another important environmental issue is pollution from waste incinerators, furnaces for burning trash, garbage and ashes. These incinerators produce 210 different dioxin compounds plus mercury, cadmium, nitrous oxide, hydrogen chloride, sulfuric acid and fluorides [Bolden et al., 2013]. Additionally, waste incinerators generate more CO_2 emissions than coal, oil, or natural gas-fueled power plants. Therefore, replacing raw materials with recycled materials has become crucial for the sustainability of the construction industry. Knowing that the quantity of our current resources is at such a rate that the facility of future generations is endangered, it is clear that the conception of resource efficiency has gained huge significance in all over the world, especially in Europe. Europe is dependent on the rest of the world for many resources, such as fuel and raw materials, which are part of products imported from outside the European Union. The reduction of resources and the unpredictable product prices bring instability to the European economy. Therefore, in Europe the demand for conservation of the built environment has assumed a key role in city regeneration. The European Union promotes several strategies and polities to reuse the existing city in a sustainable way, limiting the extraction of natural resources and trying to enhance and regenerate the existing ones, through retrofitting or demolition and reconstruction operations [European Commission, 2016; European Commission, 2017; A Sustainable Europe by 2030]. These new policies to reuse the existing city in a sustainable way support the creation of a more circular organization that starts to reuse, recycle and regenerate the built environment. European policies intent to improve waste management, stimulate improvement and innovation in recycling, limit the use of landfilling and initiate change consumer behavior.

3.1.1 Linear and Circular Economy in build environment

The construction industry traditionally presents a Linear Economy model, based on “take, make dispose of” [Ellen MacArthur Foundation, 2015]. Considering the built environment, the phases that characterize the Linear Economy start from the extraction of raw materials from the environment, that are then processed to create new construction materials, often in ways that the new product cannot be disassembled, becoming obsolete at the end of life of the building, having to be disposed in landfills or incinerated, along with all the waste generated through the whole process [Mangialardo & Micelli et al., 2018; Cheshire et al., 2017; Ellen MacArthur Foundation, 2015]. In the future, the availability and price of products, resources and material will be rare and costly. Account should also be taken of the considerable costs of disposing of the waste and the environmental and economic damage from the high value of the materials that are wasted because they not being able to be disassembled. Consequently, Linear Economy model has become ever more unsustainable [Andersen M. S. et al., 2007; Bisello A. et al., 2017; Braungart & McDonough 2009; Cheshire et al., 2017; Ellen MacArthur Foundation, 2015]. On the contrary, Circular Economy model has been gaining attention in the last decades because of the better management of resources [Pomponi & Moncaster et al., 2017]. Ellen MacArthur Foundation defined Circular Economy as a regenerative system that aims to keep products, components, and materials in a closed loop at their highest utility and value at all times [Ellen MacArthur Foundation, 2015].

Another definition of Circular Economy described by Pomponi and Moncaster. They focused on the definition of Circular Economy for the Construction Industry and considered it as a building that is designed, planned, built, operated, maintained, and deconstructed in a manner consistent with Circular Economy principles [Pomponi & Moncaster et al., 2017]. As in the Linear Economy the Circular Economy model entails the extraction of the raw materials, and then these resources are used to manufacture new products which are consumed. The difference with the Linear Economy model is that the end of life building materials can be reused and their components and parts deconstructed, to act as material banks for new buildings, keeping the components and materials in a closed loop [Hopkinson et al., 2019]. C&D waste is kept in use, retaining its value and contributing to a substantial reduction in the extraction of raw materials. Optimization at the end of life building materials, such as by maintaining and reusing their durable components, constitutes the key to guaranteeing more flexibility [Addis & Schouten et al., 2004; Kohler & Yang et al., 2007]. This innovative economic model started with the recycling of high-value components in products that were consumed and thrown away once they stopped functioning. This circular model has now been strongly developed in the automotive sector or high-tech technologies, which contain in their products increasingly rare and precious components, and the extraction of which is highly polluting [McDonough et al., 2013; Sauvè et al., 2016].

The use of advanced materials and technologies such as automated maintenance systems or 3-D printing are examples of new methods and products to improve the quality and reduce the costs connected to the design and management of buildings and infrastructures. However, this model still needs development of knowledge and tools to have a larger adoption in the construction industry.

3.1.2 Principles of the Circular Economy in the Construction Industry

The principles of the Circular Economy in the construction industry can be summarized in a nested circle (Fig. 39). Fig. 39 shows a hierarchy for building approaches which maximizes use of existence materials. Diminishing returns are gained by moving through the hierarchy outwards, with the three inner circles being the most desirable [Cheshire et al., 2017; Mangialardo & Micelli et al., 2018].

The first circle which is the principle of retaining a building is the most resource-efficient and least invasive option. The second and third circle which are refitting and refurbishing the building respectively, are requiring more demanding interventions. After these circles, the more difficult operations involve reclaiming or remanufacturing principles. The last circle and the most difficult, is recycling/composting the building in order to create new products or return materials to the biosphere [Cheshire et al., 2017; Mangialardo & Micelli et al., 2018].

Common to these circles, there are five segments that represent the design principles to follow in each type of intervention. The first segment is the concept of building in layers. This concept distinguishes the various components that constitute a building and their different lifespans in order to recycle and replace them. To achieve that it is important that each component presents different rules that are independent of the others. Thus, layers make it possible to easily locate and replace something damaged, without affecting the nearby layers. As a result, building in layers helps to quickly recover the damaged components.

Therefore, it makes the building more flexible and adaptable than a building without this differentiation. The second segment is designing-out waste. This concept aims to help reduce, as far as possible consumption of raw materials at the stage of construction projects in order to optimize the resource efficient maintenance and repair. It means that repairing elements (refitting and refurbishment operations) are preferable to interventions such as demolition and reconstruction. This helps to significantly reduce the quantity of waste created during the construction process and maximize re-use of materials at the end. The third element is design for adaptability. The fundamental basis of the design for adaptability approach is that a product can be designed as a dynamic adaptable system, and as in all adaptable systems, control and feedback can be used to modify system performance [Kasarda et al., 2007]. In some cases, this process will involve remanufacture, and in other cases the utilization of self-healing materials and approaches such as a self-tightening bolt [Antonious et al., 2006].

The fourth principle is design for disassembly. In this concept building components can be reused at the end of their life. Once a building has been abandoned, elements can be disassembled and transferred elsewhere, acting as material banks and retaining their value for a longer time and becoming independent of the value of the original site. As a result, buildings are more flexible and easier to repair or reconfigure. The last principle to design through a Circular Economy model is selecting the correct materials. It is necessary to split the constituent elements that compose a building into biological (i.e. the eco materials) and technical materials (i.e. the elements that are more difficult to recycle). In this way, it is easier to distinguish those who are destined for the biosphere, for an industrial loop or to be recycled [Cheshire et al., 2017; Mangialardo & Micelli et al., 2018].

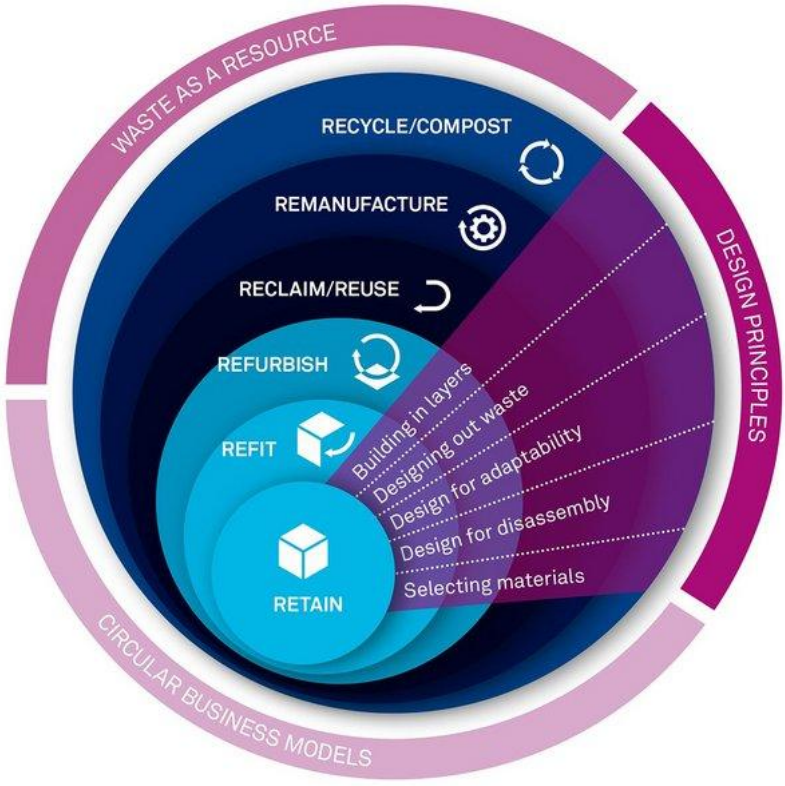

Fig. 39 Circular Economy hierarchy for building approaches in the construction industry. [Cheshire et al., 2017]

3.1.3 Economic benefits of the Circular Economy in the Construction Industry

The economic benefits of the Circular Economy model for the construction industry are shown in the Fig. 3 [Cheshire et al., 2017]. In this diagram (Fig. 40) the Linear and the Circular Economy approach in the construction industry are compared in terms of potential changes in revenues and costs associated with designing buildings with a long term, starting from the design to the end of life of the building. The costs and time associated with construction operations are almost the same in the two models. The difference starts when the building needs to be refitted, increasing the lifespan of the assets [Cheshire et al., 2017; Mangialardo & Micelli et al., 2018.]

In the Linear Economy, when the building becomes obsolete, it needs relevant refurbishment operations to become efficient again. However, the building continues to lose its economic value. As a result, the percentage of the rental yield associated with the cost of the investment continues to reduce until the demolition of the building. The demolition also involves the costs of remediation of the site and the disposal of waste materials. At this stage the asset often becomes a liability. In economic terms, the value of the site corresponds to the value of transformation [Cheshire et al., 2017; Mangialardo & Micelli et al., 2018].

In the Circular Economy building, the costs of refitting and adaptation are lower, and they require less time. The Circular Economy building is designed to be refit, adapted to new uses and disassembled at the end of its life. This approach gives more residual value on the asset with the potential to lower the depreciation rate. The potential of the circular economy applied in the construction industry totally changes the value chain linked to all stages of intervention in existing buildings, making the operations sustainable in social, environmental and economic terms, thus contributing to an increase in the residual value of the assets [Cheshire et al., 2017; Mangialardo & Micelli et al., 2018].

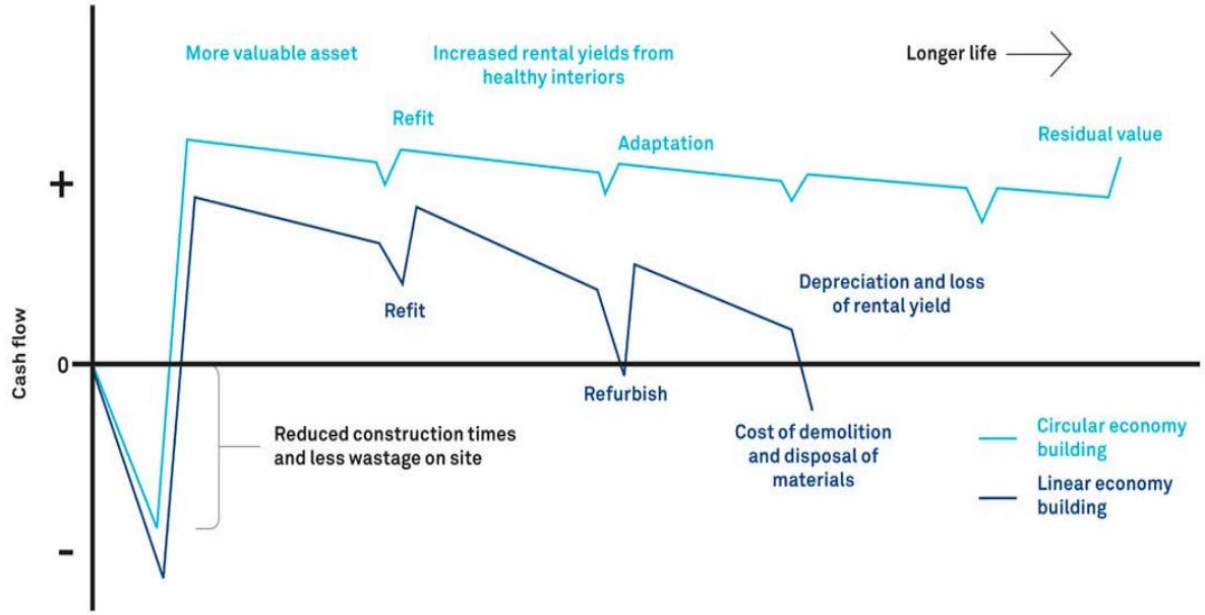

Fig. 40 Economic benefits of Linear and Circular Economy buildings. [Cheshire et al., 2017]

3.2 Recycled and waste materials

Construction industry consumes a large proportion of raw materials and accounts for a very large portion of waste to landfill spaces compared to other sectors of global economy [Knoeria et al., 2011]. One way to prevent the irreparable damage because of materials consumption and waste generation is to promote the use of recycled materials. The use of recycled materials has positive impact through different aspects, including the benefits in enhancing sustainability of the construction industry while reducing cost, providing solutions to environmental pollution and reducing the need for natural resources. Waste from different origins such as households, post-consumer waste generated from commercial, institution or industrial have become sources of various construction products [Oyedele et al., 2014]. Examples of such materials include newsprint for cellulose insulation, wallpaper, glass, rubber tires, asphalt road surfacing and plastic bottles for use as a lightweight geotechnical material [Bolden et al., 2013; Woolley et al., 1997; Graettinger et al., 2005]. More common in construction industry is recycled concrete aggregate and fly ash, which is powdery substance, produced as a result of combustion. Other materials include roof shingles cut-offs used as constituent of hot mix asphalt (HMA), granulated ground blast furnace slag (GGBFS) used as constituent of cement mix [El-Assaly & Ellis et al., 2001; Bolden et al., 2013], metal waste such as steel scrap and silica fume. Research is also focusing on more environmentally friendly solutions such as “green cement materials” in order to reduce consumption of natural resources and energy and pollution of the environment [Hameed & Sekar et al., 2009]. Moreover, materials deriving from industrial waste such as tire rubber [Valente & Sibai et al., 2019] or paper [Raut et al., 2011], can be added in partial replacement of the aggregates to optimize several physical properties of the product such as density, thermal insulation and sound insulation. The addition of chemical additives during preparation could confer specific rheological or functional properties to the product, such as self-sensing, self-compacting, self-healing, and self-cleaning [Ma GuoWei et al., 2017]. Potential methods for better sustainability is to replace the concrete contents with other materials such as fly ash or recycle the previously used concrete aggregate [Nithesh Nadarajah et al.,2018].

Tire Rubber

All vehicles on road uses tires made of rubber. During their use, the tread of tires gets consumed and then they are not fit for further use as they have lived their life. Ninety two percent of all end of life tires in Europe were collected and used in 2017 for either material recycling or energy recovery, according to a report from the European Tire & Rubber Manufacturers' Association [ETRMA et al., 2019]. Whole tires have been used in artificial reefs, break waters, dock bumpers, soil erosion control mats and playground equipment. By weight, some 1.96 million metric tons of scrap tires went to material recovery [ETRMA et al., 2019]. Several studies have shown that tire waste can be successfully used in concrete, grass turf, asphalt mix, embankments, stone cladding, flowable fill and clay composite [Bolden et al., 2013].

Glass aggregate

Glass is composed of silica, soda ash (sodium carbonate) and limestone to form a rigid physical state. Glass that ends up in the landfill won't break down for over a million years. Glass is a permanent material that can be endlessly recycled into new packaging, always maintaining its safety characteristics no matter how many times it's recycled [FEVE et al., 2019]. European Container Glass Federation [FEVE et al., 2019] show that the EU28 average collection for recycling rate for glass packaging grew to the record rate of 76 % in 2017.

Glass aggregate is a byproduct of recycled glass. Glass aggregate, also known as glass cullet, is 100 % crushed material that is generally angular, flat and elongated in shape. Foamed glass is made from glass cullet (Fig. 41). It has numerous applications, for example it is an ultralight extender, it improves the sound absorption, and its spherical shape has a positive effect on the workability of the mortar [Scarinci et al., 2006]. This additive is used for the production of lightweight building blocks with excellent thermal insulation and sound insulation due to their high porosity [Dachowski & Stepien et al., 2011]. Possible applications of glass foam blocks are in precast concrete panels, concrete bricks, piping insulation, storage vessel wall insulation, block paving but mainly floor and roof insulation [Scarinci et al., 2006].

Fig. 41 Foamed glass gravel. [Geocell]

Plastic

Plastics are nondegradable materials so it cannot be decomposed. After use most plastics are either thrown out at landfill spaces or incinerated, causing land and air pollution. Some plastics can be reused or recycled by converting them to granular form and then re-rolling them in the form of sheets. Uses of recycled plastics in the construction industry include plastic strips to add to soil embankments, which has positive results of increasing the measured strength in reinforcement of soils. Hot Mix Asphalt (HMA) mixture has a higher stability and reduced pavement deformation. Moreover, recycled plastics increase fatigue resistance and provide better adhesion between the asphalt and the aggregate [Awwad & Shbeeb et al., 2007].

Silica Fume

Silica fume (Fig. 42) is a byproduct of the reduction of high-purity quartz with carbonaceous materials like coal, in electric furnaces in the production of silicon and ferrosilicon alloys. Silica Fume is also collected as a byproduct in the production of other silicon alloys such as ferrochromium, ferromanganese, ferromagnesium, and calcium silicon. The environmental concerns necessitated the collection and use of silica fume in various applications to be mandatory.

Fig. 42 Silica in powder form. [ACV/GARDS]

Perhaps the most important use of this material is as mineral admixture in concrete to improve its properties like compressive strength, bond strength and abrasion resistance [Bolden et al., 2013]. Additionally, reduces permeability and therefore more durable and helps in protecting reinforcing steel from corrosion. These improvements stem from both the mechanical improvements resulting from addition of a very fine powder to the cement paste mix as well as from the pozzolanic reactions between the silica fume and free calcium hydroxide in the paste [Bolden et al., 2013]. Silica fume can be very useful in applications such as bridge deck overlays, water retaining structures, monumental structures and in high performance concrete for structural repairs.

Asphalt Roofing Shingles

Each year, the U.S. generates approximately 13.2 million tons of waste asphalt roofing shingles [ARMA et al., 2015]. This is an increase from the commonly cited figure of 11 million tons [NAHB et al., 1998], reflecting changes in housing stock and the housing market since 1998. In 2009, it was estimated that 702000 tons of reclaimed asphalt shingles (RAS) was utilized in asphalt mixtures. The use of RAS peaked in 2014 with 1964000 tons of RAS utilized. In 2017, the amount of RAS utilized in asphalt mixtures was estimated to be 944000 tons, which equates to a 34.5 % increase over 2009 usage, but a 52 % decrease from the peak RAS usage in 2014 [NAPA et al., 2019; FHWA et al., 2018; Williams et al., 2018].

Fig. 43 Asphalt Shingles before (left) and after (right) recycling. [J.N. Davis Roofing Co.]

Asphalt roofing shingles composition (Fig. 44) is asphalt cement, fiberglass or organic felt, fine aggregate or granules and mineral fillers such as limestone dolomite and silica. Some applications of RAS include to Hot Mix Asphalt (HMA), cold patch mix asphalt, aggregate substitute, base course, mineral filler and granular base stabilizer. The use of asphalt roofing shingles offers economic benefits, reducing the disposal costs for shingle scrap manufactures and reducing cost in the production of HMA. Moreover, using asphalt roofing shingles improves the rutting resistance of the mixtures considerably, due to a combination of the fibers and harder asphalt and improves resistance to pavement cracking.

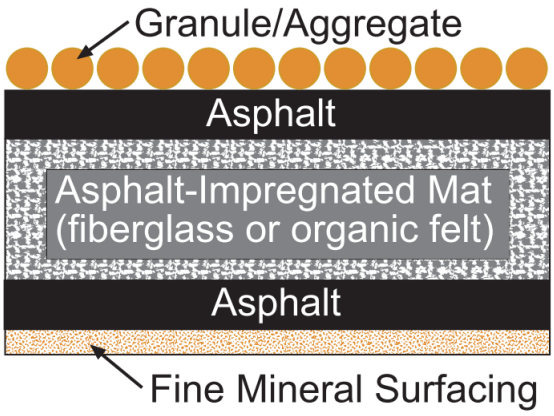

Fig. 44 Typical Asphalt Shingle Composition. [NAPA et al., 2019]

Fly ash

Fly ash is the byproduct of coal combustion in coal-fired power plants. Fly ash is a powdery substance laced with heavy metals such as arsenic, mercury and lead [Bolden et al., 2013]. Because of environmental concerns, fly ash is removed from flue gases by mechanical collectors and electrostatic precipitators before they are discharged into the atmosphere. The amount of carbon in fly ash affects its color. Gray to black represents increasing percentages of carbon, while tan color is indicative of lime and/or calcium content.

Some applications of fly ash include to cement and concrete products, structural fill and cover material, roadway and pavement utilization, infiltration barrier and underground void filling. Some of the technical benefits of fly ash use in concrete are the lower water demand for similar workability, reduced bleeding, increased durability, increased resistance to sulfate attack, reduced cracking at early age and lower evolution of heat. High-lime fly ash has permitted normal replacements of 25-40 and up to 75% of cement in concrete materials for parking lots, driveways and roads [Bolden et al., 2013].

Metals waste

Metals waste such as steel have good material properties including favorable frictional properties, high stability, and resistance to rutting. For the steel industry, using old steel products and other forms of ferrous scrap to produce new steel lowers a variety of steelmaking costs and reduces the amount of energy used in the process. Recycling steel scrap also saves landfill space and natural resources. By recycling one ton of steel, 2500 pounds of iron ore, 1400 pounds of coal and 120 pounds of limestone are conserved [SRI]. Steel scrap can be recycled into new steel to be used for any variety of new products. For example, such steel scrap and metals waste can be shredded in small elongated pieces and used in making Fiber Reinforced Concrete or SIFCON (Slurry infiltrated concrete) which is similar to Fiber Reinforced Concrete [Jagarapu & Prasad et al., 2019; Pilakoutas & Strube et al., 2001].

Blast furnace slag

Blast furnace slag (Fig. 45) is a byproduct from the manufacture of pig iron and steel. Blast furnace slag consists primarily of silicates, aluminates, silicates, and calcium-alumina-silicates. It's a valuable material with many uses in agriculture, environmental applications and in the construction industry. Crushed Air-Cooled Blast Furnace Slag (ACBFS aggregate) has significant material properties including favorable frictional properties, high stability, and resistance to stripping and rutting. It is used in concrete and asphalt mixes, fill material in embankments, road base material and as treatments for the improvement of soils. Ground Granulated Blast Furnace Slag (GGBFS) has a positive effect on the flexural and compressive strength of concrete [Bolden et al., 2013]. Expanded Blast Furnace Slag aggregate have higher porosity than ACBFS aggregate and low density allowing for good mechanical binding with hydraulic cement paste. Due to his suitable bulk density, particle size, porosity, water holding capacity and surface area, it can be used as an adsorbent [Bolden et al., 2013].

Fig. 45 Blast furnace slag aggregates. [Hwang-Hee & Chan-Gi et al., 2016]

Gypsum

It is possible to recycle gypsum from demolition gypsum waste and gypsum collected from recycling centers and renovation sites. The gypsum crusher crushes the gypsum into a fine gypsum powder and separates it from paper, insulation materials, steel rods, plastic, wood, cables, nails and screws for subsequent removal [ACA Industry]. The recycled gypsum powder makes up 100% of the gypsum waste recycled and can substitute virgin gypsum raw materials at the gypsum consuming industries [Plasterboard recycling]. Plasterboard recycling means that waste that would otherwise have been disposed of in landfills now is being recycled and turned into a gypsum powder that the plasterboard manufacturers can use when making new boards, reducing the need to acquire natural gypsum resources. Moreover, plasterboard waste in landfills under certain circumstances is known to cause hydrogen sulfite gasses, which potentially are lethal, and obviously by recycling plasterboard waste instead such dangerous situations can be avoided [Gypsum recycling International]. Another use of recycled gypsum, which is derived from gypsum waste plasterboard, is for ground improvement in different projects such as embankments and highways [Ahmed & Ugai et al., 2011].

Recycled Concrete Aggregate

It's predicted that aggregate production would have to increase to about 2.5 billion tons per year by the year 2020 [Gonzalez & Moo-Young et al., 2004]. This doesn't only induce economic strains but also posts grave environmental impact. Using recycled demolished concrete as an alternative aggregate for structural concrete is gaining popularity as a viable solution [Sarraz et al., 2017]. Crushed aggregate has been used as base course or granular base in highway construction. Its primary function is to increase the load capacity of the pavement and to distribute the applied load to avoid damage to the sub grade [Bolden et al., 2013]. Additionally, it can be used in making concrete. Such concrete can be used in dry lean concrete, curbs or block making.

3.2.1 Concrete recycling

In the present-day world CO_2 emissions has been a major factor for the global warming issue. Approximately 8% of the global CO_2 emissions are from manufacturing cement for industrial and commercial purposes [Andrew et al., 2019]. The huge quantity of products made of concrete in the construction industry due to its properties, make it the most consumed material worldwide and the second most consumed resource worldwide [Low M. et al., 2005].

Concrete recycling is becoming an increasingly popular way to utilize aggregates left behind when structures or roadways are demolished. Concrete recycling allows reuse of the aggregates for different fields of application such as road construction, pavements, foundation, substructure and structural concrete. Using recycled concrete aggregates promotes sustainability by reducing waste that may otherwise ended up in the landfill, conserving natural resources and reducing greenhouse gases emissions, energy consumption and production costs related to using natural aggregates [V. Tam et al., 2008; M. Behera et al., 2014; A. Shah et al., 2013].

How concrete is recycled

Recycled concrete aggregate is generally produced by two-stage procedure. Firstly, crushing of demolished concrete and secondly filtering, screening and removal of unwanted contaminants such as reinforcement, paper, wood, plastics and gypsum [Atik Sarraz et al., 2017; Shah & Pitroda et al., 2011]. Crushing and screening systems start with primary jaws, cones and/or large impactors taking aggregates with various dimensions depending on hardness and size of the material to be crushed and the characteristics of the system such as capacity [Shah & Pitroda et al., 2011]. For example, Sandvik CH440 cone crusher has a motor of 220KW, with nominal capacity of 50-388tonnes/hour and can handle feed sizes of 80-215mm [Sandvik]. Depending upon the project, the equipment used and the final product desired, there is the possibility of using a secondary cone or impactor and secondary screens. Subsequently a scalping screen will remove dirt and foreign particles. Next a fine harp deck screen will remove fine from coarse aggregates. The removal of unwanted contaminants can be done by water floatation, hand picking, air separators and electromagnetic separators, to ensure the recycled concrete product is free of dirt, clay, wood, plastic and organic materials [Shah & Pitroda et al., 2011].

Concrete crushing plants

Depending on the needs of the user, the concrete crushing plant might be available in stationary, mobile and portable configurations. Stationary concrete plants are systems that are permanently fixed to the ground (Fig. 46). Mobile crushing plants can be moved to various locations economically [Shah & Pitroda et al., 2011]. They have their own onboard drive system (Fig. 47a). They are typically track driven allowing superior on-site mobility where several moves are required [Shah & Pitroda et al., 2011]. Portable crushing plants are mounted on rubber-tired chassis and towed to the site by truck (Fig. 48a). On site, they are moved by loaders or tugs [Shah & Pitroda et al., 2011]. This type of crusher is typically used in a recycling yard where all material is trucked on the site [Shah & Pitroda et al., 2011].

Fig. 46 Stationary crusher plant. [Fabo-Stationary]

Types of crushers

Crushers are machines used to reduce the size of rocks and stones in aggregates production, construction material recycling applications, and in mining operations. Crushers can be classified into two main categories [Neikov et al., 2019]. The first category is compressive crushers that press the material until it breaks and the second one is impact crushers that use the principle of quick impacts to crush the material. There are three main types of crushers. The first two are Jaw and cone crushers, which operate according to the compression principle. The third type is impact crushers, which utilize the impact principle [Neikov et al., 2019]. All of the below crusher types are available in portable, mobile and stationary configurations.

Jaw crushers compress the concrete between a stationary and moveable plate in order to crush it (Fig. 47b). The moving jaw is mounted on a pitman that has a reciprocating motion, and the fixed jaw stays put. When the material runs between the two jaws, the jaws compress larger boulders into smaller pieces [Shah & Pitroda et al., 2011].

(a)

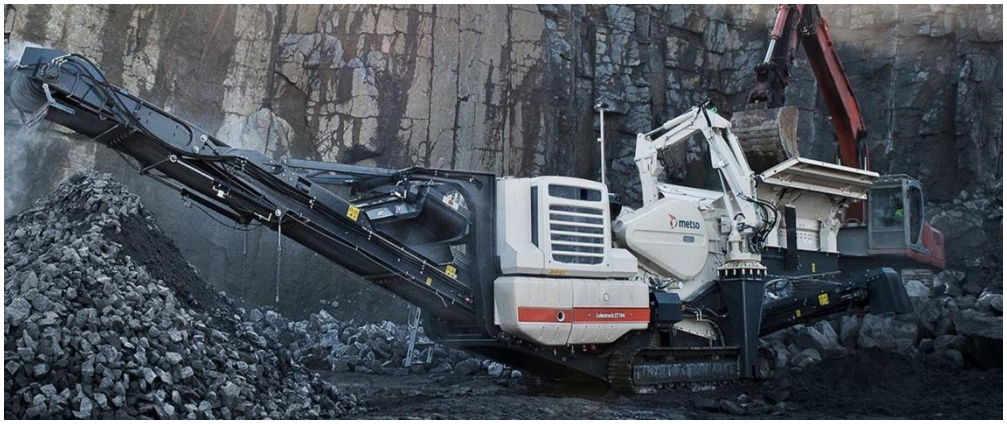

(b)

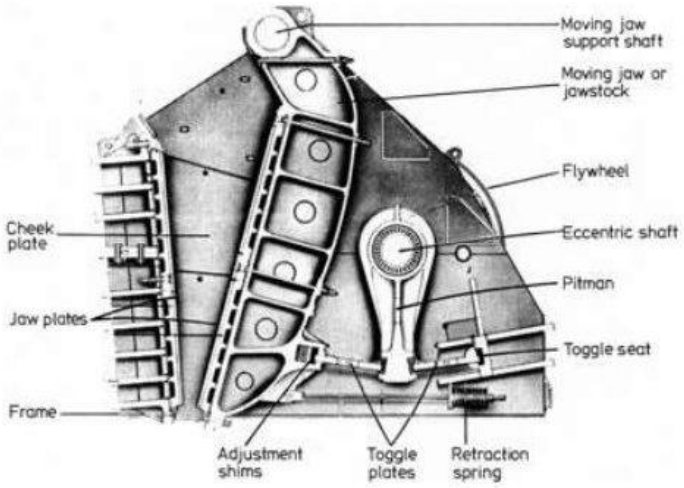

Fig. 47 (a) Mobile jaw crusher plant and (b) jaw crusher mechanism. [Metso-Mobile; CPC Equipment]

Cone crushers reduce the material size in a crushing cavity by continuous compression between two cone-shaped plates, a fixed element (bowl liner) and a moving element (cone mantle) [A. Jankovic et al., 2015]. The fragmentation of the material results from the continuous compression that takes place between the liners around the chamber [A. Jankovic et al., 2015]. An additional crushing effect occurs between the compressed particles, resulting in less wear of the liners [A. Jankovic et al., 2015]. Cone crushers are very suitable for size reduction and shaping in the downstream of a crushing circuit, so they are used mostly as secondary crushers [Shah & Pitroda et al., 2011].

(a)

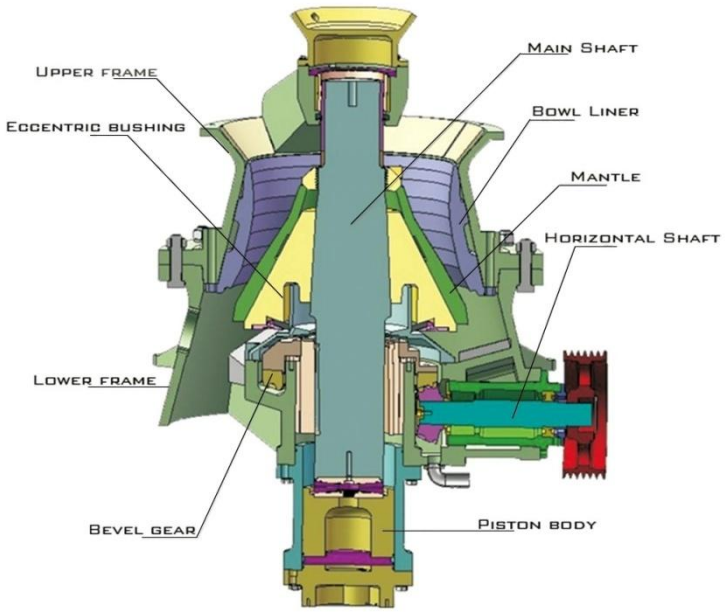

(b)

Fig. 48 (a) Portable cone crusher plant and (b) cone crusher mechanism. [Metso-Portable; CLMM]

Impact crushers, or impactors have a spinning rotor with bars or hammers that accelerates the feed material to high speed and then flings it into a solid plate, several plates, or rods and each other (Fig. 49). Impactors can be used as primary, secondary, and even tertiary crushers and produce [Shah & Pitroda et al., 2011]. These collisions cause the material to break down to smaller sizes. Impactors are generally divided into two main types. The conventional type has horizontal shaft configuration and for that reason it is known as a horizontal shaft impact (HIS) crusher (Fig. 50a). The other type has a centrifugal crusher with vertical shaft, and it is called a vertical shaft impact (VSI) crusher (Fig. 50b).

Fig. 49 Mobile vertical shaft impact (VSI) crusher plant. [Metso-Impact]

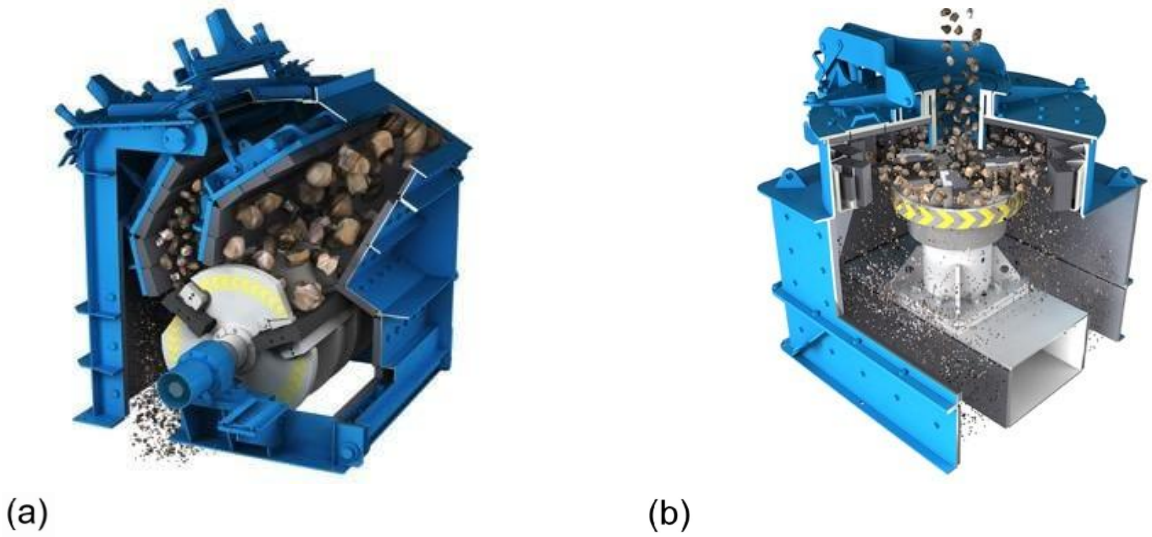

Fig. 50 (a) Horizontal shaft impact (HIS) crusher and (b) vertical shaft impact (VSI) crusher. [Stedman Machine Company]

3.2.2 Applications for recycled aggregate

Recycled aggregate is generally used as bulk backfill in sub-base, base or surface material in road construction, lean concrete bases, hydraulically bound materials and in the manufacture of new concrete [J. de Brito & N. Saikia et al., 2013; Hansen & Narud et al., 1983]. The most common use of recycled aggregate encountered was its reuse as an aggregate base. Recycled aggregate can be used as replacement material for virgin aggregate in the construction of base layers [Bakoss & Ravindrarajah et al., 1999; Herrador et al., 2012], showing similar geo-mechanical and physical performance to conventional graded base material [Haider et al., 2014; Kolay & Akentuna et al., 2014].

The properties of recycled aggregate greatly influence the performance of unbound granular pavement layers [Aqil et al., 2005; Barbudo et al., 2012; Gokce et al., 2011; Vegas et al., 2011]. The quality of recycled construction products remains a big subject of controversial literatures. Some studies claim that the quality of concrete reduces with increasing recycled concrete aggregate [Mefteh et al., 2013; Etxeberria et al., 2007]. The main problems identified in pavements are fatigue cracking, rutting, depressions and frost- related heaving, which can result from the poor performance of the unbound base and sub-base layers. Other studies argue that the quality of concrete remains unaffected as a result of recycled aggregate [Yang et al., 2011; Thomas et al., 2013; Nassar & Soroushian et al., 2016]. For example, Nassar and Soroushian investigated the field performance of recycled concrete aggregate in pavement construction subjected to heavy traffic loads under aggressive weather conditions [Nassar & Soroushian et al., 2016]. They showed that the recycled concrete aggregate performs similar or even better than the control concrete. So recycled concrete aggregate is suitable for use in concrete based infrastructure such as pavement construction.

Moreover, recycled aggregate can be used to make light weight concrete molds using 3-D printing process. The recycled concrete can be also used in powder-based binder jetting 3-D printing method for reducing the amount of cement used for construction activities. The recycled concrete can be used as a replacement for fine aggregates in few quantities [Nithesh Nadarajah et al., 2018]. Since the molds are made of recycled aggregates and 3-D printer uses few amounts of recycled aggregates, it costs less to 3-D print them and they can be destroyed and used for other construction purposed once their lifetime is over [Nithesh Nadarajah et al., 2018].

Chapter IV

Experimental Procedure

Methodology

In this chapter, the experimental procedure and methodology of the Master thesis will be presented. For this thesis TiO_2 was selected, because of its high photocatalytic activity, the high stability and the low cost. Titanium dioxide nanoparticles with self-cleaning properties can be used as coatings on building blocks or pavements, but also on interior decorative items such as ceiling panels, curtains and wallpapers. Therefore, both these scenarios were studied, firstly as coating on 3-D printed panels and then as coating on fabrics.

The specific characteristics of nanomaterials were studied under different techniques. The characterization techniques used were, X-Ray Diffraction (XRD) and BET (Brunauer, Emmett and Teller). Metal doping has proved to be a successful approach for enhancing the visible light absorption by photocatalysts and to hinder electron–hole recombination. By shifting the optical response towards higher wavelengths, the photoactivity under visible irradiation is increasing. This shifting may allow using sunlight (44% visible and 3% UV light) as an inexpensive and renewable energy source in photocatalytic applications. Besides optical absorption, other parameters that affect the photocatalytic activity, such as surface area, size and defects, can also be modified by metal doping.

The decolorization of coatings on 3-D printed panels and fabrics was then studied under different techniques and methods due to the specific availability of the instrumentations. For eliminating errors in all the decolorization experiments, a reference -blank sample was constantly examined simultaneously for a good comparison between the tested samples.

4.1 Synthesis and Characterization Techniques

4.1.1 Microwave oven synthesized undoped and doped TiO_2 nanoparticles

In this section, the synthesis and characterization techniques used for the fabrication of bulk nanomaterials are being presented.

Synthesis

Undoped and In-Ni-, Mn-In, Mn-Cu-, Mn-Ni- bimetallic doped TiO_2 nanostructures were synthesized using the microwave-assisted hydrothermal method. Solution (0.1 M) of Titanium (IV) oxysulfate-sulfuric acid hydrate (99.95% trace metals basis, Sigma Aldrich), was dissolved into 250 mL of distilled water and were mixed under fast stirring for 45 min. The obtained solution was transferred into four Teflon vessels and irradiated in an advanced flexible microwave synthesis platform (Milestone flexiWAVE), using the high-pressure setup at 120 °C for 30 min (max 1500 Watt). When the reaction was finished and cooled to room temperature, the precipitate was collected, centrifuged (1000 rpm for 2 min) and washed several times with ethanol and distilled water.

In-Ni-, Mn-In-, Mn-Cu-, and Mn-Ni- doped TiO_2 nanostructures were prepared following the same experimental procedure used to prepare undoped TiO_2 by also adding into the precursor solution, 0.25 at. % of indium (III) nitrate hydrate ($In(NO_3)_3 \cdot H_2O$, 99.9% Sigma-Aldrich) with nickel (II) nitrate hexahydrate (Ni(NO3)2 · 6H2O, ≥97.0%, Honeywell Fluka™), manganese (II) nitrate tetrahydrate ($Mn(NO_3)_2 \cdot 4H_2O$, ≥97.0% , Honeywell Fluka™) with indium (III) nitrate hydrate , manganese (II) nitrate tetrahydrate with copper (II) nitrate trihydrate ($Cu(NO_3)_2 \cdot 3H_2O$, 99-104%, Honeywell Fluka™) and manganese (II) nitrate tetrahydrate with nickel (II) nitrate hexahydrate, respectively.

In all cases the microwave was programmed with a first temperature ramp where the target temperature was reached after 15 min. All products were kept at room temperature overnight and totally dried using an oven at 100 ℃ for 1 hour.

Fig. 51 Milestone flexiWAVE microwave oven. [Milestone]

Sample	Description	Concentration	Microwave Oven	Magnetic Stirring
1	Titanium Dioxide, undoped	[0.1 M]	1500W 120°C 30 min	45 min
2	Titanium Dioxide, doped Indium and Nickel	[0.1 M], doped 0.25 at. %		
3	Titanium Dioxide, doped Manganese and Indium			
4	Titanium Dioxide, doped Manganese and Copper			
5	Titanium Dioxide, doped Manganese and Nickel			

Table 6. Synthesis method of nanomaterials.

Characterization Techniques

Their crystallographic structure was examined using a Siemens D5000, X-ray diffractometer, equipped with a Cu-Kα (λ = 0.15405 nm) monochromatic radiation source. The specific surface area of the samples was examined by nitrogen (N_2) physisorption using a Micromeritics' Gemini VII 2390 Surface Area Analyzer. The samples were prior degassed at 100°C for 2 hours under continuous nitrogen gas flow using a Micromeritics' FlowPrep 060, in order to remove moisture.

Fig. 52 Siemens D5000, X-ray diffractometer. [LabX]

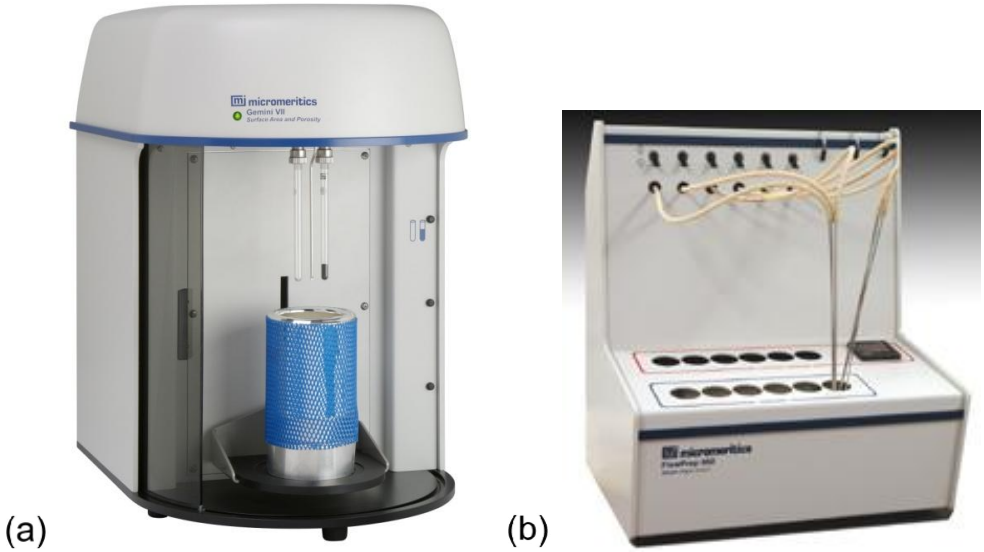

Fig. 53 (a) Micromeritics' Gemini VII 2390 Surface Area Analyzer and (b) Micromeritics' FlowPrep 060. [Micromeritics; FlowPrep]

4.1.2 Synthesis of panels and fabrics

In this section, the synthesis of 3-D printed panels and fabrics are being presented.

Synthesis

A mix of equal amounts of recycled concrete aggregate and recycled gypsum powder, supplied by ATTICA RECYCLING CD & EW SA, was used for the 3-D printing of panels (Fig. 55a). The dimensions of each panel were 5 x 5 x 1 cm and printed with a Z Corporation 3-D printer (ZPrinter 310 Plus). The composition of recycled concrete aggregate during 3-D printing varies. This problem solved by 3-D printing simultaneously a pair of panels, one panel as reference (blank) and one with the nanocoating.

Fig. 54 The ZPrinter 310 Plus (Left) and the ZD5 Powder Recycling Unit (Right).

While the synthesis of fabrics is 98% cotton and 2% viscose, with a grey color (Fig. 55b). The dimensions of each fabric sample were 7 x 7 cm. The fabric mass per unit area was 125 gram per square meter.

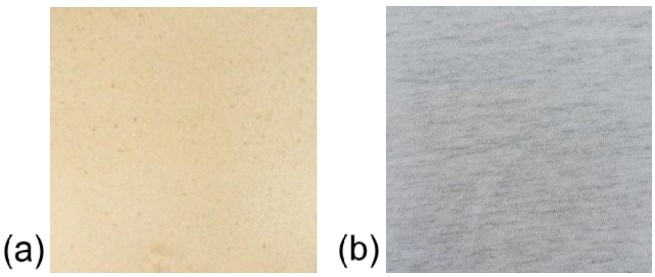

Fig. 55 (a) Initial state of 3-D printed panels and (b) fabric samples.

4.2 Decolorization experiments

Decolorization of applied coatings was evaluated by the use of a self-made apparatus for the test of the decolorization effect of Methylene Blue (MB). Degradation of pollutant was assessed by a colorimetric method and by a Varian CARY-5000 DRA 2500 UV-VIS-NIR Spectrophotometer (Fig.56). The color analysis was performed using the CIELAB model. Unlike RGB and CMYK color models, color definitions characterized by CIE systems are unambiguous, absolute, and device independent. For example, a CIE system isn't tied to, influenced by or dependent on the characteristics or capabilities of any color capturing or rendering device [Sappi]. CIE L*a*b* (CIELAB) is the most complete color space specified by the International Commission on Illumination. It describes all the colors visible to the human eye [Bianchi et al., 2013].

The three coordinates (L*, a*, b*) determine the CIELAB components are (Fig. 55):

a*: red/magenta and green

b*: blue and yellow

L*: black/white (luminance/brightness).

The lightness, L*, represents the darkest black at L*=0 and the brightest white at L*=100. The color channels, a* and b*, represent true neutral gray values at a*=0 and b*=0. The red/green opponent colors are represented along the a* axis, with green at negative a* values and red at positive a* values. The yellow/blue opponent colors are represented along the b* axis, with blue at negative b* values and yellow at positive b* values.

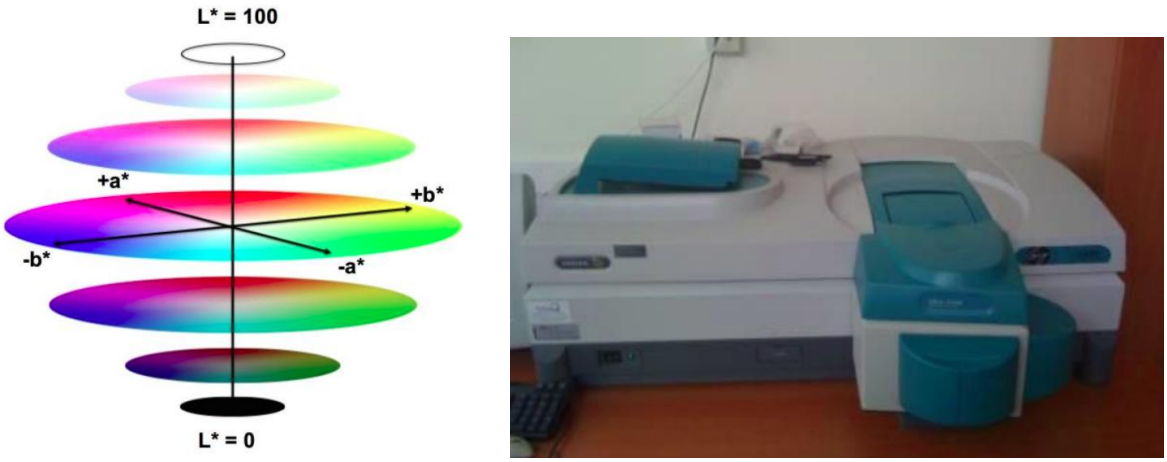

Fig. 56 Color coordinates of CIELAB model and Varian CARY-5000 DRA 2500 UV-VIS-NIR Spectrophotometer. [Sappi]

The color difference is expressed as delta E (ΔE) and is calculated by comparing reference and sample L*a*b* coordinate values.

The color difference (ΔE) is calculated by the Eq.1:

$$\Delta E = [(\Delta a)^2 + (\Delta b)^2 + (\Delta L)^2]^{½} \qquad \text{(Eq. 1)}$$

where Δa, Δb, ΔL were the differences of coordinates a*, b*, and L* before irradiation and at the specific time of irradiation.

MB is a thiazine dye often used as standard to evaluate the decolorization. Solar radiation exposure changes the dye color intensity and can be used as an indicator of the efficiency of sample's photocatalytic capacity with respect to sample's configuration. The sample with the greatest dye decolorization would indicate the sample with the greatest photocatalytic efficiency for self-cleaning performance and air pollution removal.

4.2.1 3-D printed panels

The 3-D printed panels were separated into five pairs of panels and each one consists of the nanocoated panel and its reference (blank) panel (Table 7). Each nanocoated panel was covered with 0.1 gram of a photocatalytic nanomaterial as slurry, which was left to dry. To evaluate the color change in dye on the surface of 3-D printed panels following exposure to UV light, the panels were dip-coated with a MB solution. The exposure to UV light was held into a handmade photocatalytic apparatus (Fig. 57). The apparatus consists of a wooden box, which is equipped with two Prinz UV Test lamps (4W, UV-A 366 nm) and a base for supporting the pair of panels. The horizontal distance of the panels with the lamps was 3 cm, the height of the base was 3.5 cm while the distance between lamps was 4 cm and between panels 2 cm. The decolorization of the MB dye applied to the surfaces of the panels was monitored by the use of chromatic measurements before UV irradiation and after 1 and 2 hours of exposure.

Fig. 57 Handmade photocatalytic apparatus.

Sample	Nanomaterial	Coating
TiOP	Titanium Dioxide, undoped	0,004 gr/cm^2 as slurry
Ref1	Reference of TiOP	Blank
MnInP	Titanium Dioxide, doped Manganese and Indium	0,004 gr/cm^2 as slurry
Ref2	Reference of MnInP	Blank
MnNiP	Titanium Dioxide, doped Manganese and Nickel	0,004 gr/cm^2 as slurry
Ref3	Reference of MnNiP	Blank
InNiP	Titanium Dioxide, doped Indium and Nickel	0,004 gr/cm^2 as slurry
Ref4	Reference of InNiP	Blank
MnCuP	Titanium Dioxide, doped Manganese and Copper	0,004 gr/cm^2 as slurry
Ref5	Reference of MnCuP	Blank

Table 7. 3-D printed panel samples and the method of coating.

4.2.2 Fabrics

For the decolorization of applied coatings on fabric six samples were used, one for each nanomaterial and one blank as reference (Table 8). Each nanocoated fabric sample was covered with 4 wt. % of a photocatalytic nanomaterial as slurry, then pressed with a roller and left to dry. Next the fabrics were dip-coated with a MB solution and left to dry under indirect sunlight for a day. The decolorization of the MB dye applied to the surfaces of the fabrics was monitored by the use of chromatic measurements before and after the exposure to indirect sunlight. After that the samples were exposed to UV irradiation. For this purpose, the initial photocatalytic apparatus was modified. The base was replaced by a thread and three hooks to hold each fabric sample in its place (Fig. 58). The horizontal distance of the fabrics with the lamps was 4 cm, lamps and fabric samples were respectively 8 cm and 12 cm above the surface of the box, while the distance between lamps was 12 cm and between fabrics 8 cm. The decolorization of the MB dye applied to the surfaces of the fabrics was monitored by a Cary 5000 UV-VIS-NIR spectrophotometer before UV irradiation and after 1 and 2 hours of exposure.

Fig. 58 Handmade photocatalytic apparatus for the case of fabrics.

Sample	Nanomaterial	Coating
Ref	Reference	Blank
TiOF	Titanium Dioxide, undoped	4 wt. % as slurry
InNiF	Titanium Dioxide, doped Indium and Nickel	
MnInF	Titanium Dioxide, doped Manganese and Indium	
MnCuF	Titanium Dioxide, doped Manganese and Copper	
MnNiF	Titanium Dioxide, doped Manganese and Nickel	

Table 8. Fabric samples and the method of coating.

Chapter V

Characterization Results

5.1 TiO_2 characterization results

5.1.1 XRD analysis of doped and undoped TiO_2 nanostructures

The XRD patterns for undoped and doped TiO_2 nanoparticles are shown to Figure 59. These samples only exhibited patterns assigned to the TiO_2 anatase phase (JCPDS file card No.-01-071-1166). No signal from the crystalline phase containing metal or metal oxide of the doping elements could be observed. Furthermore, careful analyses of the main peak (101) of the XRD patterns (Fig. 59, inset) indicated a slight shift to the higher angle side for Mn-In doped TiO_2, Mn-Cu doped TiO_2, In-Ni doped TiO_2 and mainly for Mn-Ni doped TiO_2 nanoparticles.

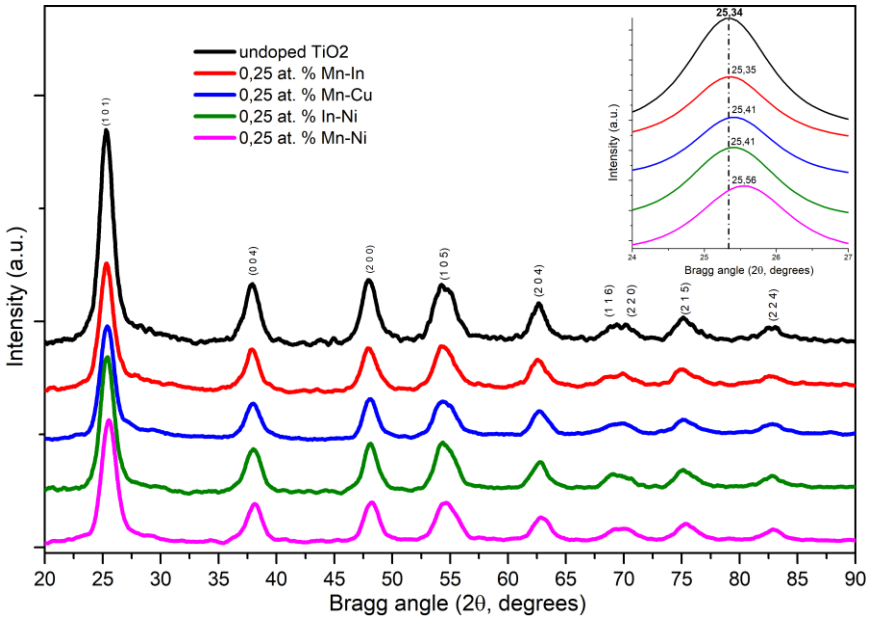

Fig. 59 X-Ray Diffraction (XRD) patterns of undoped and doped TiO_2. The inset shows the peak (101) of doped and undoped TiO_2.

By comparing the ionic radius values [Rohrer et al., 2001; Pauling et al., 1960; Francis Galasso et al., 1970; D. Papadaki et al., 2019] of Ti^{+4} (0.68 Å) to that of In^{+3} (0.81 Å), Mn^{+2} (0.80 Å), Ni^{+2} (0.72 Å) and Cu^{+2} (0.73 Å), we hypothesize that some of the doping elements were incorporated into the structures of TiO_2 and replaced the titanium ions, which induced a perturbation in anatase crystal structure.

Replacement of Ti^{+4} by In^{+3}, Mn^{+2}, Ni^{+2} and Cu^{+2} dopant ions may cause expansion/compression of the unit cell resulting to variation in various parameters including micro-strain due to lattice mismatch and distortion. The increase in micro-strain can be explained by the dopant substitution on the oxygen sites of TiO_2 surface.

The lattice constants a, b and c have been calculated (Table 9) from the XRD patterns using the following equation [Wilso et al., 2006]:

$$\frac{1}{d^2} = \frac{(h^2+k^2)}{a^2} + \frac{l^2}{c^2}, \quad \text{(Eq. 2)}$$

where d (calculated from $\lambda = 2d\sin\theta$) denotes the interplanar distance and h, k, l show the miller indices.

Crystallite size of each nanomaterial was calculated by two methods, the modified Scherrer equation and the Halder-Wagner (H-W) Method. In both methods the crystallite sizes are increasing in the order of In-NI, Mn-In, Mn-Ni and Mn-Cu (Table 9).

A) Modified Scherrer equation

Modified Scherrer equation estimates crystallite size (D) more accurately then the formal Scherrer equation. Modified Scherrer equation is based on the fact that we must decrease the errors and obtain the average value of crystallite size (D) though all the peaks (or any number of selected peaks) by using least squares method to mathematically decrease the source of errors.

Scherrer equation is given by:

$$\beta = \frac{K\cdot\lambda}{D\cdot\cos\theta} = \frac{K\cdot\lambda}{D}\cdot\frac{1}{\cos\theta}, \quad \text{(Eq. 3)}$$

where D is the average crystallite size, λ is the wavelength of the incident X-ray beam (1.5405 Å), θ is the Bragg diffraction angle, K is the shape factor (Scherrer constant) usually taken as 0.9 and β is the peak width at half width maximum (FWHM).

Now by making logarithm on both sides:

$$ln\beta = ln\frac{K\cdot\lambda}{D\cdot cos\theta} = ln\frac{K\cdot\lambda}{D} + ln\frac{1}{cos\theta}, \quad \text{(Eq. 4)}$$

Equation 4 is known as modified Scherrer equation. If we plot the results of lnβ against ln(1/cosθ), then a straight line with a slope of around one and an intercept of about ln(Kλ/D) must be obtained. Theoretically this straight line must be with a slope of 45° since tan45° = 1. But, since errors are associated with experimental data, the least squares method gives the best slope and most accurate ln(Kλ/D) [Monshi et al., 2012].

After getting the intercept, then the exponential of the intercept is obtained and finally calculate the crystallite size D:

$$y_{intercept} = \ln\frac{K\cdot\lambda}{D} \rightarrow e^{y_{intercept}} = e^{\ln\frac{K\cdot\lambda}{D}} = \frac{K\cdot\lambda}{D} \rightarrow D = \frac{K\cdot\lambda}{e^{y_{intercept}}}, \quad \text{(Eq. 5)}$$

Figure 60 indicates five plots of lnβ vs. ln(1/cosθ) for each nanomaterial, together with the equations of linear least squares method obtained from linear regression of data. The modified Scherrer equation can provide the advantage of decreasing the sum of absolute values of errors, $\Sigma\ (\pm\Delta\ln\beta)^2$ and producing a single line through the points to give a single value of intercept ln(Kλ/L) [Monshi et al., 2012]. As observed from Table 9, the average crystallite size increased from 5.69 to 5.96, 6.16, 6.21 and 6.29 with In-Ni, Mn-In, Mn-Ni and Mn-Cu doping, respectively.

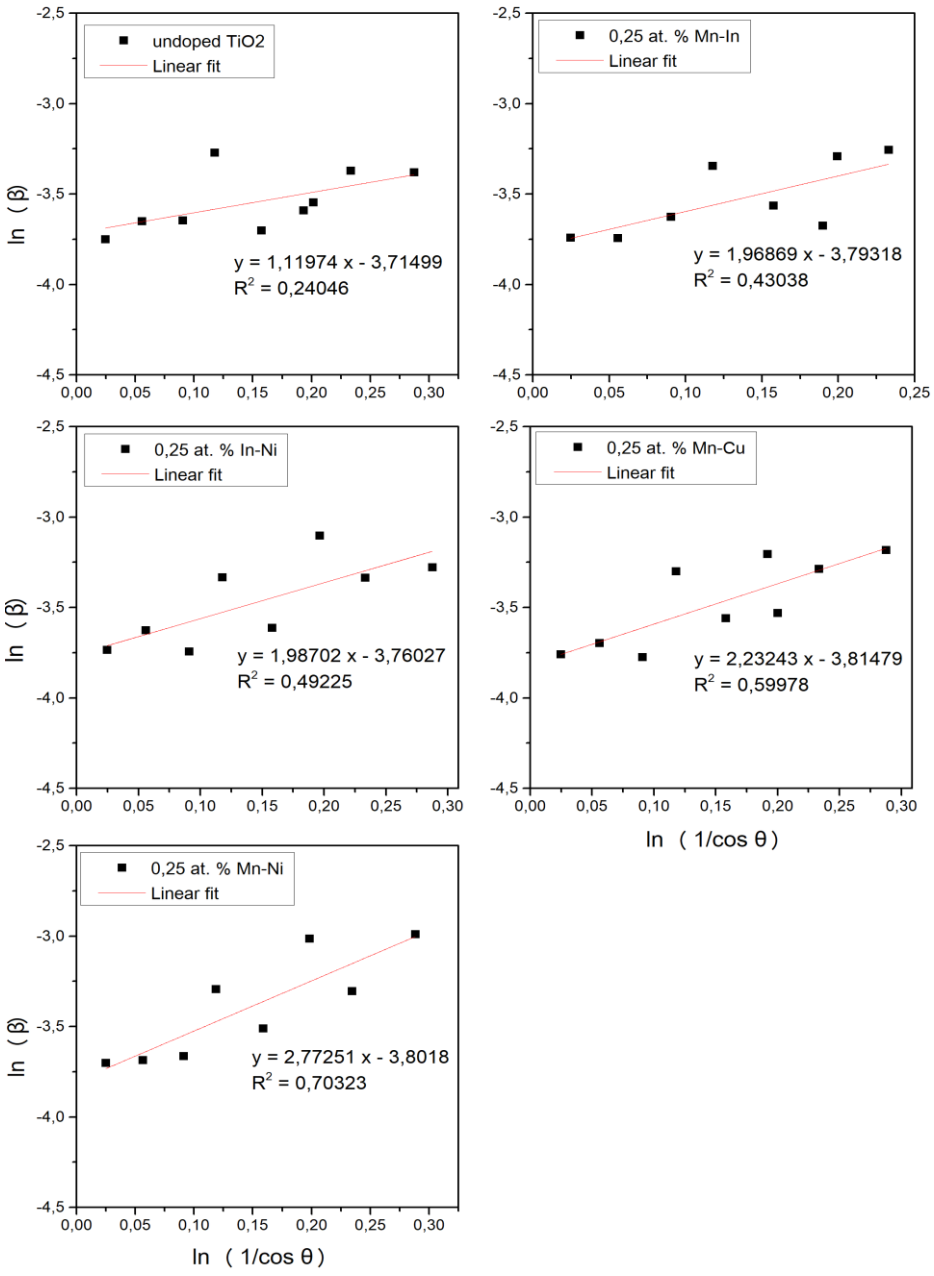

Fig. 60 Five plots of lnβ vs. ln(1/cosθ) for each nanomaterial, together with the equations of linear least squares method obtained from linear regression of data.

B) Halder–Wagner (H-W) method

In fact, XRD peak is neither Lorentzian function nor Gaussian function, as XRD peak region matches well with the Gaussian function, whereas its tail falls off too rapidly without matching and on the other hand, tails of the profile fits quite well with Lorentz function, but that fails to match the XRD peak region [Halder & Wagner et al., 1966; Hepp & Baerlocher et al., 1988; Nath et al., 2019]. The solution to this problem is the Halder-Wagner method. This method is based on the assumption that peak broadening is a symmetric Voigt function, as it is a convolution of Lorentzian function and Gaussian function [Halder & Wagner et al., 1966; Balzar & Ledbetter et al., 1993; Langford et al., 1992]. This method has the advantage that data for reflections at low and mid-angles are given more weight than those at higher angles where the precision is often lower, because the overlapping of the higher diffracting peaks is greater.

Equation 6 gives the full width at half maximum of the physical profile as per Halder-Wagner Method.

$$\beta_{hkl}^2 = \beta_L \cdot \beta_{hkl} + \beta_G^2 , \quad \text{(Eq. 6)}$$

where, β_L and β_G are the full width at half maximum of the Lorentzian and Gaussian function.

The crystallite size D, and the micro-strain ε, are related to β^* by the following expression [Halder & Wagner et al., 1966]:

$$\left(\frac{\beta_{hkl}^*}{d_{hkl}^*}\right)^2 = \frac{K}{D} \cdot \frac{\beta_{hkl}^*}{{d_{hkl}^*}^2} + (2 \cdot \varepsilon)^2 , \quad \text{(Eq. 7)}$$

where $\beta_{hkl}^* = \beta_{hkl} \frac{\cos\theta}{\lambda}$, (Eq. 8) and $d_{hkl}^* = 2 \cdot d_{hkl} \cdot \frac{\sin\theta}{\lambda}$, (Eq. 9)

Equation 8 and 9 are substituted in the Equation 7 and the resulting expression is:

$$\left(\frac{\beta_{tot} \cdot \cos\theta}{\sin\theta}\right)^2 = \frac{K \cdot \lambda}{D} \cdot \frac{\beta_{tot} \cdot \cos\theta}{\sin^2\theta} + 16 \cdot \varepsilon^2, \quad \text{(Eq. 10)}$$

So, from equation 10 plotting with $(\beta_{hkl}/\tan\theta)^2$ term along X-axis and $(\beta_{hkl}/ \tan\theta \sin\theta)$ along Y-axis for each peak of the XRD pattern, we can calculate the crystallite size D, and the micro-strain ε (Fig.61). From linear fitted data to the plot, y-intercept gives the mean value of the micro-strain ($16\varepsilon^2$) and the slope gives the crystallite size (Kλ/D) [Halder & Wagner et al., 1966; Kibasomba et al., 2018; Izumi Fujio & Takuji Ikeda et al., 2014]. As observed from Table 9 the micro-strain increased from 0.41 to 0.54, 0.62, 0.62, 0.78 with Mn-In, Mn-Cu, In-Ni and Mn-Ni doping, respectively. The average crystallite size calculated with this method increased from 6.02 to 6.21, 6.24, 6.32 and 6.40 with In-Ni, Mn-In, Mn-Ni and Mn-Cu doping, respectively (Table 9).

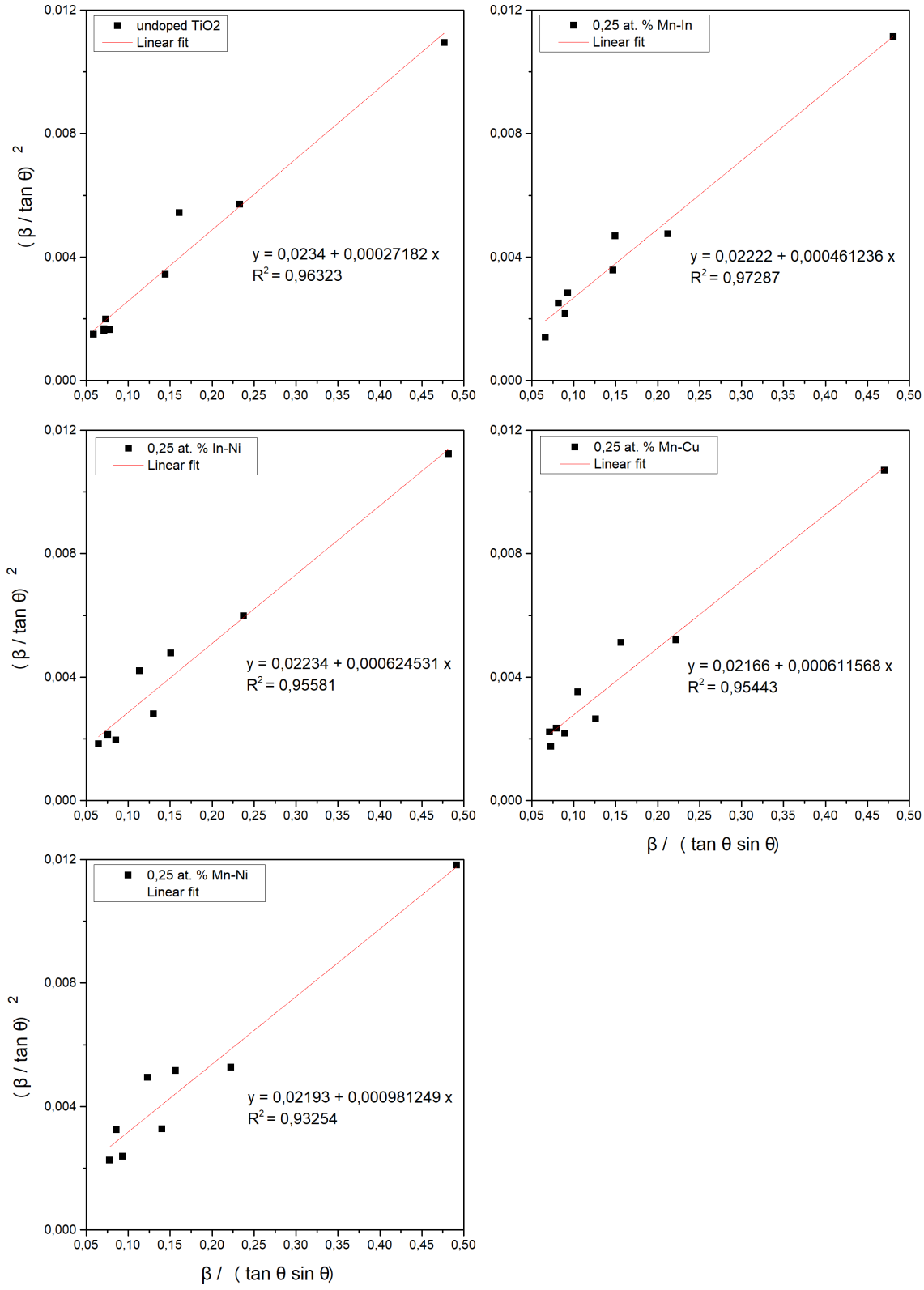

Fig. 61 Halder-Wagner method plot for each nanomaterial, together with the equations of linear least squares method obtained from linear regression of data.

5.1.2 BET surface area of doped and undoped TiO_2 nanostructures

The photocatalytic activity of nanoparticles is highly related to their surface properties such as surface area. As surface area (and porosity) increases, the number of active sites also increases [Suwarnkar et al.,2014]. The selection of dopants plays a significant role on the surface area of the nanomaterial. More specifically, undoped TiO_2 showed the surface area of 96.7 m^2/g, the TiO_2 doped with Mn-Cu and In-Ni revealed higher surface area of 98.8 and 98.4 m^2/g respectively, while Mn-In and Mn-Ni displayed lower surface areas accounting to 81.5 and 94.1 m^2/g respectively (Table 9). Lower surface area may be justified by aggregation of nanoplatelets. The IUPAC classification of adsorption isotherms is illustrated in Figure 62. The six types of isotherm (IUPAC classification) are characteristic of adsorbents that are microporous (type I), nonporous or macroporous (types II, III, and VI), or mesoporous (types IV and V) [Sing et al., 1985; Broekhoff et al., 1979; Shields et al., 2004; Abebe et al., 2018; G. Leofantia et al., 1998]. In Figure 63, N_2 adsorption isotherms are shown for undoped and Mn-In, Mn-Cu, In-Ni and Mn-Ni doped TiO_2 nanostructures. It is well demonstrated that the nature of dopant ions is affecting the BET-specific surface area. For both the undoped and the doped TiO_2 nanostructures, the gas adsorption measurement revealed a type-I curve, according to the IUPAC classification. Type I isotherm approaches a limiting value and usually is used to describe adsorption on microporous adsorbents [Donohue & Aranovich et al., 1998]. The adsorbate adsorption rate depends on the available micropore volume instead total interior surface area [Abebe et al., 2018]. Each curve has a point of inflection called a 'knee' around $P/P_0 = 0.1$. This point indicates that monolayer adsorption is complete and multilayer formation starts to take place. Over this point the adsorbed volume was increased predominantly, which means that there are also mesopores on doped and undoped TiO_2 nanostructures [Lee Hyemin et al., 2013].

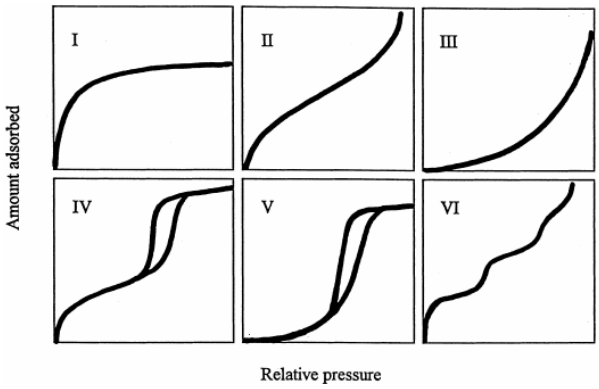

Fig. 62 The six types of isotherm (IUPAC classification). [Donohue & Aranovich et al., 1998]

Sample	2θ [1 0 1] (degrees)	Lattice parameters		Unit Cell Volume ($Å^3$)	d spacing [1 0 1] (nm)	Crystallite Size, D (nm)		Micro-strain, e (%)	Surface Area (m2/g)
		a=b (Å)	c (Å)			Modified Scherrer Eq.	H-W Method	H-W Method	BET
undoped TiO2	25,34	3,786	9,490	136,04	3,512	5,69	6,02	0,41	96,7
0,25 % at. doped Mn-In	25,35	3,785	9,489	135,98	3,510	6,16	6,24	0,54	81,5
0,25 % at. doped Mn-Cu	25,41	3,780	9,470	135,30	3,503	6,29	6,40	0,62	98,8
0,25 % at. doped In-Ni	25,41	3,778	9,466	135,10	3,503	5,96	6,21	0,62	98,4
0,25 % at. doped Mn-Ni	25,56	3,771	9,439	134,25	3,482	6,21	6,32	0,78	94,1

Table 9. Characterization results for undoped and doped TiO_2 nanostructures.

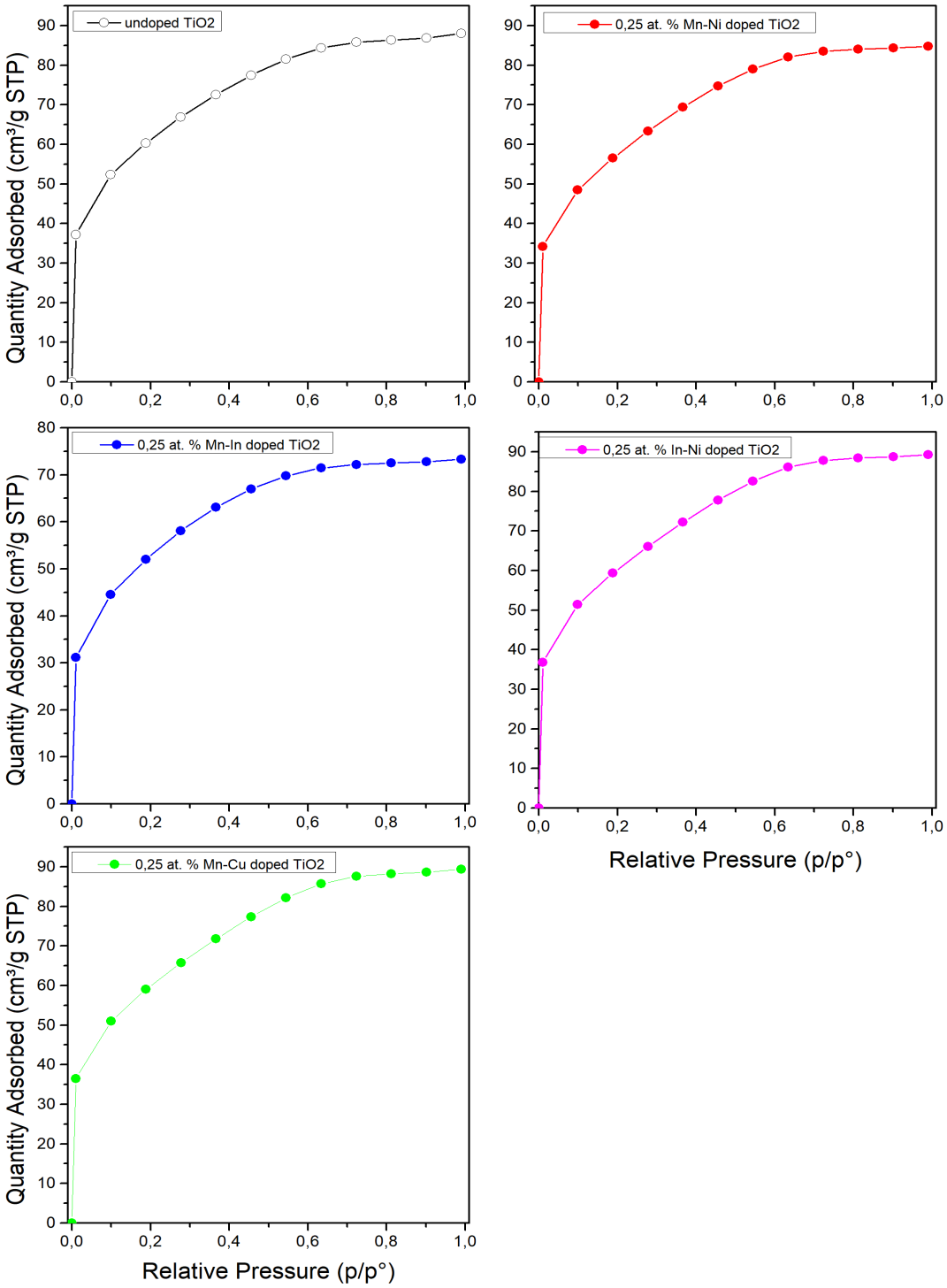

Fig. 63 N_2 adsorption isotherms for undoped and Mn-In, Mn-Cu, In-Ni and Mn-Ni doped TiO_2 nanostructures.

Chapter VI

Decolorization Results

6.1 Decolorization of Methylene Blue

In this chapter the decolorization of the coatings on 3-D printed panels and fabrics was studied. Decolorization of applied coatings was evaluated by the decolorization of Methylene Blue (MB). The exposure to UV light was held into a handmade photocatalytic apparatus..

6.1.1 Application on 3-D printed panels

The decolorization of the MB dye applied to the surfaces of the 3-D printed panels under UV exposure, was monitored by the use of chromatic measurements. For better evaluation of initial conditions of substrate and the effect of any color differences between analyzed surfaces before test, decolorization values (D) were normalized with respect to the original aspect of substrate before deposition of MB dye.

The decolorization D has been calculated using the following equation:

$$D\ (\%) = \frac{\Delta E(t)}{\Delta E(0)} \cdot 100\,, \quad \text{(Eq. 11)}$$

where ΔE(t) is the total color difference of chromatic coordinates calculated from Equation 1 at a specific time under UV irradiation with respect to the sample before the UV exposure, and ΔE(0) is the total color difference of the sample prior to UV exposure with respect to the sample before the deposition of MB dye (original panel).

As observed from Table 10, the decolorization values of nanocoated 3-D printed panels, after 120 minutes of UV irradiation, are 44.5, 31.6, 34.4, 34.1 and 19.6 for sample TiOP, InNiP, MnInP, MnNiP and MnCuP, respectively. While the decolorization percentage values of reference 3-D printed panels (Table 11), after 120 minutes of UV irradiation, are 23.8, 9.3, 16.0, 9.0 and 7.7 for sample Ref1, Ref2, Ref3, Ref4 and Ref5, respectively. The decolorization of reference 3-D printed panels is mainly caused by the sorption (absorption and adsorption) of MB dye onto the panels.

Nanocoated 3-D printed panels					
Time (min)	Decolorization Percentage, D %				
	TiOP	MnInP	MnNiP	InNiP	MnCuP
60	41,5	31,8	29,7	20,0	11,7
120	44,5	34,4	34,1	31,6	19,6

Table 10. Decolorization percentage of nano-coated 3-D printed panels after 60 and 120 minutes of UV light exposure.

Reference 3-D printed panels					
Time (min)	Decolorization Percentage, D %				
	Ref1	Ref2	Ref3	Ref4	Ref5
60	22,7	8,6	15,6	4,9	5,5
120	23,8	9,3	16,0	9,0	7,7

Table 11. Decolorization percentage of reference 3-D printed panels after 60 and 120 minutes of UV light exposure.

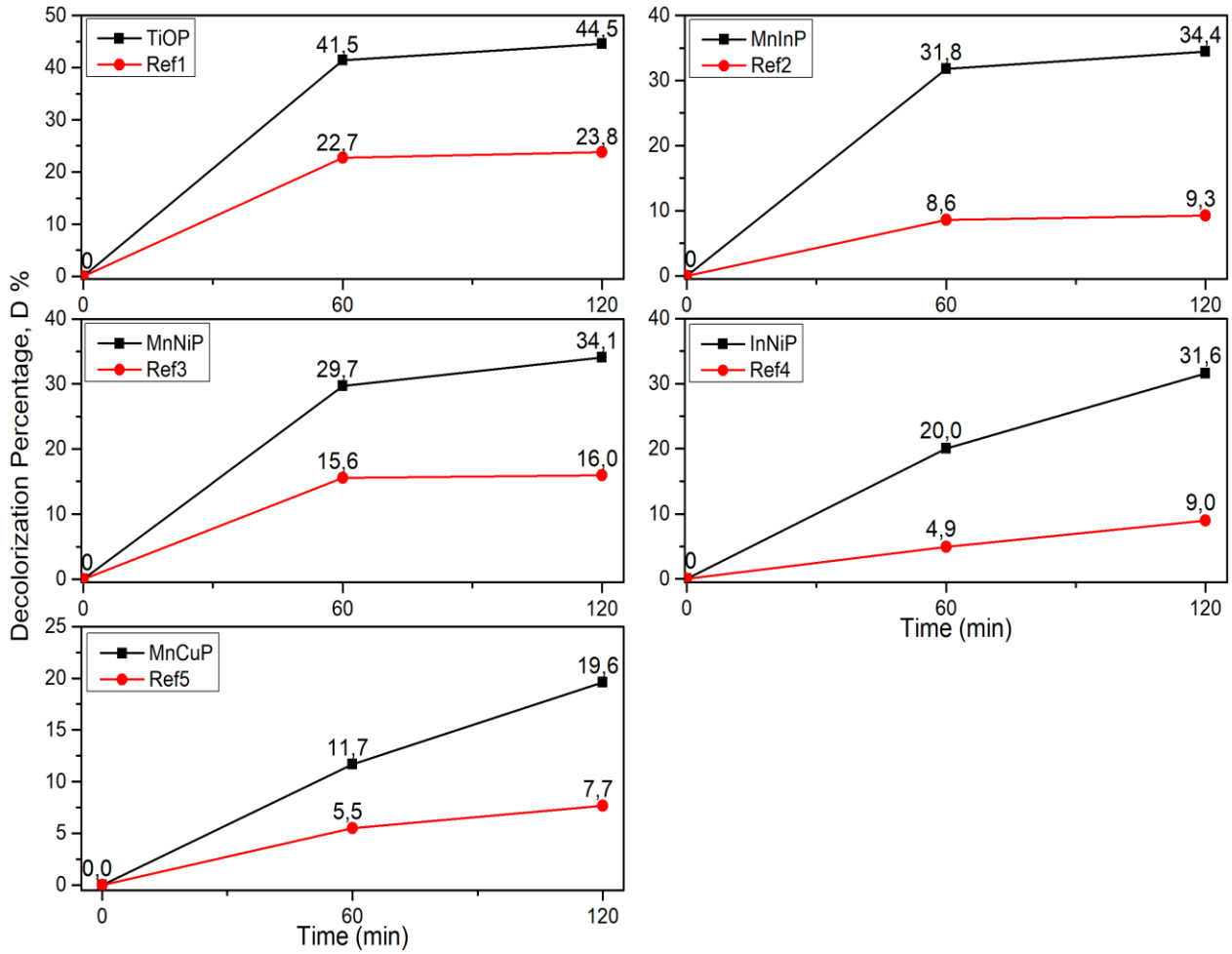

Fig. 64 Decolorization of each pair of 3-D printed panels under UV light. The black and red lines describe the decolorization of nanocoated and reference panels, respectively.

It is important to compare each pair of panels in order to distinguish the sorption processes from the decolorization of each nanomaterial applied. So, Table 12 shows the decolorization of panels caused by the nanomaterial used for the coating of the 3-D printed panels. Comparing the results from Table 12 and Figure 65 it is obvious that the sample coated with 0.25 at. % Mn-In doped TiO_2 showed the best decolorization percentage of MB dye.

Net Decolorization Percentage - Panels					
Time (min)	$\lvert D_{Nanocoated} - D_{Reference} \rvert$ %				
	$\lvert D_{TiOP} - D_{Ref1} \rvert$	$\lvert D_{MnInP} - D_{Ref2} \rvert$	$\lvert D_{MnNiP} - D_{Ref3} \rvert$	$\lvert D_{InNiP} - D_{Ref4} \rvert$	$\lvert D_{MnCuP} - D_{Ref5} \rvert$
60	18,8	23,2	14,1	15,1	6,2
120	20,7	25,1	18,1	22,6	12,0

Table 12. Net decolorization percentage of 3-D printed panels after 60 and 120 minutes of UV light exposure.

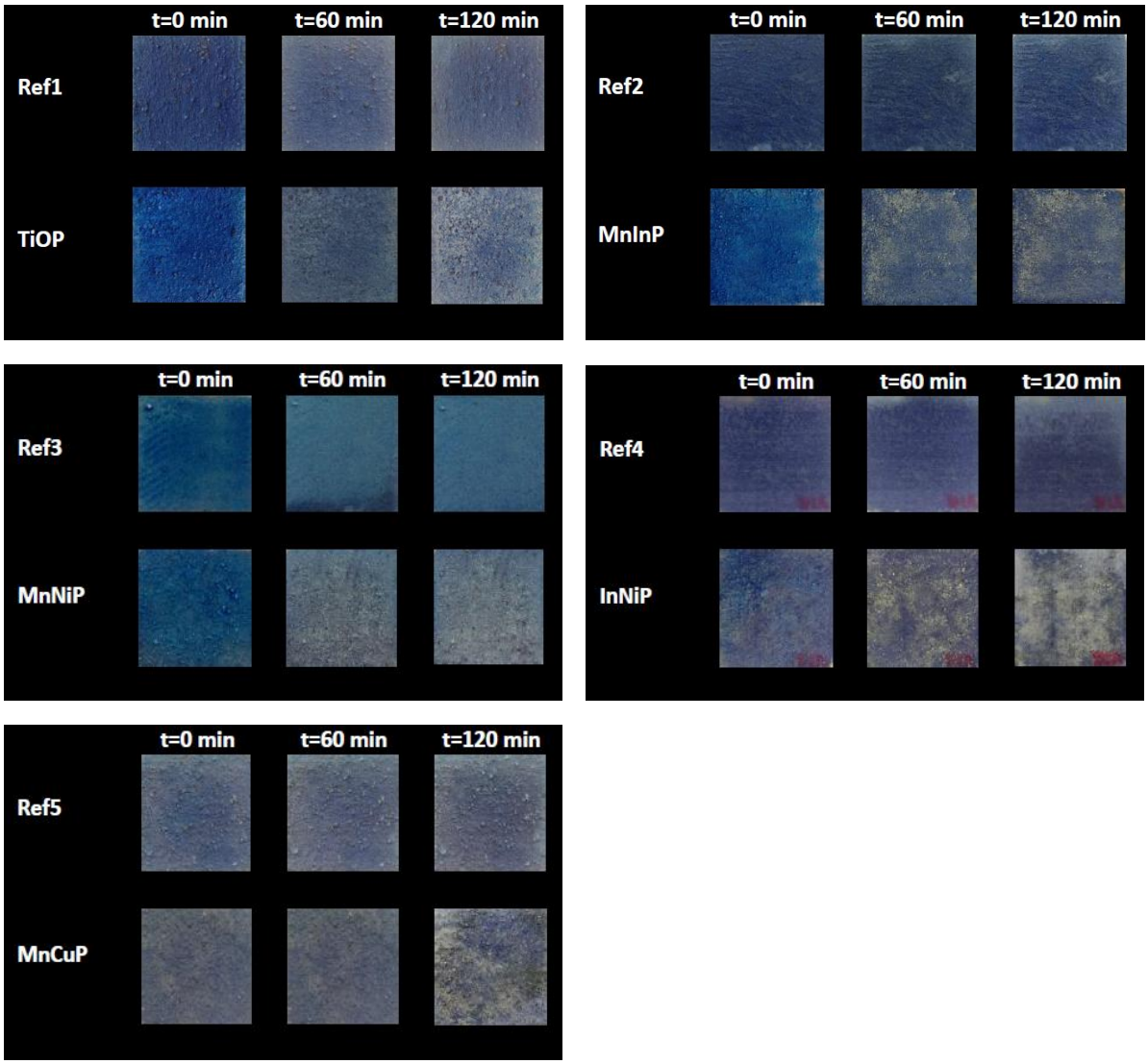

Fig. 65 MB decolorization test: pairs of 3-D printed panels at the beginning of the test before UV exposure (t=0) and after 60 and 120 minutes of UV irradiation.

6.1.2 Application on fabrics

The decolorization of MB dye applied to the surfaces of the fabrics was studied, firstly under exposure to indirect sunlight and then under UV exposure. The decolorization of MB under exposure to indirect sunlight was monitored by the use of chromatic measurements, while the decolorization of MB under UV exposure was monitored by a UV-VIS measurement.

A) Indirect sunlight exposure

For the case of indirect sunlight exposure, the decolorization percentage of fabrics was calculated using the Equation 11. Ass observed from Table 13, the decolorization percentage values of reference and nanocoated fabrics, after indirect sunlight exposure, are 10.8, 13.3, 52.7, 58.1, 18.6 and 47.6 for sample Ref, TiOF, InNiF, MnInF, MnNiF and MnCuF, respectively.

Fabrics						
Decolorization Percentage, D %						
Exposure	**Ref**	**TiOF**	**InNiF**	**MnInF**	**MnNiF**	**MnCuF**
Indirect Sunlight	10,8	13,3	52,7	58,1	18,6	47,6

Table 13. Decolorization percentage of reference and nano-coated fabrics after indirect sunlight exposure.

The results from Table 13 are in accordance with the decolorization shown in Figure 66. Three fabric samples showed great decolorization under sunlight. Specifically, the fabrics coated with 0.25 at. % Mn-In doped TiO_2, 0.25 at. % In-Ni doped TiO_2 and 0.25 at. % Mn-Cu doped TiO_2. The fabric coated with 0.25 at. % Mn-In doped TiO_2 showed the best decolorization percentage of MB dye, 47.3 % more than the decolorization of the reference fabric, while fabric coated with undoped TiO_2 showed the smallest decolorization, 2.5 % more than the decolorization of the reference fabric.

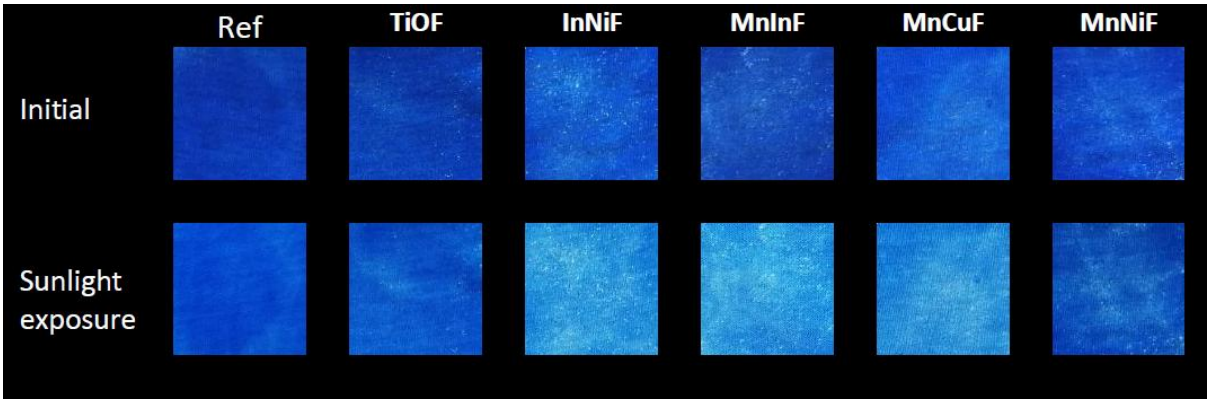

Fig. 66 MB decolorization test: reference and nanocoated fabrics at the beginning of the test before indirect sunlight exposure (Initial) and after exposure.

B) UV light exposure

The decolorization of fabrics was determined according to the Beer-Lambert law at the maximum absorbance (λ_{max} = 670 nm) using a UV-Vis spectrophotometer (Fig. 67). The decolorization percentage D, was calculated using Equation 12:

$$D\ (\%) = \frac{(A_0 - A_t)}{A_o} \cdot 100\ , \quad \text{(Eq. 12)}$$

where A_0 and A_t stand for the absorbance before UV exposure and after a specific time under UV irradiation, respectively.

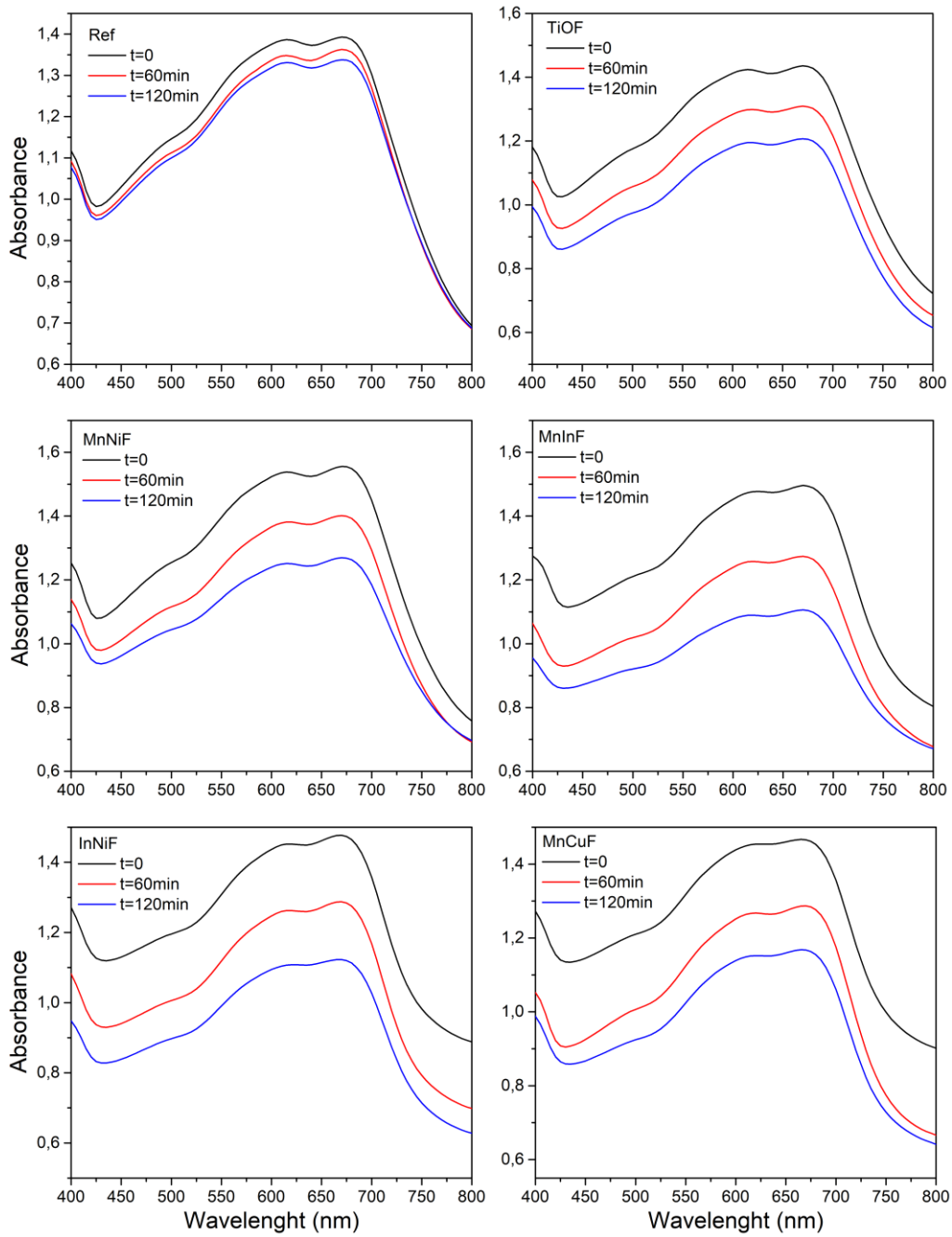

Fig. 67 Absorption spectra of reference and nanocoated fabrics, before UV exposure (t=0) and after 60 and 120 minutes of UV irradiation.

As observed from Table 14, the decolorization percentage values of reference and nanocoated fabrics, after 120 minutes of UV irradiation, are 3.9, 15.9, 18.4, 26.1, 24.0 and 20.4 for sample Ref, TiOF, InNiF, MnInF, MnNiF and MnCuF, respectively. The fabric coated with 0,25 at. % Mn-In doped TiO_2 showed the best decolorization, 22.2 % more than the decolorization of the reference fabric, while the fabric coated with undoped TiO_2 and 0,25 at. % Mn-Ni doped TiO_2 showed the smallest decolorization (Fig. 68), 12.0 % and 14.5 % more than the decolorization of the reference fabric, respectively.

Fabric	**Decolorization Percentage, D (%)**	
	Time (min)	
	60	120
Ref	2,2	3,9
TiOF	8,8	15,9
MnNiF	9,9	18,4
MnInF	14,9	26,1
InNiF	12,8	24,0
MnCuF	12,2	20,4

Table 14. Decolorization percentage of reference and nanocoated fabrics after 60 and 120 minutes of UV light exposure.

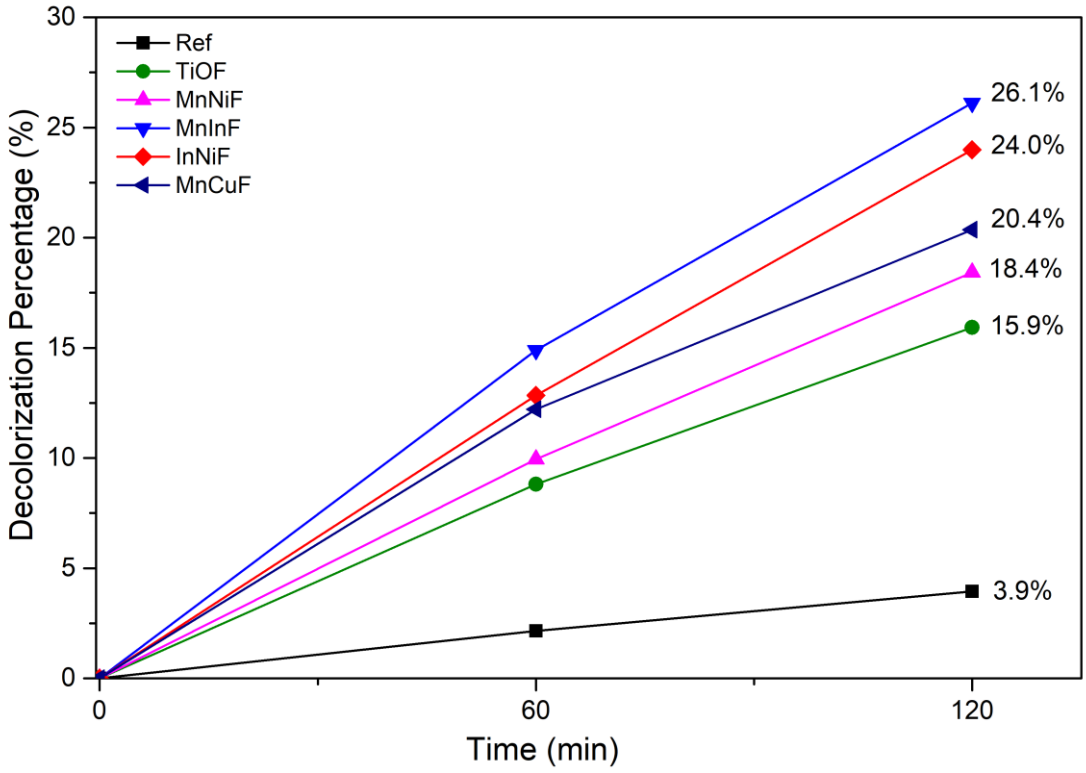

Fig. 68 Decolorization percentage of reference and nanocoated fabrics.

Conclusions & Recommendations

During this Master Thesis synthesis and characterization of photocatalytic titanium dioxide nanoparticles took place, followed by the assessment of their decolorization effectiveness as coatings on fabrics and 3-D printed panels made of recycled materials. Photocatalytic efficiency is enhanced by doping. Undoped and In-Ni-, Mn-In, Mn-Cu-, Mn-Ni- bimetallic doped (0.25 at. %) TiO_2 nanostructures were synthesized using the microwave-assisted hydrothermal method. The structure of nanoparticles was investigated by X-Ray Diffraction (XRD) and the specific surface area by the BET (Brunauer, Emmett and Teller) analysis.

Undoped and doped TiO_2 nanoparticles only exhibited patterns assigned to the TiO_2 anatase phase (JCPDS file card No.-01-071-1166). No signal from the crystalline phase containing metal or metal oxide of the doping elements could be observed. By comparing the ionic radius values of Ti^{+4} (0.68 Å) to that of In^{+3} (0.81 Å), Mn^{+2} (0.80 Å), Ni^{+2} (0.72 Å) and Cu^{+2} (0.73 Å), we hypothesize that some of the doping elements were incorporated into the structures of TiO_2 and replaced the titanium ions, which induced a perturbation in anatase crystal structure. Replacement of Ti^{+4} by In^{+3}, Mn^{+2}, Ni^{+2} and Cu^{+2} dopant ions may cause expansion/compression of the unit cell resulting to variation in various parameters including micro-strain due to lattice mismatch and distortion. Crystallite size of each nanomaterial was calculated by two methods, the modified Scherrer equation and the Halder-Wagner (H-W) Method. In both methods the crystallite sizes are in good agreement and increasing in the order of In-Ni-, Mn-In-, Mn-Ni- and Mn-Cu-doping. Specifically, the average crystallite size calculated by the modified Scherrer equation, increased from 5.69 to 5.96, 6.16, 6.21 and 6.29 nm, while the average crystallite size calculated with H-W method increased from 6.02 to 6.21, 6.24, 6.32 and 6.40 nm with In-Ni-, Mn-In-, Mn-Ni- and Mn-Cu- doping, respectively. Moreover, the micro-strain of nanomaterials was calculated by the H-W method, increased from 0.41 to 0.54, 0.62, 0.62 and 0.78 % with Mn-In-, Mn-Cu-, In-Ni- and Mn-Ni- doping, respectively. The increase in micro-strain can be explained by the dopant substitution on the oxygen sites of TiO_2 surface.

For both undoped and doped TiO_2 nanostructures, the gas adsorption measurement revealed a type-I curve, according to the IUPAC classification, describing adsorption on microporous adsorbents. For type-I the adsorbate adsorption rate depends on the available micropore volume instead total interior surface area. Additionally, over the 'knee' point (P/P_0 = 0.1) of each curve the adsorbed volume was increased predominantly, which means that there are also mesopores on doped and undoped TiO_2 nanostructures. Specifically, undoped TiO_2 showed the surface area of 96.7 m^2/g, the TiO_2 doped with Mn-Cu- and In-Ni- revealed higher surface area of 98.8 and 98.4 m^2/g respectively, while Mn-In- and Mn-Ni- displayed lower surface areas accounting to 81.5 and 94.1 m^2/g respectively. Lower surface area may be justified by aggregation of nanoplatelets.

The decolorization of reference 3-D printed panels is mainly caused by the sorption (absorption and adsorption) of MB dye onto the panels. The variance in sorption between reference 3-D printed panels is due to the different composition of recycled concrete aggregate during the 3-D printing of each pair of panels. So, it is important to compare each pair of panels in order to distinguish the sorption processes from the decolorization caused by the nanomaterial applied. The 3-D printed panel coated with Mn-In- and In-Ni- doped TiO_2 showed the highest net MB decolorization, 25.1 and 22.6 %, respectively, after 2 hours of UV light exposure.

For the case of nanocoated fabrics, three samples (Mn-In-, In-Ni- and Mn-Cu- doped TiO_2) showed great MB decolorization (58.1, 52.7 and 47.6 % respectively) under indirect sunlight. Specifically, the fabric coated with Mn-In- doped TiO_2 showed the best decolorization percentage of MB dye, 47.3 % more than the decolorization of the reference fabric, while fabric coated with undoped TiO_2 showed the smallest decolorization, 2.5 % more than the decolorization of the reference fabric. Under UV light the fabric coated with Mn-In- doped TiO_2 showed the best decolorization, 22.2 % more than the decolorization of the reference fabric, while the fabric coated with undoped TiO_2 and Mn-Ni- doped TiO_2 showed the smallest decolorization, 12.0 % and 14.5 % more than the decolorization of the reference fabric, respectively. Therefore, nanocoated samples showed high MB decolorization and great potential in self-cleaning applications.

This research has thrown up many questions in need of further investigation. It is recommended that further research be undertaken in the structure and properties of nanomaterials, for example analyze the photocatalyst samples by using X-ray photoelectron spectroscopy (XPS) to study the valence state of the metal dopant. A future study investigating the antimicrobial properties of nanomaterials incorporating with different surfaces, in small and large-scale applications would be very interesting.

References

A Sustainable Europe by 2030, publiced at 30 January 2019, viewed on 13 June 2020,<https://ec.europa.eu/commission/sites/beta-political/files/rp_sustainable_europe_3001_en_web.pdf>

A. Bandyopadhyay, B. Heer, Additive manufacturing of multi-material structures, Mater. Sci. Eng.: R: Rep. 129 (2018) 1–16.

A. D. Basiago, "METHODS OF DEFINING 'SUSTAINABILITY'," Sustainable Development, vol. 3, pp. 109-119, 1995.

A. Hepp, C. Baerlocher, Learned peak shape functions for powder diffraction data, Aust. J. Phys. 41 (1988) 229–236.

A. Jankovic, (2015), "8 - Developments in iron ore comminution and classification technologies", Iron Ore, Woodhead Publishing, Pages 251-282, ISBN 9781782421566, https://doi.org/10.1016/B978-1-78242-156-6.00008-3.

A. Perrot, D. Rangeard, A. Pierre, Structural built-up of cement-based materials used for 3D-printing extrusion techniques, Mater. Struct. (2015) 1–8.

A.K. Kamrani, E.A. Nasr, Engineering Design and Rapid Prototyping, Springer US, Boston, MA, 2010.

Abebe, B. , Murthy, H. and Amare, E. (2018) Summary on Adsorption and Photocatalysis for Pollutant Remediation: Mini Review. Journal of Encapsulation and Adsorption Sciences, 8, 225-255. doi: 10.4236/jeas.2018.84012.

Abulmagd S, Etman ZA (2018) Nanotechnology in Repair and Protection of Structures State-of-the-Art. J Civil Environ Eng 8: 306. doi: 10.4172/2165-784X.1000306

ACA Industry, "ACA gypsum crusher for recycling of gypsum waste from demolition and recycling stations", viewed on 10 August 2020, < https://acaindustry.com/gypsum-waste/ >.

Adair CG, Gorman SP, Feron BM, Byers LM, Jones DS, Goldsmith CE, et al. Implications of endotracheal tube biofilm for ventilator-associated pneumonia. Intensive Care Med. 1999;25(10):1072-6

Addis, W., & Schouten, J. (2004). Design for deconstruction: Principles of design to facilitate reuse and recycling. London: CIRIA.

Agustí-Juan, Isolda & Müller, Florian & Hack, Norman & Wangler, Timothy & Habert, Guillaume. (2017). Potential benefits of digital fabrication for complex structures: Environmental assessment of a robotically fabricated concrete wall. Journal of Cleaner Production. 154. 330-340. 10.1016/j.jclepro.2017.04.002.

Ahmed, A. & Ugai, K. 2011. Environmental effects on durability of soil stabilized with recycled gypsum. Cold Regions Science and Technology., Vol. 66, Iss. 2–3, p. 84–92.

Albanese, Alexandre & Tang, Peter & Chan, Warren. (2012). The Effect of Nanoparticle Size, Shape, and Surface Chemistry on Biological Systems. Annual review of biomedical engineering. 14. 1-16. 10.1146/annurev-bioeng-071811-150124.

Allen NS, Edge M, Verran J et al. (2008) Photocatalytic titania based surfaces: environmental benefits. Polymer Degradation and Stability 93(9): 1632–1646.

Allouzi, Rabab. (2019). 3D Printing of Nanomaterials for Concrete Construction.

Alnaser, N.W. & Flanagan, Roger & Alnaser, Waheeb. (2008). Model for calculating the sustainable building index (SBI) in the kingdom of Bahrain. Energy and Buildings. 40. 2037-2043. 10.1016/j.enbuild.2008.05.015.

Aloise, P., Ricca, M., La Russa, M. F., Ruffolo, S. A., Belfiore, C. M., Padeletti, G., et al. (2014). Diagnostic analysis of stone materials from underwater excavations: the case study of the Roman archaeological site of Baia (Naples, Italy). Appl. Phys. A Mater. Sci. Proc. 114, 655–662. doi: 10.1007/s00339-013-7890-1

An, Seongpil & Lee, Minwook & Yarin, Alexander & Yoon, Sam. (2018). A Review on Corrosion-Protective Extrinsic Self-Healing: Comparison of Microcapsule-Based Systems and Those Based on Core-Shell Vascular Networks. Chemical Engineering Journal. 344. 10.1016/j.cej.2018.03.040.

Andersen, M. S. (2007). An introductory note on the environmental economics of the circular economy. Sustainable Science, 2(1), e133–e140.

Andrew, Robbie. (2019). Global CO2 emissions from cement production, 1928–2018. Earth System Science Data Discussions. 1-67. 10.5194/essd-2019-152.

Ansari, M. A., Khan, H. M., Alzohairy, M. A., Jalal, M., Ali, S. G., Pal, R., et al. (2015). Green synthesis of Al2O3 nanoparticles and their bactericidal potential against clinical isolates of multi-drug resistant Pseudomonas aeruginosa. World J. Microbiol. Biotechnol. 31, 153–164. doi: 10.1007/s11274-014-1757-2

Antonios, Charbel & Inman, Daniel & Smaili, A. (2006). Experimental and Theoretical Behavior of Self-healing Bolted Joints. Journal of Intelligent Material Systems and Structures - J INTEL MAT SYST STRUCT. 17. 499-509. 10.1177/1045389X06058872.

Aqil, U., Tatsuoka, F., Uchimura, T., Lohani, T.N., Tomita, Y., Matsushima, K., 2005. Strength and deformation characteristics of recycled concrete aggregate as a backfill material. Soils Found. 45 (5), 53–72.

ARMA (2015). Personal communication from R.X. Gumucio, Asphalt Roofing Manufacturers Association, Washington, D.C.

Asbestos Council of Victoria/Gippsland Asbestos Related Disease Support Inc. (ACV/GARDS), viewed on 19 June 2020, < https://gards.org/what-is-silica/ >

ASTM. ‘‘ASTM F2792-10 Standard Terminology for Additive Manufacturing Technologies.” American Society for Testing and Materials (ASTM)

Awwad, M.T. and L. Shbeeb, 2007. The use of polyethylene in hot asphalt mixtures. Am. J. Eng. Applied Sci., 4: 390-396. DOI: 10.3844/ajassp.2007.390.396

B. Berman, 3-D printing: the new industrial revolution, Bus. Horiz. 55 (2) (2012) 155–162.

B. Khoshnevis, “Toward total automation of on-site construction an integrated approach based on contour crafting”, Proc. ISARC (2003) 61–66.

B. Khoshnevis, Automated construction by contour crafting—related robotics and information technologies, Autom. Constr. 13 (1) (2004) 5–19.

B. Khoshnevis, D. Hwang, K. Yao, Z. Yeh, Mega-scale fabrication by contour crafting, International journal of Industrial and System Engineering Vol 1 (no. 3) (2006) 301–320.

B. Khoshnevis, Dutton R. Innovative rapid prototyping process makes large sized, smooth surfaced complex shapes in a wide variety of materials. Mater Technol, 1998, 13: 53–56

B. Khoshnevis, R. Russell, H. Kwon, S. Bukkapatnam, Contour crafting—a layered fabrication technology, Spec. Issue IEEE Robot. Autom. Mag. 8 (3) (2001) 33–42.

B.-J. De Gans, P.C. Duineveld, U.S. Schubert, Inkjet printing of polymers: state of the art and future developments, Adv. Mater. 16 (3) (2004) 203–213.

Baglioni, P., Carretti, E., Chelazzi, D., 2015. Nanomaterials in art conservation. Nature Nanotechnology 10, 287-290.

Barbudo, A., Agrela, F., Ayuso, J., Jiménez, J.R., Poon, C.S., 2012. Statistical analysis of recycled aggregates derived from different sources for sub-base applications. Constr. Build. Mater. 28 (1), 129–138.

Barnett, Eric & Gosselin, Clément. (2015). Large-Scale 3D Printing with A Cable-Suspended Robot. Additive Manufacturing. 7. 10.1016/j.addma.2015.05.001.

Beaujuge, P. M.; Reynolds, J. R. Color Control in Π-Conjugated Organic Polymers for Use in Electrochromic Devices. Chem. Rev. 2010, 110, 268–320.

Behzadnia, A., Montazer, M., Rashidi, A. and Rad, M.M. (2014). Sonosynthesis of nano TiO2 on wool using titanium isopropoxide or butoxide in acidic media producing multifunctional fabric. Ultrason. Sonochem. 21: 1815-1826.

Benedix, Roland & Dehn, Frank & Quaas, Jana & Orgass, Marko. (2000). Application of Titanium Dioxide Photocatalysis to Create Self-Cleaning Building Materials. Lacer. 5.

Bergamonti, L., Predieri, G., Paz, Y., Fornasini, L., Lottici, P.P., Bondioli, F., 2017. Enhanced self-cleaning properties of N-doped TiO2 coating for cultural heritage. Microchemical Journal 133, 1-12.

Bianchi, Claudia & Gatto, S. & Nucci, S. & Cerrato, Giuseppina & Capucci, V.. (2013). Self-cleaning measurements on tiles manufactured with micro-sized photoactive TiO2. Advances in materials Research. 2. 10.12989/amr.2013.2.1.065.

Bickley RI, Munuera G, Stone FS (1973) Photoadsorption and photocatalysis on rutile surface. II. Photocatalytic oxidation of isopropanol. J Catal 31:398–407

Binas, V. D., Sambani, K., Maggos, T., Katsanaki, A., & Kiriakidis, G. (2012). Synthesis and photocatalytic activity of Mn-doped TiO2 nanostructured powders under UV and visible light. Applied Catalysis B: Environmental, 113–114, 79–86. https://doi.org/10.1016/j.apcatb.2011.11.021

Biscarini, F., Taliani , C., Chen , J., and Komanduri , R. (April 29, 2002). "Nanomanufacturing and Processing—Research, Education, Infrastructure, Security, Resource." ASME. J. Manuf. Sci. Eng. May 2002; 124(2): 489–490. https://doi.org/10.1115/1.1471359

Bisello, A., Grilli, G., Balest, J., Stellin, G., & Ciolli, M. (2017). Co-benefits of smart and sustainable energy district projects: An overview on economic assessment methodologies. In Green Energy and Technology, 127–164. https://doi.org/10.1007/978-3-319-44899-2_9.

Blaauw C, et al. The metal-non-metal transition in VO2: X-ray photoemission and resistivity measurements. J Phys C: Solid State Phys 1975;8(4):459.

Bolden, Johnny & Abu-Lebdeh, Taher & Fini, Ellie. (2013). UTILIZATION OF RECYCLED AND WASTE MATERIALS IN VARIOUS CONSTRUCTION APPLICATIONS. American journal of environmental sciences. 9. 14-24.

Bridget B M. Eindhoven University of Technology (TU/e) unveils massive robotic concrete 3D printer, displays new pavilion. 2016, https://3dprint.com/139988/tue-concrete-3d-printer-pavilion.

Broekhoff, J.C.P. Mesopore determination from nitrogen sorption isotherms: Fundamentals, scope, limitations. Stud. Surf. Sci. Catal. 1979, 3, 663–684.

Bruinink, Arie & Wang, Jing & Wick, Peter. (2015). Effect of particle agglomeration in nanotoxicology. Archives of toxicology. 89. 10.1007/s00204-015-1460-6.

Bystrzejewska-Piotrowska G, Golimowski J, Urban P. Nanoparticles: their potential toxicity, waste and environmental management. Waste Manage 2009; 29:2587–95.

C. Harty, Implementing innovation in construction: contexts, relative boundedness and actor-network theory, Constr. Manag. Econ. 26 (10) (2008) 1029–1041.

C. Ladd, J.H. So, J. Muth, M.D. Dickey, 3D printing of free standing liquid metal microstructures, Adv. Mater. 25 (36) (2013) 5081–5085.

C. V. Konstantinidou and A. Novoselac, “Integration of thermal energy storage in buildings,” Univ. Tex. Austin, 2010

C. Vielkanowitz, New silver based antimicrobial systems for hygiene coatings, in: American Coatings Conference, Charlotte, NC, June 2–4, 2008.

C.B. Hiragond, A.S. Kshirsagar, V.V. Dhapte, T. Khanna, P. Joshi, P.V. More, Enhanced anti-microbial response of commercial face mask using colloidal silver nanoparticles, Vacuum 156 (2018) 475–482, http://dx.doi.org/10.1016/j.vacuum.2018.08.007.

Caratto, Valentina & Ball, Lorenzo & Sanguineti, Elisa & Insorsi, Angelo & Firpo, Iacopo & Alberti, Stefano & Ferretti, Maurizio & Pelosi, Paolo. (2017). Antibacterial activity of standard and N-doped titanium dioxide-coated endotracheal tubes: An in vitro study. Revista Brasileira de Terapia Intensiva. 29. 55-62. 10.5935/0103-507X.20170009.

Castaño, Victor & Rodriguez, Rodolfo. (2004). A nanotechnology approach to high-performance anti graffiti coatings. Inter J Appl Manag Technol. 2. 53-58.

Cesaretti, Giovanni & Enrico, Dini & De Kestelier, Xavier & Colla, Valentina & Pambaguian, Laurent. (2014). Building Components for an Outpost on the Lunar Soil by Means of a Novel 3D Printing Technology. Acta Astronautica. 93. 430-450. 10.1016/j.actaastro.2013.07.034.

Charles Hull, patent application for "Apparatus for production of three-dimensional objects by stereolithography", U.S. patent US4575330 A, granted on March 11, 1986

Chen, F., Yang, X., Wu, Q., 2009. Antifungal capability of TiO2 coated film on moist wood. Building and Environment 44, 1088-1093. https://doi.org/10.1016/j.buildenv.2008.07.018.

Chen, J., Kou, S., Poon, C., 2012. Hydration and properties of nano-TiO2 blended cement composites. Cement and Concrete Composites 34 (5), 642-649.

Chen, J., Poon, C.S., 2009. Photocatalytic construction and building materials: from fundamentals to applications. Building and Environment 44, 1899-1906.

Cheshire, D. (2017). Building revolutions—Applying the circular economy to the built environment (1st ed.). London: Riba Publishing.

Cho, M., Chung, H., Choi, W., Yoon, J., 2004. Linear correlation between inactivation of E. coli and OH radical concentration in TiO2 photocatalytic disinfection. Water Research 38, 1069-1077. https://doi.org/10.1016/j.watres.2003.10.029.

Chongqing Longxin Machinery Manufacturing Co. LTD (CLMM), "Cone crusher", viewed on 24 June 2020, <https://cqljgs.diytrade.com/sdp/2312578/4/pd/136818932773227/used_cone_crusher_machine_PYY_200.html>.

Chung CJ, Lin HI, Tsou HK, Shi ZY, He JL. An antimicrobial TiO2 coating for reducing hospital acquired infection. Journal of Biomedical Materials Research Part B: Applied Biomaterials. 2008;85B:220-224

CMP Cientifica, 'NANOTECH: The Tiny Revolution', November 2001.

Colangiuli, D., Calia, A., & Bianco, N. (2015). Novel multifunctional coatings with photocatalytic and hydrophobic properties for the preservation of the stone building heritage. Construction and Building Materials, 93, 189–196. https://doi.org/10.1016/j.conbuildmat.2015.05.100

Colangiuli, D., Lettieri, M., Masieri, M., and Calia, A. (2019). Field study in an urban environment of simultaneous self-cleaning and hydrophobic nanosized TiO2-based coatings on stone for the protection of building surface. Sci. Total Environ. 650, 2919–2930. doi: 10.1016/j.scitotenv.2018.10.044

Contera, Sonia. 2019. Interfaces and Mechanical Properties of Nanomaterials and Biological Systems with AFM. AZoNano, viewed 27 April 2020, https://www.azonano.com/article.aspx?ArticleID=3012.

Contour Crafting CORP, http://contourcrafting.com

Coronado J.M. (2013) A Historical Introduction to Photocatalysis. In: Coronado J., Fresno F., Hernández-Alonso M., Portela R. (eds) Design of Advanced Photocatalytic Materials for Energy and Environmental Applications. Green Energy and Technology. Springer, London https://doi.org/10.1007/978-1-4471-5061-9_1

CPC Equipment Pvt. Ltd, "JAW CRUSHERS", viewed on 24 June 2020, <https://www.cpcequipments.com/blog/index.php/2019/07/24/difference-between-double-and-single-toggle-jaw-crusher/>.

Cros, C.J., Terpeluk, A.L., Burris, L.E., Crain, N.E., Corsi, R.L., Juenger, M.C.G., 2015a. Effect of weathering and traffic exposure on removal of nitrogen oxides by photocatalytic coatings on roadside concrete structures. Materials and Structures/Materiaux et Constructions 48,3159-3171.

Cui, Yuanyuan & Ke, Yujie & Liu, Chang & Chen, Zhang & Wang, Ning & Liangmiao, Zhang & Zhou, Yang & Wang, Shancheng & Gao, Yanfeng. (2018). Thermochromic VO 2 for Energy-Efficient Smart Windows. Joule. 2. 10.1016/j.joule.2018.06.018.

Cultrone, G., Madkour, F., 2013. Evaluation of the effectiveness of treatment products in improving the quality of ceramics used in new and historical buildings. Journal of Cultural Heritage 14, 304-310.

CustomPartNet, https://www.custompartnet.com/wu/laminated-object-manufacturing

D. Asprone, F. Auricchio, C. Menna, V. Mercuri, "3D printing of reinforced concrete elements: Technology and design approach", Construction and Building Materials 165 (2018) 218–231

D. Balzar, H. Ledbetter, Voigt-function modeling in fourier analysis of size- and strain-broadened X-ray diffraction peaks, J. Appl. Crystallogr. 26 (1) (1993) 97–103.

D. Bozsaky, Special Thermal Insulation Methods of Building Constructions with Nanomaterials, Acta Technica Jaurinensis, Vol. 9, No. 1,2016, pp.29-41.

D. Smith, Printed buildings: an international race for the ultimate in automation, Constr. Research Innovation 3 (2) (2012) 26–31.

Dachowski, Ryszard & Stepien, Anna. (2011). The Impact of Various Additives on the Microstructure of Silicate Products. Procedia Engineering. 21. 1173-1178. 10.1016/j.proeng.2011.11.2127.

Dalmora CH, Deutschendorf C, Nagel F, dos Santos RP, Lisboa T. Defining ventilator-associated pneumonia: a (de)construction concept. Rev Bras Ter Intensiva. 2013;25(2):81-6.

De Longchamp, D. M.; Kastantin, M.; Hammond, P. T. High-Contrast Electrochromism from Layer-by-Layer Polymer Films. Chem. Mater. 2003, 15, 1575–1586.

Delgado Camacho, Daniel & Clayton, Patricia & O'Brien, William & Ferron, Raissa & Salamone, Salvatore. (2018). Applications of additive manufacturing in the construction industry – A forward-looking review. Automation in Construction. 89. 10.1016/j.autcon.2017.12.031.

Dhawan, A.; Sharma, V.: Toxicity assessment of nanomaterials: methods and challenges. Anal. Bioanal. Chem. 398, 589–605 (2010)

Dhir, R. K., Newlands, M. D., and Csetenyi, L. J. "Introduction". Proceedings of the International Conference – Application of Technology in Concrete Design, p. IV, 2005, Scotland, UK International, Journal of Recent Trends in Engineering, Vol 1, No. 4, May 2009

Diamanti, M.V., Del Curto, B., Ormellese, M., Pedeferri, M.P., 2013b. Photocatalytic and self-cleaning activity of colored mortars containing TiO2. Construction and Building Materials 46, 167-174.

Diamanti, M.V., Gadelrab, K.R., Pedeferri, M.P., Stefancich, M., Pehkonen, S.O., Chiesa, M., 2013. Nanoscale investigation of photoinduced hydrophilicity variations in anatase and rutile nanopowders. Langmuir 29 (47), 14512-14518.

Diamanti, Maria Vittoria & Pedeferri, M.P. (2019). Photocatalytic performance of mortars with nanoparticles exposed to the urban environment. 10.1016/B978-0-08-102641-0.00022-0.

Dimitra Papadaki, Gugu H. Mhlongo, David E. Motaung, Steven S. Nkosi, Katerina Panagiotaki, Emmy Christaki, Margarita N. Assimakopoulos, Vassileios C. Papadimitriou, Federico Rosei, George Kiriakidis, and Suprakas Sinha Ray. "Hierarchically Porous Cu-, Co-, and Mn-Doped Platelet-Like ZnO Nanostructures and Their Photocatalytic Performance for Indoor Air Quality Control" .ACS Omega 2019 4 (15), 16429-16440DOI: 10.1021/acsomega.9b02016

Ding, Zhen & Yuan, Chao & Peng, Xirui & Wang, Tiejun & Qi, H. & Dunn, Martin. (2017). Direct 4D Printing via Active Composite Materials. Science Advances. 3. 10.1126/sciadv.1602890.

Dini Engineering S.R.L., 3-D Printers, viewed on 10 June 2020, < https://d-shape.com/3d-printers/ >

Dini Engineering S.R.L., Materials, viewed on 4 June 2020, < https://d-shape.com/materials/ >

Dini Engineering S.R.L., viewed on 4 June 2020, < https://d-shape.com/our-technology/ >

Doehne, E.F., Price, C.A., 2010. Stone Conservation: An Overview of Current Research, second ed. Getty Conservation Institute, Los Angeles.

Donohue, Marc & Aranovich, G.L. (1998). Classification of Gibbs adsorption isotherms. Advances in Colloid and Interface Science. 76. 137-152. 10.1016/S0001-8686(98)00044-X.

Dr. Inas Hosny Ibrahim Anous, American International Journal of Research in Humanities, Arts and Social Sciences, 7(1), June-August, 2014, pp. 16-27

Dresselhaus, M & Dresselhaus, G & Charlier, Jean-Christophe & Hernandez, Eduardo. (2004). Electronic, thermal and mechanical properties of carbon nanotubes. Philosophical transactions. Series A, Mathematical, physical, and engineering sciences. 362. 2065-98. 10.1098/rsta.2004.1430.

Drexler, K.E., 'Engines of Creation: The Coming Era of Nanotechnology' (Anchor/Doubleday, 1986).

Drexler, K.E., 'Molecular engineering: An approach to the development of general capabilities for molecular manipulation', Proceedings of the National Academy of Sciences 78 (9) (Sept. 1981) 5275-78.

Dubas S.T., Kumlangdudsana P., Potiyaraj P., Colloids & Surfaces A: Physiochemical & Engineering Aspects 2006, 289, 105-109

E. Bagda, Photocatalytic effects on masonry coatings, International Paint, Varnish, Ink and Auxiliary Products Industry Congress, Smart Coatings and New Technologies, vol. 6, Istanbul, May 17–19, 2006.

Edie News, 'EU smart construction materials to absorb pollution', http://www.greenbiz.com/news/2004/03/11/eu-smart-construction-materials-absorb-pollution.

EEA, 2018b 'Exceedance of air quality standards in urban areas'

EEA, 2019a Air quality in Europe – 2019 report, EEA report No 10/2019, European Environmental Agency

El Sakka, F & Hamzeh, F 2017, "3D concrete printing in the service of lean construction. IGLC 2017 - Proceedings of the 25th Annual Conference of the International Group for Lean Construction."

El-Assaly A, Ellis R. Evaluation of recycling waste materials and by-products in highway construction. Int J Sustainable Dev World Ecol 2001;8(4):299–308.

Ellen MacArthur Foundation, (2015), Towards a Circular Economy: business rationale for an accelerated transition. < https://www.ellenmacarthurfoundation.org/publications/towards-a-circular-economy-business-rationale-for-an-accelerated-transition >

Enrico Dini, Moreno Chiarugi, Roberto Nannini, patent application for "Method and Device for Building Automatically Conglomerate Structures", U.S. patent US20080148683A1, granded on June 26, 2008.

Enrico Dini, Moreno Chiarugi, Roberto Nannini, patent application for "Method and Device for Building Automatically Conglomerate Structures", WO patent WO2006100556A2, granted on March 16, 2006.

Etxeberria M, Mari AR, Vazquez E. Recycled aggregate concrete as structural material. Mater Struct 2007;40(2007):529–41.

European Commission – Department: Energy – In focus Energy efficiency in buildings Brussels, 17 February 2020

European Commission. (2016), Construction and demolition waste, viewed on 13 June 2020, < http://ec.europa.eu/environment/waste/construction_demolition.htm >

European Commission. (2017), Circular economy strategy, viewed on 13 June 2020, < http://ec.europa.eu/environment/circular-economy/index_en.htm >

European Container Glass Federation (FEVE), publiced 29 October 2019, < https://feve.org/wp-content/uploads/2019/10/FEVE-PR-Recycling-Data-2017-Final.pdf >

European Environment Agency (EEA), Signals 2013, Every breath we take

European Tire & Rubber Manufacturers' Association (ETRMA), released 19 November 2019, < https://www.etrma.org/wp-content/uploads/2019/11/20191119-Europe-92-of-all-End-of-Life-Tyres-collected-and-treated-in-2017.pdf >

Executive summary (2012) of the EFFACEUR project.

F. D. Mai, C. S. Lu, C. W. Wu, C. H. Huang, J. Y. Chen, and C. C. Chen, "Mechanisms of photocatalytic degradation of Victoria Blue R using nano-TiO2," Separation and Purification Technology, vol. 62, no. 2, pp. 423–436, 2008.

F. Liang, Y. Liang, Study on the status quo and problems of 3D printed buildings in China, Glob. J. Hum. Soc. Sci. 14 (5) (2014) 7–10.

F. Rengier, A. Mehndiratta, H. von Tengg-Kobligk, C.M. Zechmann, R. Unterhinninghofen, H.U. Kauczor, F.L. Giesel, 3D printing based on imaging data: review of medical applications, Int. J. Comput. Assisted Radiol. Surg. 5 (4) (2010) 335–341.

F. Yuan, L.-y. Shen, and Q.-m. Li, "Emergy analysis of the recycling options for construction and demolition waste," Waste Management, vol. 31, pp. 2503-2511, 12// 2011.

F.P.W. Melchels, J. Feijen, D.W. Grijpma, A review on stereolithography and its applications in biomedical engineering, Biomaterials 31 (24) (2010) 6121–6130.

FABO, Stationary crusher plant, viewed 25 June 2020, < https://fabo.com.tr/product/stationary-crushing-plant/stationary-crushing-plants/150-250-tph-capacity-crushing-screening-plant-with-primary-impact-crusher/ >.

Fadlalla M.I., Senthil Kumar P., Selvam V., Ganesh Babu S. (2019) Recent Advances in Nanomaterials for Wastewater Treatment. In: Naushad M., Rajendran S., Gracia F. (eds) Advanced Nanostructured Materials for Environmental Remediation. Environmental Chemistry for a Sustainable World, vol 25. Springer, Cham. https://doi.org/10.1007/978-3-030-04477-0_2

Fan, F. R.; Tian, Z. Q.; Lin Wang, Z. Flexible Triboelectric Generator. Nano Energy 2012, 1, 328–334.

Faraldos, M. & Bahamonde, Ana. (2019). Multifunctional photocatalytic coatings for construction materials. 10.1016/B978-0-08-102641-0.00023-2.

Farid, M. M., Khudhair, A. M., Razack, S. A. K., & Al-Hallaj, S. (2004). A review on phase change energy storage: Materials and applications. Energy Conversion and Management, 45(9–10), 1597–1615. https://doi.org/10.1016/j.enconman.2003.09.015

Feilden, Ezra. (2017). Additive Manufacturing of Ceramics and Ceramic Composites via Robocasting. 10.13140/RG.2.2.29343.25765.

Feynman, R.P. There's Plenty of Room at the Bottom: An Invitation to Enter a New Field of Physics.In Proceedings of the Annual meeting of the American Physical Society, California Institute of Technology,Pasadena, CA, USA, 29 December 1959; California Institute of Technology: Pasadena, CA, USA, 1960.

FHWA (2018). Tech Brief: State of the Knowledge for the Use of Asphalt Mixtures with Reclaimed Binder Content (Report FHWA-HIF-18-059). Office of Asset Management, Pavement, and Construction, Federal Highway Administration, Washington, D.C.

Flores e Colen, I., de Brito, J., de Freitas, V.P., 2008. Stains in facades' rendering e diagnostic and maintenance techniques' classification. Construction and Building Materials 22,211-221.

FlowPrep, Micromeritics' FlowPrep 060, viewed on 13 August 2020, <https://www.micromeritics.com/Product-Showcase/Sample-Preparation-Systems/FlowPrep-060-Accessory-Literature.aspx>.

Fn Nano Inc., News (13 September 2019), PEOPLE DO NOT BREATHE FUMES AT NORTH LAS VEGAS AIRPORT ANYMORE, http://fnnanoinc.com/news.html/.

Fonseca, A.J., Pina, F., Macedo, M.F., Leal, N., Romanowska-Deskins, A., Laiz, L., Gomez-Bolea, A., Saiz-Jimenez, C., 2010. Anatase as an alternative application for preventing biodeterioration of mortars: evaluation and comparison with other biocides. International Biodeterioration & Biodegradation 64, 388-396. https://doi.org/10.1016/j.ibiod.2010.04.006.

Frank SN, Bard AJ (1977) Heterogeneous photocatalytic oxidation of cyanide ion in aqueous solutions at titanium dioxide powder. J Am Chem Soc 99:303–304

Fraser, T.W.K.; Reinardy, H.C.; Shaw, B.J.; Henry, T.B.; Handy, R.D.: Dietary toxicity of single-walled carbon nanotubes and fullerenes (C60) in rainbow trout (Oncorhynchus mykiss). Nanotoxicology. 5, 98–108 (2010).

Friel, Ross & Harris, Russell. (2013). Ultrasonic Additive Manufacturing – A Hybrid Production Process for Novel Functional Products. Procedia CIRP. 6. 35–40. 10.1016/j.procir.2013.03.004.

Fujishima A, Honda K (1972) Electrochemical photolysis of water at a semiconductor electrode. Nature 238:37–38

Fujishima, A. K. Hashimoto, T. Watanabe, TiO2 Photocatalysis: Fundamentals and Applications, BKC, Tokyo, 1999

Fujishima, A., Rao, T., & Tryk, D. (2000). Titanium dioxide photocatalysis. Journal of Photochemistry and Photobiology C: Photochemistry Reviews, 1(1), 1-21-5567(00)00002-2.

Fujishima, A., Zhang, X., & Tryk, D. (2008). TiO2 photocatalysis and related surface phenomena. Journal of Photochemistry and Photobiology C: Photochemistry Reviews, 63(12), 515–582. https://doi.org/http://doi.org/10.1016/j.surfrep.2008.10.001

Fujishima, Akira & Zhang, Xintong. (2006). Titanium Dioxide Photocatalysis: Present Situation and Future Approaches. Comptes Rendus Chimie - C R CHIM. 9. 750-760. 10.1016/j.crci.2005.02.055.

G Elvin. Nanotechnology for Building Security. International Journal of Architectural Computing 2 (2), 177-187, 2004.

G. Leofantia, M. Padovanb, G. Tozzolac, B. Venturelli. Surface area and pore texture of catalysts. Catalysis Today 41 (1998) 207-219.

Gagaoudakis, E., Kortidis, I., Michail, G., Tsagaraki, K., Binas, V., Kiriakidis, G., & Aperathitis, E. (2016). Study of low temperature rf-sputtered Mg-doped vanadium dioxide thermochromic films deposited

Galasso, Francis S. Structure and Properties of Inorganic Solids. Oxford: Pergamon Press, 1970.

Galeta, Tomislav & Raos, Pero & Stojšić, Josip & Pakši, Ivana. (2016). Influence of Structure on Mechanical Properties of 3D Printed Objects. Procedia Engineering. 149. 100-104. 10.1016/j.proeng.2016.06.644.

Geocell, Geocell foam glass gravel, viewed on 19 June 2020, < https://www.geocell-schaumglas.eu/en/products/foam_glass_gravel/properties/ >.

Gherardi, F., Colombo, A., D'Arienzo, M., Di Credico, B., Goidanich, S., Morazzoni, F., Simonutti, R., Toniolo, L., 2016. Efficient self-cleaning treatments for built heritage based on highly photo-active and well-dispersible TiO2 nanocrystals. Microchemical Journal 126, 54-62. https://doi.org/10.1016/j.microc.2015.11.043.

Gibson I., Rosen D., Stucker B. (2015) Directed Energy Deposition Processes. In: Additive Manufacturing Technologies. Springer, New York, NY, doi.org/10.1007/978-1-4939-2113-3_10.

Gnanaprakasam, Arul & Sivakumar, V.M. & Thirumarimurugan, M. (2015). Influencing Parameters in the Photocatalytic Degradation of Organic Effluent via Nanometal Oxide Catalyst: A Review. Indian Journal of Materials Science. 2015. 1-16. 10.1155/2015/601827.

Godbert, Nicolas & Mastropietro, Teresa & Poerio, Teresa. (2018). Mesoporous TiO2 Thin Films: State of the Art. 10.5772/intechopen.74244.

Goffredo, Giovanni Battista & Accoroni, Stefano & Totti, Cecilia. (2019). Nanotreatments to inhibit microalgal fouling on building stone surfaces. 10.1016/B978-0-08-102641-0.00025-6.

Gogotsi Y. (2006) Nanomaterials Handbook. Taylor & Francis Group, LLC, USA.

Gonzalez, G. and Moo-Young, H., (2004). Transportation Applications of Recycled Concrete Aggregate, FHWA State of the Practice National Review. Washington DC: Federal Highway Administration (pp. 1-47).

Gonzalez, L.; Lison, D.; Kirsch-Volders, M.: Genotoxicity of engineered nanomaterials: a critical review. Nanotoxicology. 2,252–273 (2008).

Goodsite M.E., Hertel O. (2012) Urban Air Quality: Sources and Concentrations. In: Meyers R.A. (eds) Encyclopedia of Sustainability Science and Technology. Springer, New York, NY

GOWRI,S., ALMEIDA,L., AMORIM,T., CARNEIRO,N., SOUTO,A.P., ESTEVES,M.F.: (2010), Polymer Nanocomposites for Multifunctional Finishing of Textiles – a Review, Textile Research Journal, 0, 1–17.

Graettinger AJ, Johnson PW, Sunkari P, Duke MC, Effinger J. Recycling of plastic bottles for use as a lightweight geotechnical material. Manage Environ Qual 2005;16(6):658–69 (An International Journal).

Greßler S and Gazsó A (2012) Nano Trust Dossier No. 032en Nano in the Construction Industry. Institute of Technology Assessment of the Austrian Academy of Sciences, Vienna, Austria. See http://epub.oeaw.ac.at/ita/nanotrust-dossiers/dossier032en.pdf.

Grigoratos, T.; Martini, G. Non-exhaust traffic related emissions. Brake and tyre wear PM, JRC Science and Policy Reports. Jt. Res. Cent. 2014.

Guerrini GL (2012) Photocatalytic performances in a city tunnel in Rome: NOx monitoring results. Construction and Building Materials 27(1): 165–175.

Guo, M.-Z., Maury-Ramirez, A., Poon, C.S., 2015. Versatile photocatalytic functions of self- compacting architectural glass mortars and their inter-relationship. Materials and Design 88, 1260-1268. https://doi.org/10.1016/j.matdes.2015.09.133.

Guo, M.Z., Maury-Ramirez, A., Poon, C.S., 2015a. Photocatalytic activities of titanium dioxide incorporated architectural mortars: effects of weathering and activation light. Building and Environment 94, 395-402.

Guo, M.-Z., Poon, C.-S., 2013. Photocatalytic NO removal of concrete surface layers intermixed with TiO2. Building and Environment 70, 102-109.

Gupta, M. & Das, A. & Subramanian, S. .(2017). A mini review on application of TiO2 nanoparticle in wool technology. Journal of Industrial Pollution Control. 33. 1633-1638.

Gypsum recycling International, "General Overview of Plasterboard Recycling", viewed on 10 August 2020, < http://gipsrecycling.no/17085-1_Generaloverview/ >.

H. Lipson, M. Kurman, Fabricated: The New World of 3D Printing, John Wiley & Sons, 2013.

H.W. Kang, D.W. Cho, Development of an indirect stereolithography technology for scaffold fabrication with a wide range of biomaterial selectivity, Tissue Eng. Part C Methods 18 (9) (2012) 719–729.

Hameed, M.S.; Sekar, A.S.S. Properties of green concrete containing quarry rock dust and marble sludge powder as fine aggregate. J. Eng. Appl. Sci. 2009, 4, 83–89.

Hansen TC, Narud H (1983) Strength of recycled concrete made from crushed concrete coarse aggregate. Concr Int 5(1):79–83

Haruehansapong, S., Pulngern, T., Chucheepsakul, S., 2014. Effect of the particle size of nanosilica on the compressive strength and the optimum replacement content of cement mortar containing nano-SiO2. Construction and Building Materials 50, 471-477.

Haugen, Håvard & Lyngstadaas, Staale. (2016). Antibacterial effects of titanium dioxide in wounds. 10.1016/B978-1-78242-456-7.00021-0.

Hemeida F.A.E.A.O. Green nanoarchitecture, MSc thesis, University of Alexandria, Egypt (2010)

Hoffmann MR, Martin ST, Choi W et al (1995) Environmental applications of semiconductor photocatalysis. Chem Rev 95(1):69–96

Hopkinson, P., Wang, Y., Chen, H., Lam, D., Zhou, K., 2019. Recovery and reuse of structural products from end-of-life buildings. Eng. Sustain. 172 (3), 119-128. https://doi.org/10.1680/jensu.18.00007.

Hou, P-k, Kawashima, S., Wang, K-j, Corr, D.J., Qian, J-s, Shah, S.P., 2013. Effects of colloidal nanosilica on rheological and mechanical properties of fly ash cement mortar. Cement and Concrete Composites 35 (1), 12-22.

Hu, C., Lu, T., Chen, F., & Zhang, R. (2013). A brief review of graphene–metal oxide composites synthesis and applications in photocatalysis. Journal of the Chinese Advanced Materials Society, 1(1), 21–39. https://doi.org/10.1080/22243682.2013.771917

Hussein-Al-Ali, S. H., El Zowalaty, M. E., Hussein, M. Z., Geilich, B. M., and Webster, T. J. (2014). Synthesis, characterization, and antimicrobial activity of an ampicillin-conjugated magnetic nanoantibiotic for medical applications. Int. J. Nanomed. 9, 3801–3814. doi: 10.2147/IJN.S61143

Hydrotect1, viewed on 8 September 2020, < https://jp.toto.com/products/hydro/en/index.htm >.

Hydrotect2, viewed on 8 September 2020, <https://jp.toto.com/hydrotect/eng/about04.html >.

I. Gibson, D. Rosen and B. Stucker, Additive Manufacturing Technologies: 3D Printing, Rapid Prototyping, and Direct Digital Manufacturing, Springer, New York, 2014.

I. Gibson, D.W. Rosen, B. Stucker, Additive Manufacturing Technologies, 238 Springer, New York, 2010, http://dx.doi.org/10.1007/978-1-4939-2113-3 ISBN 978-1-4939-2112-6.

I. Gibson, T. Kvan, L.W. Ming, Rapid prototyping for architectural models, Rapid Prototyp. J. 8 (2) (2002) 91–95.

I. Haider, B. Cetin, Z. Kaya, M. Hatipoglu, A. Cetin, H.A. Ahmet, Evaluation of the Mechanical Performance of Recycled Concrete Aggregates Used in Highway Base Layers, Geo-Congress 2014, Tech Pap, 2014, 3686–2594, doi:10.1061/9780784413272.357.

International Energy Agency (IEA) 2012, "IEA Solar HC Roadmap FoldOut Print"

International Institute of Building Enclosure Consultants (IIBEC) http://rci-online.org/wp-content/uploads/molleti-et-al-fig-2.jpg

IPCC, 2018: Global warming of 1.5°C. An IPCC Special Report on the impacts of global warming of 1.5°C above pre-industrial levels and related global greenhouse gas emission pathways, in the context of strengthening the global response to the threat of climate change, sustainable development, and efforts to eradicate poverty [V. Masson-Delmotte, P. Zhai, H. O. Pörtner, D. Roberts, J. Skea, P.R. Shukla, A. Pirani, W. Moufouma-Okia, C. Péan, R. Pidcock, S. Connors, J. B. R. Matthews, Y. Chen, X. Zhou, M. I. Gomis, E. Lonnoy, T. Maycock, M. Tignor, T. Waterfield (eds.)]. In Press.

ISO/ASTM, 52900-15, Standard Terminology for Additive Manufacturing – General Principles-Terminology, ASTM International, West Conshohocken, 2015, dx.doi.org/10.1520/ISOASTM52900-15.

Izumi, Fujio and Takuji Ikeda. "Implementation of the Williamson-Hall and Halder-Wagner Methods into RIETAN-FP." (2014).

J. de Brito, N. Saikia, Concrete with recycled aggregates in international codes, Recycl. Aggregates Concr. (2013), https://doi.org/10.1007/978-1-4471-4540-0.

J. Kośny, PCM-Enhanced Building Components. Cham: Springer International Publishing, 2015.

J. Mireles, D. Espalin, D. Roberson, B. Zinniel, F. Medina, R. Wicker, Fused deposition modelling of metals, Proceedings of Solid Freeform Fabrication Symposium 2012, pp. 836–845.

J. Pegna, Exploratory investigation of solid freeform construction, Autom. Constr. (1997) 427–437, http://dx.doi.org/10.1016/S0926-5805(96)00166-5.

J. Saurav, "Application of nanotechnology in building materials", International Journal of Engineering Research and Applications, 2 (5), 2012, 1077-1082.

J. Tidd, J. Bessant, K. Pavitt, Managing Innovation Integrating Technological, Market and Organizational Change, John Wiley and Sons, Chichester, 1997.

J. Baghdachi, D. Clemans, Formulation and evaluation of antimicrobial waterborne and high solids coatings, in: Smart Coatings Conference, Orlando, FL, February 15–17, 2006.

J.A. Inzana, D. Olvera, S.M. Fuller, J.P. Kelly, O.A. Graeve, E.M. Schwarz, H.A. Awad, 3D printing of composite calcium phosphate and collagen scaffolds for bone regeneration, Biomaterials 35 (13) (2014) 4026–4034.

J.M. Makar and J.J. Beaudoin, "Carbon nanotubes and their application in the construction Industry", 1s International Symposium on Nanotechnology in Construction, 2003, pp. 331-341

J.M. Pearce, C.M. Blair, K.J. Laciak, R. Andrews, A. Nosrat, I. Zelenika-Zovko, 3-D printing of open source appropriate technologies for self-directed sustainable development, J. Sustain. Dev. 3 (4) (2010) 17–29.

J.N. Davis Roofing Co., “IS SHINGLE RECYCLING A GOOD IDEA?”, viewed on 19 June 2020, < https://jndavis.com/recycled-shingles/ >

J.-P. Kruth, L. Froyen, J. Van Vaerenbergh, P. Mercelis, M. Rombouts, B. Lauwers, Selective laser melting of iron-based powder, J. Mater. Process. Technol. 149 (1-3) (2004) 616–622.

J.-P. Kruth, P. Mercelis, J. Van Vaerenbergh, Binding mechanisms in selective laser sintering and selective laser melting, Rapid Prototyp. J. 11 (1) (2005) 26–36.

J.R. Castrejon-Pita, W.R.S. Baxter, J. Morgan, S. Temple, G.D. Martin, I.M. Hutchings, Future, opportunities and challenges of Inkjet technologies, Atomization Sprays 23 (2013) 541–565.

J.-Y. Lee, J. An, C.K. Chua, Fundamentals and applications of 3D printing for novel materials, Appl. Mater. Today 7 (2017) 120–133.

Jagarapu, Durga Chaitanya Kumar & Prasad, B.. (2019). Experimental Examination of Fiber Reinforced Concrete Incorporation with Lathe Steel Scrap. International Journal of Innovative Technology and Exploring Engineering. 9. 3729 - 3732. 10.35940/ijitee.B6692.129219.

Jalal, M., Fathi, M., Farzad, M., 2013. Effects of fly ash and TiO2 nanoparticles on rheological, mechanical, microstructural and thermal properties of high strength self-compacting concrete. Mechanics of Materials 61, 11-27.

Janjua, Z.A. Icephobic Nanocoatings for Infrastructure Protection. In Nanotechnology in Eco-Efficient Construction, 2nd ed.; Pacheco-Torgal, F., Diamanti, M.V., Nazari, A., Goran-Granqvist, C., Pruna, A., Amirkhanian, S., Eds.; Woodhead Publishing: Duxford, UK, 2019; Chapter 13; pp. 281–302.

Janus, Magdalena & Zając, Kamila. (2019). Self-cleaning efficiency of nanoparticles applied on facade bricks. 10.1016/B978-0-08-102641-0.00024-4.

Jasim KE (2015) Quantum dots solar cells, chapter 11. In: Kosyachenko LA (ed) Solar cells: new approaches and reviews. InTech Open Publishing Company, Croatia

Jelena Božić, Nano insulation materials for energy efficient buildings Contemporary Materials (Renewable energy sources), VI−2 (2015)

K. Davidson, B. Moyer, K. Ramanathan, A. Preuss, B. Pomper, Formulating coatings with silver-based antimicrobials: a systematic approach, JCT Coatings Technology (January 2007) 56–62.

K. Venkatraman, Dr. V. Tamizharasan, “Electrically Conductive Concrete” Vol. 4, Issue 8, August 2015.

Kale, Ravindra & Meena, Drchet. (2012). Synthesis of Titanium dioxide Nanoparticles and Application on Nylon fabric using Layer by Layer technique for Antimicrobial Property. Advances in Applied Science Research. 3. 3073.

Kalogeropoulou S, Pantazopoulou P (2015) Study of corrosion protection offered to concrete reinforcement by organic coatings and inhibitors. A -Technology and Sciences 15: 31-40.

Kapridaki, Ch., Pinho, L., Mosquera, M.J., Maravelaki e Kalaitzaki, P., 2014. Producing photoactive, transparent and hydrophobic SiO2-crystalline TiO2 nanocomposites at ambient conditions with application as self-cleaning coatings. Applied Catalysis B: Environmental 156e157, 416-427.

Kasarda, M. & Terpenny, Janis & Inman, Daniel & Precoda, Karl & Jelesko, John & Sahin, Asli & Park, Jaeil. (2007). Design for adaptability (DFAD)—a new concept for achieving sustainable design. Robotics and Computer-Integrated Manufacturing. 23. 727-734. 10.1016/j.rcim.2007.02.004.

Kashani, Alireza & Ngo, Tuan. (2018). Optimisation of Mixture Properties for 3D Printing of Geopolymer Concrete. 10.22260/ISARC2018/0037.

Khan, Mohd. (2020). Mix suitable for concrete 3D printing: A review. Materials today: proceedings. 10.1016/j.matpr.2020.03.825.

Khoshnevis, B. (1999). "Contour Crafting — state of development", 10th Solid Freeform Fabrication Proceedings, Austin, 743–750.

Kibasomba, Pierre & Dhlamini, M. & Maaza, Malik & Liu, Chuan-Pu & Rashad, Mohamed & Rayan, Diaa & Mwakikunga, Bonex. (2018). Strain and grain size of TiO 2 nanoparticles from TEM, Raman spectroscopy and XRD: The revisiting of the Williamson-Hall plot method. Results in Physics. 9. 10.1016/j.rinp.2018.03.008.

Kifayah Abbood Alsaffar, Review of the Use of Nanotechnology in Construction Industry, International Journal of Engineering Research and Development Volume 10, Issue 8 (August 2014), PP.67-70

Kim, Hwang-Hee & Park, Chan-Gi. (2016). Plant Growth and Water Purification of Porous Vegetation Concrete Formed of Blast Furnace Slag, Natural Jute Fiber and Styrene Butadiene Latex. Sustainability. 8. 386. 10.3390/su8040386.

Kim, S.M., In, I. and Park, S.Y. (2016). Study of photo-induced hydrophilicity and self-cleaning property of glass surfaces immobilized with TiO2 nanoparticles using catechol chemistry. Surf. Coatings Technol. 294 : 75-82.

Kittusamy, N.K., Buchholz, B., 2004. Whole-body vibration and postural stress among operators of construction equipment: a literature review. J. Saf. Res. 35 (3), 255-261.

Klompas M, Anderson D, Trick W, Babcock H, Kerlin MP, Li L, Sinkowitz-Cochran R, Ely EW, Jernigan J, Magill S, Lyles R, O'Neil C, Kitch BT, Arrington E, Balas MC, Kleinman K, Bruce C, Lankiewicz J, Murphy MV, E Cox C, Lautenbach E, Sexton D, Fraser V, Weinstein RA, Platt R; CDC Prevention Epicenters. The preventability of ventilator-associated events. The CDC Prevention Epicenters Wake Up and Breathe Collaborative. Am J Respir Crit Care Med. 2015;191(3):292-301.

Knoeria C, Binderb CR, Althausa H. Decisions on recycling: construction stakeholders' decisions regarding recycled mineral construction materials. Resour Conserv Recycl 2011; 55:1039–50.

Kohler, N., & Yang, W. (2007). Long-term management of building stocks. Building Research and Information, 34(3), 287–294.

Kolokotsa, D. (2017). Smart cooling systems for the urban environment. Using renewable technologies to face the urban climate change. Solar Energy.

Kolokotsa, D. Tsoutsos, T and Papantoniou, S. 2012 Energy conservation techniques for hospital buildings. Advances In Building Energy Research Vol. 6, Iss. 1

Kolokotsa, D., Rovas, D., Kosmatopoulos, E., Kalaitzakis, K., 2011. A roadmap towards intelligent net zero- and positive-energy buildings. Sol. Energy 85, 3067–3084.

Korayem, A.H., Tourani, N., Zakertabrizi, M., Sabziparvar, A.M., Duan, W.H., 2017. A review of dispersion of nanoparticles in cementitious matrices:Nanoparticle geometry perspective. Construction and Building Materials 153, 346-357.

Krassenstein E. D-Shape intern unveils plans to 3D print unique buildings in Australia & beyond. 2015, viewed on 6 June 2020, < https://www.3dprint.com/64469/3d-printed-buildings-australia/ >

Krassenstein E. D-Shape looks to 3D print bridges, a military bunker, and concrete/metal mixture. 2014, viewed on 6 June 2020, < https://www.3dprint.com/27229/d-shape-3d-printed-military >

Krystek, M. and Górski, M. (2018). Nanomaterials in Structural Engineering. In New Uses of Micro and Nanomaterials. IntechOpen.

Kurapati S. (2014). Nanomaterials for Concrete Technology. International Journal of Civil, Structural, Environmental and Infrastructure Engineering Research and Development (IJCSEIERD), 4(3), 79–90.

LabX, Siemens D5000, viewed on 13 Aygust 2020, < https://www.labx.com/item/siemens-bruker-d5000-x-ray-powder-diffraction-xrd-system/10423995 >.

Langford J. I. (1992). The Use of the Voigt Function in Determining Microstructural Properties from Diffraction Data by means of Pattern Decomposition. NIST Spec. Publ. 846 110

Laplaza, A., Jimenez-Relinque, E., Campos, J., Castellote, M., 2017. Photocatalytic behavior of colored mortars containing TiO2 and iron oxide based pigments. Construction and Building Materials 144, 300-310.

Le, Thanh & Austin, Simon & Lim, Sungwoo & Buswell, R.A. & Gibb, A. & Thorpe, Antony. (2012b). Mix design and fresh properties for high-performance printing concrete. Materials and Structures. 45. 1-12. 10.1617/s11527-012-9828-z.

Le, Thanh & Austin, Simon & Lim, Sungwoo & Buswell, R.A. & Law, R. & Gibb, Alistair & Thorpe, Antony. (2012a). Hardened properties of high-performance printing concrete. Cement and Concrete Research. 42. 558–566. 10.1016/j.cemconres.2011.12.003.

Leach, Neil & Carlson, Anders & Khoshnevis, Behrokh & Thangavelu, Madhu. (2012). Robotic Construction by Contour Crafting: The Case of Lunar Construction. International Journal of Architectural Computing. 10. 423-438. 10.1260/1478-0771.10.3.423.

Lee, Hyemin & Kang, Hyo-Rang & An, Kay-Hyeok & Kim, Hong-Gun & Kim, Byung-Joo. (2013). Comparative studies of porous carbon nanofibers by various activation methods. Carbon letters. 14. 10.5714/CL.2013.14.3.180.

Lee, J.; Mahendra, S.; Alvarez, P.J.J. Nanomaterials in the Construction Industry: A Review of Their Applications and Environmental Health and Safety Considerations. ACS Nano 2010,4, 3580–3590.

Lee, Y.C., Hong, Y.P., Lee, H.Y., Kim, H., Jung, Y.J., Ko, K.H., Jung, H.S., Hong, K.S., 2003. Photocatalysis and hydrophilicity of doped TiO2 thin films. Journal of Colloid and Interface Science 267, 127-131.

Leung, Y. H., Ng, A. M., Xu, X., Shen, Z., Gethings, L. A., Wong, M. T., et al. (2014). Mechanisms of antibacterial activity of MgO: non-ROS mediated toxicity of MgO nanoparticles towards Escherichia coli. Small 10, 1171–1183. doi: 10.1002/smll.201302434

Levy, Karyne 2014, A Chinese Company 3D Printed 10 Houses In A Day, Business Insider Australia, viewed 1 June 2020, < https://www.businessinsider.com/a-chinese-company-3d-printed-10-houses-in-a-day-2014-4 >.

Leyland, Nigel & Carroll (Podporska), Joanna & Browne, John & Hinder, Steven & Quilty, Brid & Pillai, Suresh. (2016). Highly Efficient F, Cu doped TiO2 anti-bacterial visible light active photocatalytic coatings to combat hospital-acquired infections. Scientific Reports. 6. 24770. 10.1038/srep24770.

Li, H., Xiao, H.-G., Yuan, J., Ou, J., 2004. Microstructure of cement mortar with nanoparticles. Composites Part B: Engineering 35, 185e189.

Lim, Sungwoo & Buswell, R.A. & Le, Thanh & Austin, Simon & Gibb, Alistair & Thorpe, Antony. (2012). Developments in construction-scale additive manufacturing processes. Automation in Construction - Automation in Construction, 21 (1), pp. 262-268.

Lim, Sungwoo & Buswell, R.A. & Le, Thanh & Wackrow, Rene & Austin, Simon & Gibb, Alistair & Thorpe, Antony. (2011). Development of a Viable Concrete Printing Process. 10.22260/ISARC2011/0124.

Low, M.-S. (2005). Material flow analysis of concrete in the United States. Unpublished Master of Science in Building Technology thesis, Massachusetts: Institute of Technology.

Lowke, Dirk & Enrico, Dini & Perrot, Arnaud & Weger, Daniel & Gehlen, Christoph & Dillenburger, Benjamin. (2018). Particle-bed 3D printing in concrete construction – Possibilities and challenges. Cement and Concrete Research. 112. 60-65. 10.1016/j.cemconres.2018.05.018.

M. Behera, S. K. Bhattacharyya, A. K. Minocha, R. Deoliya, and S. Maiti, "Recycled aggregate from C&D waste & its use in concrete – A breakthrough towards sustainability in construction sector: A review," Construction and Building Materials, vol. 68, pp. 501-516, 10/15/ 2014.

M. d. R. Merino, P. I. Gracia, and I. S. W. Azevedo, "Sustainable construction: construction and demolition waste reconsidered," Waste Management & Research, vol. 28, 2010.

M. Rajeh, J.E. Tookey, J.O.B. Rotimi, Estimating transaction costs in the New Zealand construction procurement: a structural equation modelling methodology, Eng. Constr. Archit. Manag. 22 (2) (2015) 242–267.

M. Yeheyis, K. Hewage, M. Alam, C. Eskicioglu, and R. Sadiq, "An overview of construction and demolition waste management in Canada: a lifecycle analysis approach to sustainability," Clean Technologies and Environmental Policy, vol. 15, pp. 81-91, Feb 2013 2013-09-25 2013.

M. Yossef, A. Chen, Applicability and Limitations of 3D Printing for Civil Structures, The Proceedings of the 2015 Conference on Autonomous and Robotic Construction of Infrastructure, 2015 http://lib.dr.iastate.edu/intrans_reports/141/.

M. Zahid, E.L. Papadopoulou, G. Suarato, V.D. Binas, G. Kiriakidis, I. Gounaki, O. Moira, D. Venieri, I.S. Bayer, A. Athanassiou, Fabrication of visible light-induced antibacterial and self-cleaning cotton fabrics using manganese doped TiO2 nanoparticles, ACS Appl. Bio Mater. 1 (2018) 1154–1164, http://dx.doi.org/10.1021/acsabm.8b00357.

M.-J. Gaoa, X.-D. Wanga, M. Guob, and M. Zhang, “Contrast on COD photo-degradation in coking wastewater catalyzed by TiO2 and TiO2-TiO2 nanorod arrays,” Catalysis Today, vol. 174, no. 1, pp. 79–87, 2011.

Ma, GuoWei & Wang, Li & Ju, Yang. (2017). State-of-the-art of 3D printing technology of cementitious material—An emerging technique for construction. Science China Technological Sciences. 10.1007/s11431-016-9077-7.

MacDonald, Mark. Technical Paper: “Graffiti: Addressing $12 Billion Annual and Growing Problem.” Valsparcoilextrusion.com, Valspar (2017).

Magill SS, Edwards JR, Bamberg W, Beldavs ZG, Dumyati G, Kainer MA, et al. Multistate point-prevalence survey of health care-associated infections. N Engl J Med. 2014;370(13):1198–208.

Makar, J. M., Margeson, J., & Luh, J. (2005, August 22–24). Carbon nanotube/cement composites– Early results and potential applications. Proceedings of 3rd international conference on Construction Materials: Performance, Innovations and Structural Implications, Vancouver, pp. 1–10.

Mangialardo, A., Micelli, E., 2018. Rethinking the construction industry under the circular economy: principles and case studies. In: Proceedings of the International conference on Smart and Sustainable Planning for Cities and Regions, 1, pp. 333e344. https://doi.org/10.1007/978-3-319-75774-2_23.

Mann, S. (2006). "Nanotechnology and Construction, " Nanoforum Report. www.nanoforum.org, May 30, 2008. MMFX Steel Corp. http://www. mmfx.com /products.shtml, May 30, 2008.

Mansour, A.M.H., Al-Dawery, S.K., 2018. Sustainable self-cleaning treatments for architectural facades in developing countries. Alexandria Engineering Journal in press.

Maraveas, Chrysanthos. (2012). Fiber-Reinforced Polymer-Strengthened/Reinforced Concrete Structures Exposed to Fire: A Review. Structural Engineering International. 22. 500-513. 10.2749/101686612X13363929517613.

Matoh, Lev & Žener, Boštjan & Cerc Korošec, Romana & Lavrencic Stangar, Urska. (2019). Photocatalytic water treatment. 10.1016/B978-0-08-102641-0.00027-X.

Maury-Ramirez, A., De Muynck, W., Stevens, R., Demeestere, K., De Belie, N., 2013. Titanium dioxide-based strategies to prevent algal fouling on cementitious materials. Cement and Concrete Composites 36, 93-100. https://doi.org/10.1016/j.cemconcomp.2012.08.030.

McDonough, W., Braungart, M., & Clinton, B. (2013). The upcycle: Beyond sustainability. London: Macmillan.

Mefteh H, Kebaïli O, Oucief H, Berredjem L, Arabi N. Influence of moisture conditioning of recycled aggregates on the properties of fresh and hardened concrete. J Cleaner Prod 2013;54(2013):282–8.

Metso, Mobile Jaw crusher, viewed on 24 June 2020, <https://www.metso.com/products/crushers/mobile-crushers/mobile-jaw-crushers/lokotrack-lt106-mobile-jaw-crusher/>.

Metso, Mobile Vertical Shaft Impact crusher, viewed on 24 June 2020 <https://www.metso.com/products/crushers/mobile-crushers/mobile-impact-crushers/lokotrack-lt7150-mobile-vsi-crusher/>.

Metso, Portable Cone crusher, viewed on 24 June 2020, <https://www.metso.com/products/crushers/portable-crushers/portable-cone-crushers/nw220gpd-rapid-portable-cone-crusher/>.

Micromeritics, Gemini VII 2390 Surface Area Analyzer, viewed on 13 August 2020, <https://www.micromeritics.com/Product-Showcase/Gemini-VII-2390-Series-Surface-Area-Analyzers.aspx>.

Milestone, Milestone flexiWAVE, viewed on 13 August 2020 <https://www.milestonesrl.com/products/microwave-assisted-synthesis/flexiwave>.

Miller, Ana & Sanmartín, Patricia & Pereira-Pardo, Lucía & Dionísio, Amelia & Saiz-Jimenez, C & Macedo, Maria & Prieto, Beatriz. (2012). Bioreceptivity of building stones: A review. The Science of the total environment. 426. 1-12. 10.1016/j.scitotenv.2012.03.026.

Min-Hsin Yeh, Long Lin, Po-Kang Yang, and Zhong Lin Wang "Motion-Driven Electrochromic Reactions for Self-Powered Smart Window System" ACS Nano 2015 9 (5), 4757-4765 DOI: 10.1021/acsnano.5b00706

Miranda-García N, Suárez S, Sánchez B, Coronado JM, Malato S, Maldonado MI (2011) Photocatalytic degradation of emerging contaminants in municipal wastewater treatment plant effluents using immobilized TiO2 in a solar pilot plant. Appl Catal B Environ 103 (3–4):294–301. doi.org/10.1016/j.apcatb.2011.01.030.

Moellmann, Jonas & Ehrlich, Stephan & Tonner, Ralf & Grimme, Stefan. (2012). A DFT-D study of structural and energetic properties of TiO 2 modifications. Journal of physics. Condensed matter: An Institute of Physics journal. 24. 424206. 10.1088/0953-8984/24/42/424206.

Moga, Ligia & Bucur, Adrian. (2018). Nano insulation materials for application in nZEB. Procedia Manufacturing. 22. 309-316. 10.1016/j.promfg.2018.03.047.

Mohajerani, A.; Kadir, A.A.; Larobina, L. A practical proposal for solving the world's cigarette butt problem: Recycling in fired clay bricks. Waste Manag. 2016, 52, 228–244.

Mohajerani, A.; Ukwatta, A.; Jeffrey-Bailey, T.; Swaney, M.; Ahmed, M.; Rodwell, G.; Bartolo, S.; Eshtiaghi, N.; Setunge, S. A Proposal for Recycling the World's Unused Stockpiles of Treated Wastewater Sludge (Biosolids) in Fired-Clay Bricks. Buildings 2019, 9, 14.

Mohajerani, Abbas & Burnett, Lucas & Smith, John & Kurmus, Halenur & Milas, John & Arulrajah, Arul & Abdul Kadir, Kadir. (2019). Nanoparticles in Construction Materials and Other Applications, and Implications of Nanoparticle Use. Materials. 12. 10.3390/ma12193052.

Mohamed, A.S.Y. Nano-Innovation in Construction, A New Era of Sustainability. In Proceedings of the International Conference on Environment and Civil Engineering, Pattaya, Thailand, 24–25 April 2015; ICEACE: Pattaya, Thailand.

Monshi, Ahmad & Foroughi, Mohammad Reza & Monshi, Mohammad. (2012). Modified Scherrer Equation to Estimate More Accurately Nano-Crystallite Size Using XRD. World Journal of Nano Science and Engineering. 2. 154-160. 10.4236/wjnse.2012.23020.

Morin F. Oxides which show a metal-to-insulator transition at the Neel temperature. Phys Rev Lett 1959;3(1):34.

Mudimela, P. R., Nasibulina, L. I., Nasibulin, A. G., Cwirzen, A., Valkeapää, M., Habermehl-Cwirzen, K., Kauppinen, E. I. (2009). Synthesis of carbon nanotubes and nanofibers on silica and cement matrix materials. Journal of Nanomaterials, 2009. https://doi.org/10.1155/2009/526128

Mukhopadhyaya, P., Maclean, D., Korn, J., Reenen, D. Van, & Molleti, S. (2014). Building application and thermal performance of vacuum insulation panels (VIPs) in Canadian subarctic climate. Energy & Buildings, 85, 672–680. https://doi.org/10.1016/j.enbuild.2014.08.038

Munafo, P., Goffredo, G.B., Quagliarini, E., 2015. TiO2-based nanocoatings for preserving architectural stone surfaces: an overview. Construction and Building Materials 84, 201-218. https://doi.org/10.1016/j.conbuildmat.2015.02.083.

N.C. Halder, C.N.J. Wagner, Separation of particle size and lattice strain in integral breadth measurements, Acta Crystallogr. 20 (2) (1966) 312–331.

NAHB (1998). From Roofs to Roads... Recycling Asphalt Roofing Shingles into Paving Materials. NAHB Research Center, National Association of Home Builders, Upper Marlboro, Maryland.

NASA/JPL, http://stardust.jpl.nasa.gov/photo/aerogel.html

Nath, Debojyoti & Singh, Fouran & Das, Ratan. (2019). X-Ray Diffraction Analysis by Williamson-Hall, Halder-Wagner and Size-Strain Plot Methods of CdSe Nanoparticles- A comparative study. Materials Chemistry and Physics. 239. 122021. 10.1016/j.matchemphys.2019.122021.

Nath, R.K., Zain, M.F.M., Jamil, M., 2016. An environment-friendly solution for indoor air purification by using renewable photocatalysts in concrete: a review. Renewable and Sustainable Energy Reviews 62, 1184-1194.

National Asphalt Pavement Association (NAPA), authors: Brett A. Williams, J. Richard Willis, Kent R. Hansen, P.E., & Brett Stanton, P.E. (2019), Report No. Information Series 136, 'Guidelines for the Use of Reclaimed Asphalt Shingles in Asphalt Pavements, 2nd Edition'.

National Nanotechnology Initiative (NNI), What It Is and How It Works. Available online: https://www.nano.gov/nanotech-101/what.

Nazari, A., Riahi, S., 2011. Improvement compressive strength of concrete in different curing media by Al2O3 nanoparticles. Materials Science and Engineering A 528 (3), 1183-1191.

Neikov, O. D., Naboichenko, S. S., & Yefimov, N. V. (2019). HANDBOOK OF NON-FERROUS METAL POWDERS. TECHNOLOGIES AND APPLICATIONS: monograph. (Second Edition ed.) Amsterdam: Elsevier.

Niroumand, H.; Zain, M.; Alhosseini, S.N. The Influence of Nano-clays on Compressive Strength of Earth Bricks as Sustainable Materials. Procedia-Soc. Behav. Sci. 2013, 89, 862–865.

Nithesh Nadarajah (2018). Development of concrete 3D printing. Unpublished Master of Science in Building Technology thesis. Aalto University.

Nosaka, Y., and Nosaka, A. Y. (2017). Generation and detection of reactive oxygen species in photocatalysis. Chem. Rev. 117, 11302–11336. doi: 10.1021/acs.chemrev.7b00161

Nowack, B.; David, R. M.; Fissan, H.; Morris, H.; Shatkin, J. A.; Stinz, M.; Zepp, R.; Brouwer, D. Environ. Internat. 2013, 59, 1. DOI: 10.016/j.envint.2013.04.003

O.E. Semonin, J.M. Luther, M.C. Beard Quantum dots for next-generation photovoltaics Mater. Today, 15 (11) (2012), pp. 508-515

Ogunsona, Emmanuel & Muthuraj, Rajendran & Ojogbo, Ewomazino & Valerio, Oscar & Mekonnen, Tizazu. (2019). Engineered nanomaterials for antimicrobial applications: A review. 10.1016/j.apmt.2019.100473.

Oksengendler, Boris & Turaeva, Nigora & Rashidova, S. (2011). Mechanism and Statistic Theory of Multiple Exciton Generation in Quantum Dots. Arhive.

Oyedele, Lukumon & Ajayi, Saheed & Kadiri, Kabir. (2014). Use of recycled products in UK construction industry: An empirical investigation into critical impediments and strategies for improvement. Resources, Conservation and Recycling. 93. 23–31. 10.1016/j.resconrec.2014.09.011.

Ozer, Cemal. (12-15 May 2008) Monitoring of Tall Building's Dynamic Behaviour Using Precision Inclination Sensors. Fig.net. 22 March,2014.

P. Mukhopadhyaya, K. Kumaran, N. Normandin, D. van Reenen, J. Lackey High-performance vacuum insulation panel: development of alternative core materials J Cold Reg Eng, 22 (4) (2008), pp. 103-123

P. Wu, J. Wang, X. Wang, A critical review of the use of 3-D printing in the construction industry, Autom. Constr. 68 (2016) 21–31, http://dx.doi.org/10.1016/j.autcon.2016.04.005.

P.K. Kolay, M. Akentuna, Characterization and utilization of recycled concrete aggregate from illinois as a construction material, Geo-Congress 2014 Tech Pap, 2014, 3570–3561, doi: 10.1061/9780784413272.345.

Pacheco-Torgal, F., & Jalali, S. (2011). Nanotechnology: Advantages and drawbacks in the field of construction and building materials. Construction and Building Materials, 582–590.

Padmavathy, N., and Vijayaraghavan, R. (2011). Interaction of ZnO nanoparticles with microbes – a physio and biochemical assay. J. Biomed. Nanotechnol. 7, 813–822. doi: 10.1166/jbn.2011.1343

Pagliarulo, Antonella & Petronella, Francesca & Licciulli, Antonio & Rocca, A. & Diso, Daniela & Calia, Angela & Lettieri, Mariateresa & Colangiuli, Donato & Agostiano, Angela & Curri, M. & Comparelli, Roberto. (2012). Photocatalytic nanostructured TiO2 for protection of porous and compact stone. 10.13140/RG.2.1.2733.7762.

Pakdel, E., Daoud, W.A. and Wang, X. (2013). Self-cleaning and superhydrophilic wool by TiO2/SiO 2 nanocomposite. Applied surface science. 275 : 397-402.

Panda, Biranchi, Ming Jen Tan, Ian R. Gibson and Chee Kai Chua. "The Disruptive Evolution Of 3D Printing." (2016).

Parveen, S., Rana, S., Fangueiro, R., 2013. A review on nanomaterial dispersion, microstructure and mechanical properties of carbon nanotube and nanofiber reinforced cementitious composites. Journal of Nanomaterials 19.

Pauling, Linus. The Nature of the Chemical Bond, 3rd edition. Ithaca, NY: Cornell University Press, 1960.

Pérez-Nicolas, M., Navarro-Blasco, I., Fernandez, J.M., Alvarez, J.I., 2017. The effect of TiO2 doped photocatalytic nano-additives on the hydration and microstructure of portland and high alumina cements. Nanomaterials 7 (10), 329.

Phogat, Navneet & Khan, Shadab & Shankar, Shiv & Ansary, Abu & Uddin, Imran. (2016). Fate Of Inorganic Nanoparticles In Agriculture:. Advanced Materials Letters. 7. 3-12. 10.5185/amlett.2016.6048.

Pilakoutas, K. and R. Strube (2001), Re-use of Tyres Fibres in Concrete. Proceedings of the International Symposium on Recycling and Reuse of Used Tyres, Thomas Telford, University of Dundee, Dundee, UK.

Pilkington St (2001), http://www.activglass.com/.

Pino, F., Fermo, P., La Russa, M., Ruffolo, S., Comite, V., Baghdachi, J., Pecchioni, E., Fratini, F., Cappelletti, G., 2016. Advanced mortar coatings for cultural heritage protection. Durability towards prolonged UV and outdoor exposure. Environmental Science and Pollution Research. https://doi.org/10.1007/s11356-016-7611-3.

Plasterboard recycling, viewed on 10 August 2020, < http://www.plasterboardrecycling.co.uk >.

Pokropivny, V.V., Skorokhod, V.V., 2007. Classification of nanostructures by dimensionality and concept of surface forms engineering in nanomaterial science. Materials Science and Engineering C 27 (5e8), 990-993.

Pokropivny, V.V., Skorokhod, V.V., 2008. New dimensionality classifications of nano-structures. Physica E: Low-dimensional Systems and Nanostructures 40 (7), 2521-2525.

Pomponi, F., Moncaster, A., 2017. Circular economy for the built environment: a research framework. J. Clean. Prod. 143, 710e718. https://doi.org/10.1016/j.jclepro.2016.12.055.

Poon, Chi Sun & Guo, Ming-Zhi. (2015). Effect of Cement Types on Photocatalytic NOx Removal and Its Underlying Mechanisms. 10.1007/978-3-319-17088-6_43.

Pratik Dewan, "Nanotech Enabled Anti-Graffiti Clear Coating System", Bom. Tech., 59, 2009

Price, C. A., and Doehne, E. (2011). Stone Conservation: An Overview of Current Research. Los Angeles: Getty Conservation Institute.

Quagliarini, Enrico & Bondioli, Federica & Goffredo, Giovanni Battista & Licciulli, Antonio & Munafò, Placido. (2012). Self-cleaning materials on Architectural Heritage: Compatibility of photo-induced hydrophilicity of TiO2 coatings on stone surfaces. Journal of Cultural Heritage. 14. 10.1016/j.culher.2012.02.006.

R. Baetens, Aerogel Insulation for Building Applications: A State-of-the-Art Review, Energy and Buildings 43, 2011, pp.761–769.

R. Bogue, 3D printing: the dawn of a new era in manufacturing, Assem. Autom. 33 (4) (2013) 307–311.

R. Herrador, P. Pérez, L. Garach, J. Ordóñez, Use of recycled construction and demolition waste aggregate for road course surfacing, J. Transp. Eng. 138 (2012) 182–190, https://doi.org/10.1061/(ASCE)TE.1943-5436.0000320.

R. Nassar, P. Soroushian, Use of recycled aggregate concrete in pavement construction, J. Solid Waste Technol. Manage. 42 (2016) 137–144, https://doi.org/10.5276/JSWTM.2016.137.

R.A. Buswell, R. Soar, A.G. Gibb, A. Thorpe, Freeform construction: mega-scale rapid manufacturing for construction, Autom. Constr. 16 (2007) 224–231.

R.P. Mudge, N.R. Wald, Laser engineered net shaping advances additive manufacturing and repair, Weld. J. 86 (1) (2007) 44 http://www.rpm-innovations.com/index.php?page=news-article&id=5.

Radu Olar, "Nanomaterials And Nanotechnologies For Civil Engineering", Gheorghe Asachi Technical University of Iaşi, Faculty of Civil Engineering and Building Service, August 27, 2011

Rakkesh RA, Balakumar S (2013) Facile synthesis of ZnO/TiO2 core–shell nanostructures and their photocatalytic activities. J Nanosci Nanotechnol 13(1):370–376

Rana, A. K., Rana, S. B., Kumari, A., & Kiran, V. (2009). Significance of Nanotechnology in Construction Engineering. International Journal of Recent Trends in Engineering, 1(4), 6–8.

Rapidprototyping Services Canada, SLS, http://rapidprototypingservicescanada.com/selective-laser-sintering-sls.php.

Rashad, A.M., 2015. A synopsis about the effect of nano-titanium dioxide on some properties of cementitious materials e a short guide for civil engineer. Reviews on Advanced Materials Science 40, 72-88.

Raut, S.P.; Ralegaonkar, R.V.; Mandavgane, S.A. Development of sustainable construction material using industrial and agricultural solid waste: A review of waste-create bricks. Constr. Build. Mater. 2011, 25,4037–4042.

Rawat, Parul & Kumar, Ajit & Verma, Abhay. (2015). A REVIEW ON NANOTECHNOLOGY IN CIVIL ENGINEERING.

Regmi C, Joshi B, Ray SK, Gyawali G, Pandey RP. Understanding Mechanism of Photocatalytic Microbial Decontamination of Environmental Wastewater. Front Chem. 2018; 6:33. Published 2018 Feb 28. doi:10.3389/fchem.2018.00033

Reid, Matthew & Whatley, Vanessa & Spooner, Emma & Nevill, Alan & Cooper, Michael & Ramsden, Jeremy & Dancer, Stephanie. (2018). How Does a Photocatalytic Antimicrobial Coating Affect Environmental Bioburden in Hospitals?. Infection Control & Hospital Epidemiology. 39. 1-7. 10.1017/ice.2017.297.

Rello J, Ollendorf DA, Oster G, Vera-Llonch M, Bellm L, Redman R, Kollef MH; VAP Outcomes Scientific Advisory Group. Epidemiology and outcomes of ventilator-associated pneumonia in a large US database. Chest. 2002;122(6):2115-21.

Rioult, M., Stanescu, D., Le Fevre, P., Barbier, A., Magnan, H., 2016. Resonant Photo Emission spectroscopy investigation of Fe2O3 e TiO2 heterojunctions for solar water splitting. Physics Procedia 85, 4-11.

Rogers, M.A. Naturally occurring nanoparticles in food. Curr. Opin. Food Sci. 2016, 7, 14–19.2.3. Incidental Nanoparticles

Rohrer, Gregory S. Structure and Bonding in Crystalline Materials. Cambridge: Cambridge University Press, 2001.

Rosseinsky, D. R.; Mortimer, R. J. Electrochromic Systems and the Prospects for Devices. Adv. Mater. 2001, 13, 783–793.

Rudenko A., andrey rudenko constructs 3D printed concrete castle in minnesota, 28 Aug. 2014, viewed 3 June 2020, < https://www.designboom.com/technology/3d-printed-concrete-castle-minnesota-andrey-rudenko-08-28-2014/ >

Rutala, W. Environmental Control to Reduce GI Illness. Presented at the Society of Health Care Epidemiology Scientific Meeting (2006).

S. Bradshaw, A. Bowyer, P. Haufe, The intellectual property implications of low-cost 3D printing, ScriptEd 7 (1) (2010) 5–31.

S. Khoshnevis, S. Bukkapatnam, H. Kown, J. Saito, Experimental investigation of contour crafting using ceramics materials, Rapid Prototyp. J. 7 (1) (2001) 32–41.

S. Lim, T. Le, J. Webster, R. Buswell, S. Austin, A. Gibb, T. Thorpe, Fabricating construction components using layer manufacturing technology, (GICC'09), Paper presented at the Global Innovation in Construction Conference, Loughborough University, Leicestershire, UK, 2009, 13–16 September, 2009.

S. Patel Abhiyan, A.R. Hiren, D.N. SharmaAn overview on application of Nanotechnology in construction industry Int J Innov Res Sci Eng and Tech, 2 (11) (2013)

S. Tibbits, C. Mcknelly, C. Guillermo Camacho Olguín, D. Dikovsky, S. Hirsch, “4D printing and universal transformation”, ACADIA (2014) 539–548.

S. Tibbits, From automated to autonomous assembly, Archit. Design 87 (4) (2017) 6–15.

S.L. Bakoss, R.S. Ravindrarajah, Recycled construction and demolition materials for use in roadworks and other local government activities, 1999, 72.

S.-s. Chung and C. W. H. Lo, "Evaluating sustainability in waste management: the case of construction and demolition, chemical and clinical wastes in Hong Kong," Resources, Conservation and Recycling, vol. 37, pp. 119-145, 1// 2003.

Saeli, M., Tobaldi, D.M., Rozman, N., SEVER Skapin, A., Labrincha, J.A., Pullar, R.C., 2017. Photocatalytic nano-composite architectural lime mortar for degradation of urban pollutants under solar and visible (interior) light. Construction and Building Materials 152, 206e213.

Safdar N, Dezfulian C, Collard HR, Saint S. Clinical and economic consequences of ventilator-associated pneumonia: a systematic review. Crit Care Med. 2005;33(10):2184-93.

Salam MA, Obaid AY, El-Shishtawy RM, Mohamed SA (2017) Synthesis of nanocomposites of polypyrrole/carbon nanotubes/silver nano particles and their application in water disinfection. RSC Adv 7:16878–16884. doi.org/10.1039/c7ra01033h

Sanchez, F., Zhang, L., & Ince, C. (2009). Multi-scale performance and durability of carbon nanofiber/cement composites. In Z. Bittnar, P. J. M. Bartos, J. Nemecek, V. Smilauer, & J. Zeman (Eds.), Nanotechnology in construction: Proceedings of the NICOM3 (3rd international symposium on Nanotechnology in Construction) (pp. 345–350), Prague. Berlin: Springer.

Sandvik, CH440 cone crusher, viewed on 23 June 2020, < https://www.rocktechnology.sandvik/en/products/stationary-crushers-and-screens/stationary-cone-crushers/ch440-cone-crusher/ >

Sappi Fine Paper North America, "Defining and Communicating Color: The CIELAB System", viewed on 14 August 2020, <https://cdns3.sappi.com/s3fspublic/sappietc/Defining%20and%20Communi cating%20Color.pdf>.

Saptarshi Sasmal, "Can Carbon Nanotubes Make Wonders in Civil/Structural Engineering?", Progress in Nanotechnology and Nanomaterial, Oct. 2013, Vol. 2 Iss. 4, PP. 117-129

Sarraz, Atik & Hossain, Md & Rahman, A. (2017). Comparative Study of Recycle Concrete Aggregate as a Construction Material. 10.13140/RG.2.2.23742.18243.

Sauvé, S., Bernard, S., & Sloan, P. (2016). Environmental sciences, sustainable development and circular economy: Alternative concepts for trans-disciplinary research. Environmental Development, 17, 48–56.

Scarinci, Giovanni & Brusatin, Giovanna & Bernardo, Enrico. (2006). Glass Foams. 10.1002/3527606696.ch2g.

Senić, Ž & Bauk, S. & Vitorović-Todorović, M. & Pajić, N. & Samolov, Aleksandra & Rajic, Dusan. (2011). Application of TiO2 Nanoparticles for Obtaining Self- Decontaminating Smart Textiles, Scientific Technical Review, 2011,Vol.61,No.3-4,pp.63-72.

Seven, O., Dindar, B., Aydemir, S., Metin, D., Ozinel, M., Icli, S., 2004. Solar photocatalytic disinfection of a group of bacteria and fungi aqueous suspensions with TiO2, ZnO and Sahara Desert dust. Journal of Photochemistry and Photobiology A: Chemistry 165,103-107. https://doi.org/10.1016/j.jphotochem.2004.03.005.

Shah, A., Jan, I.U., Khan, R.U. and Qazi, E.U., (2013). Experimental investigation on the use of recycled aggregates in producing concrete. Structural Engineering and Mechanics, 47(4), pp.545-557.

Shah, Riddhish & Pitroda, Dr. Jayeshkumar. (2011). RECYCLING OF CONSTRUCTION MATERIALS FOR SUSTAINABILITY. National Conference on Recent Trends in Engineering & Technology (NCRTET) at BVM Engineering College, Vallabh Vidyanagar, Volume: ISBN-978-81-921358-0-9

Shah, S. P., Konsta-Gdoutos, M. S., Metaxa, Z. S., & Mondal, P. (2009). Nanoscale modification of cementitious materials. In Z. Bittnar, P. J. M. Bartos, J. Nemecek, V. Smilauer, & J. Zeman (Eds.), Nanotechnology in construction: Proceedings of the NICOM3 (3rd international symposium on Nanotechnology in Construction) (pp. 125–130), Prague. Berlin: Springer.

Shaki BA, Houbi MV, Valinejadshoubi M (2014) Useable and precautionary aspects of using nanotechnology and nano- materials in the construction industry. Int J of Sci Engineer Technol Rese (IJSETR).

Shen S, Burton M, Jobson B and Haselbach L (2012) Pervious concrete with titanium dioxide as a photocatalyst compound for a greener urban road environment. Construction and Building Materials 35: 874–883.

Shields, J.E.; Lowell, S.; Thomas, M.A.; Thommes, M. Characterization of Porous Solids and Powders: Surface Area, Pore Size and Density; Kluwer Academic Publisher: Boston, MA, USA, 2004; pp. 43–45.

Shvedova AA, Sager T, Murray A, Kisin E, Porter DW, Leonard SS, Schwegler-Berry D, Robinson VA, Castranova V [2007]. Critical issues in the evaluation of possible effects resulting from airborne nanoparticles. In: Monteiro-Riviere N and Tran L (eds). Nanotechnology: characterization, dosing and health effects. Philadelphia, PA: Informa Healthcare, pp. 221–232.

Sing, K.S.W.; Everett, D.H.; Haul, R.A.W.; Moscou, L.; Pierotti, R.A.; Rouquerol, J.; Siemieniewska, T. Reporting physisorption data for gas/solid systems with special reference to the determination of surface area and porosity. Pure Appl. Chem. 1985, 57, 603–619.

Sireesha, Merum & Lee, Jeremy & Kiran, A Sandeep & VELURU, Jagadeesh babu & Kee, Bernard & Ramakrishna, Seeram. (2018). A review on additive manufacturing and its way into the oil and gas industry. RSC Advances. 8. 22460-22468. 10.1039/C8RA03194K.

Sobolev, K., & Ferrada-Gutiérrez, M. (2005). How nanotechnology can change the concrete world: Part 1. American Ceramic Society Bulletin, 10, 14–17.

Souayfane, Farah & Fardoun, Farouk & Biwole, Pascal. (2016). Phase Change Materials (PCM) for cooling applications in buildings: A review. Energy and Buildings. 129. 10.1016/j.enbuild.2016.04.006.

Stedman Machine Company (a), “HSI Crusher Manufacturer”, viewed on 24 June 2020,<https://www.stedman-machine.com/more.html>.

Stedman Machine Company (b), “All You Need to Know About: Vertical Shaft Impactor (VSI) Primers”, viewed on 24 June 2020, <https://www.stedman-machine.com/vsi-primer-article.html>.

Steel Recycling Institute (SRI), “Steel: The Sustainable Material for Building Construction”, viewed on 22 June 2020, < https://www.steelsustainability.org/-/media/recycling-resources/steel-sustainable-material-building-construction.ashx >.

Stefanidou, M.; Karozou, A. Testing the effectiveness of protective coatings on traditional bricks. Constr. Build. Mater. 2016, 111, 482–487.

Strambeanu, N.; Demetrovici, L.; Dragos, D. Nanoparticles’ Promises and Risks: Characterization Manipulation,Potential Hazards to Humanity the Environment; Springer: Cham, Switzerland, 2015; pp. 9–19.

Sustainable development, viewed on 13 June 2020, < http://isdg.in/sustainable-development-model/ >.

Suwarnkar, M., B., Dhabbe, R., S., Kadam, A., N., Garadkar, K., M., Enhanced photocatalytic activity of Ag doped TiO2 nanoparticles synthesized by a microwave assisted method, Ceramics International 40 (2014) 5489–5496.

T. Campbell, C. Williams, O. Ivanova, B. Garrett, Could 3D Printing Change the World, Technologies, Potential, and Implications of Additive Manufacturing, Atlantic Council, Washington, DC, 2011.

T. Campbell, C. Williams, O. Ivanova, B. Garrett, Could 3D Printing Change the World: Technologies, Potential, and Implications of Additive Manufacturing, Atlantic Council, Washington, 2011.

T. Thorsell Advances in thermal insulation – vacuum insulation panels and thermal efficiency to reduce energy usage in buildings Doctoral thesis KTH Royal Institute of Technology, Stockholm (2012).

T. Wohlers, 3D Printing and Additive Manufacturing State of the Industry, Wohlers Associates Inc., Colorado, 2014.

talgaresources.com: TalgaGrapheneBoostsConcreteThermal Conductivity

Taniguchi, N.; Arakawa, C.; Kobayashi, T. On the basic concept of nano-technology. In Proceedings of the International Conference on Production Engineering, Tokyo, Japan, 26–29 August 1974.

Taurozzi, J.S., Hackley, V.A., Wiesner, M.R., 2012. Preparation of nanoparticle dispersions from powdered material using ultrasonic disruption. National Institute of Standards and Technology, Gaithersburg, p. 15. To, D.

Thomas C, Cimentada A, Polanco JA, Setién J, Méndez D, Rico J. Influence of recycled aggregates containing sulphur on properties of recycled aggregate mortar and concrete. Compos B: Eng 2013;45(1):474–85.

Thomas, Selvin & Al Mutairi, Eid & De, Sadhan. (2013). Impact of Nanomaterials on Health and Environment. ARABIAN JOURNAL FOR SCIENCE AND ENGINEERING. 38. 457-477. 10.1007/s13369-012-0324-0.

Tibaut, A., Rebolj, D., Perc, M.N., 2016. Interoperability requirements for automated manufacturing systems in construction. J. Intell. Manuf. 27 (1), 251.

Toshimi Kabeyasawa, “Recent Development of Seismic Retrofit Methods in Japan”, Japan Building Disaster Prevention Association, January, 2005.

U. Berardi, Development of glazing systems with silica aerogel, 6th International Physics Conference, Energy Procedia 78, 2015, pp. 394-399.

U. Scheithauer, E. Schwarzer, H.J. Richter, T. Moritz, Thermoplastic 3D Printing—An additive manufacturing method for producing dense ceramics, Int. J. Appl. Ceram. Technol. 12 (1) (2015) 26–31.

Udroiu, Razvan & Braga, Cristian. (2017). Polyjet technology applications for rapid tooling. MATEC Web of Conferences. 112. 03011. 10.1051/matecconf/201711203011.

Urosevic, M., Yebra-Rodríguez, A., Sebastian-Pardo, E., Cardell, C., 2012. Black soiling of an architectural limestone during two-year term exposure to urban air in the city of Granada (S Spain). The Science of the Total Environment 414, 564e575. https://doi.org/10.1016/j.scitotenv.2011.11.028.

V. Colla, E. Dini, Large scale 3D printing: From deep sea to the moon, Education & Sustainable Development, 2013, pp. 127–132.

V. Kruefu, H. Ninsonti, N. Wetchakun, B. Inceesungvorn, P. Pookmanee, and S. Phanichphant, “Photocatalytic degradation of phenol using Nb-loaded ZnO nanoparticles,” Engineering Journal, vol 16, no. 3, pp. 91–99, 2012.

V. Tam, "Economic comparison of concrete recycling: A case study approach," Resources, Conservation and Recycling, vol. 52, pp. 821-8, 2008.

V.R.G. Dev, J. Venugopal, S. Sudha, G. Deepika, S. Ramakrishna, Dyeing and antimicrobial characteristics of chitosan treated wool fabrics with henna dye, Carbohydr. Polym. 75 (2009) 646–650, http://dx.doi.org/10.1016/j.carbpol.2008.09.003.

Valente, M.; Sibai, A. Rubber/crete: Mechanical properties of scrap to reuse tire-derived rubber in concrete; A review. J. Appl. Biomater. Funct. Mater. 2019, 17, 1–8.

Vegas, I., Ibañez, J.A., Lisbona, A., Sáez de Cortazar, A., Frías, M., 2011. Pre-normative research on the use of mixed recycled aggregates in unbound road sections. Constr. Build. Mater. 25 (5), 2674–2682.

Vignesh, K. & Somasundaram, Sivaraman. (2019). Exploitation of Nanoparticles as Photocatalysts for Clean and Environmental Applications. 10.1007/978-3-030-04477-0_11.

Vinu R, Madras G (2011) Photocatalytic degradation of water pollutants using Nano-TiO2. In: Zang L (ed) Energy efficiency and renewable energy through nanotechnology. Springer, London, pp 625–677

Voxeljet, viewed on 10 June 2020, < https://www.voxeljet.com/3d-printing-systems/vx4000/ >

W. Gao, Y. Zhang, D. Ramanujan, K. Ramani, Y. Chen, C.B. Williams, C.C. Wang, Y.C. Shin, S. Zhang, P.D. Zavattieri, The status, challenges, and future of additive manufacturing in engineering, Comput. Aided Des. 69 (2015) 65–89.

Waiskopf, N., BenShahar, Y., Galchenko, M., Carmel, I., Moshitzky, G., Soreq, H., et al. (2016). Photocatalytic reactive oxygen species formation by semiconductor–metal hybrid nanoparticles. toward light-induced modulation of biological processes. Nano Lett. 16, 4266–4273. doi: 10.1021/acs.nanolett.6b01298

Wang, F., Yang, L., Wang, H., & Yu, H. (2015). Facile preparation of photocatalytic exposed aggregate concrete with highly efficient and stable catalytic performance. CHEMICAL ENGINEERING JOURNAL, 264, 577–586. https://doi.org/10.1016/j.cej.2014.11.129

Wang, W., Huang, G., Yu, J. C., and Wong, P. K. (2015). Advances in photocatalytic disinfection of bacteria: Development of photocatalysts and mechanisms. J. Environ. Sci. 34, 232–247. doi: 10.1016/j.jes.2015.05.003

Wang, Z. L. Triboelectric Nanogenerators as New Energy Technology for Self-Powered Systems and as Active Mechanical and Chemical Sensors. ACS Nano 2013, 7, 9533–9557.

Wangler, Timothy & Lloret, Ena & Reiter, Lex & Hack, Norman & Gramazio, Fabio & Kohler, Matthias & Bernhard, Mathias & Dillenburger, Benjamin & Buchli, Jonas & Roussel, N. & Flatt, Robert. (2016). Digital Concrete: Opportunities and Challenges. RILEM Technical Letters. 1. 67. 10.21809/rilemtechlett.2016.16.

Whitby, Raymond & Busquets, Rosa. (2013). Nanomaterials and the Environment: Global impact of tiny materials. Nanomaterials and the Environment. 1. 1-2. 10.2478/nanome-2012-0001.

Williams, B.A., A. Copeland, & T.C. Ross (2018). Asphalt Pavement Industry Survey on Recycled Materials and Warm-Mix Asphalt Usage: 2017, 8th Annual Survey (IS 138). National Asphalt Pavement Association, Lanham, Maryland. doi:10.13140/RG.2.2.30240.69129.

Wilso, G. J., Matijasevich, A. S., Mitchell, D. R., Schulz, J. C., & Will, G.D. (2006). Modification of TiO2 for enhanced surface properties: Finite Ostwald ripening by a microwave hydrothermal process. Langmuir, 22(5), 2016–2027.

Wong, Shane. (2014). An Overview of Nanotechnology in Building Materials. Canadian Young Scientist Journal. 2014. 18-21. 10.13034/cysj-2014-012.

Wonyong Choi, Andreas Termin, and Michael R. Hoffmann, The Role of Metal Ion Dopants in Quantum-Sized TiO2: Correlation between Photoreactivity and Charge Carrier Recombination Dynamics, The Journal of Physical Chemistry 1994 98 (51), 13669-13679 DOI: 10.1021/j100102a038

Woolley T, Kimmins S, Harrison P, Harrison R. Green building handbook: a guide to building products and their impact on the environment, 1. London: Spon Press; 1997.

Wu, Deyong & Long, Mingce & Zhou, Jiangya & Cai, Weimin & Zhu, Xiehao & Chen, Chao & Wu, Yahui. (2009). Synthesis and characterization of self-cleaning cotton fabrics modified by TiO2 through a facile approach. Surface & Coatings Technology - SURF COAT TECH. 203. 3728-3733. 10.1016/j.surfcoat.2009.06.008.

Wu, Peng & Wang, Jun & Wang, Xiangyu. (2016). A critical review of the use of 3-D printing in the construction industry. Automation in Construction. 68. 21-31. 10.1016/j.autcon.2016.04.005.

X. Zhang, F. Wu, X. Wu, P. Chen, and N. Deng, “Photodegradation of acetaminophen in TiO2 suspended solution,” Journal of Hazardous Materials, vol. 157, no. 2-3, pp. 300–307, 2008.

Xia, Ming & Sanjayan, Jay. (2016). Method of formulating geopolymer for 3D printing for construction applications. Materials & Design. 110. 10.1016/j.matdes.2016.07.136.

Y. Huang, M.C. Leu, J. Mazumder, A. Donmez, Additive manufacturing: current state, future potential, gaps and needs, and recommendations, J. Manuf. Sci. Eng. 137 (2015).

Y. Li, P. Leung, L. Yao, Q.W. Song, E. Newton, Antimicrobial effect of surgical masks coated with nanoparticles, J. Hosp. Infect. 62 (2006) 58–63, http://dx.doi.org/10.1016/j.jhin.2005.04.015.

Y. Liu, Y. Ohko, R. Zhang, Y. Yang, and Z. Zhang, “Degradation of malachite green on Pd/WO3 photocatalysts under simulated solar light,” Journal of Hazardous Materials, vol. 184, no. 1–3, pp. 386–391, 2010.

Yang J, Du Q, Bao Y. Concrete with recycled concrete aggregate and crushed clay bricks. Constr Build Mater 2011;25(4):1935–45.

Ye H, Meng X, Xu B. Theoretical discussions of perfect window, ideal near infrared solar spectrum regulating window and current thermochromic window. Energy Build 2012; 49:164–72.

Yixian Liu, William Z. Xu, Paul A. Charpentier, “Synthesis of VO2/Poly(MMA-co-dMEMUABr antimicrobial/thermochromic dual-functional coatings”, Progress in Organic Coatings 142 (2020) 105589, https://doi.org/10.1016/j.porgcoat.2020.105589

Yusuf, Mohd & Cutler, & Gao, (2019). Review: The Impact of Metal Additive Manufacturing on the Aerospace Industry. Metals. 9. 1286. 10.3390/met9121286.

Zareiyan, B. and Khoshnevis, B. (2017). Interlayer adhesion and strength of structures in Contour Crafting-Effects of aggregate size, extrusion rate, and layer thickness. Automation in Construction, 81, pp.112-121.

Zhang J, Khoshnevis B. Optimal machine operation planning for construction by Contour Crafting. Automat Constr, 2013, 29: 50–67

Zhang, H., Yang, Z., Zhang, X. and Mao, N. (2014). Photocatalytic effects of wool fibers modified with solely TiO2 nanoparticles and N-doped TiO2 nanoparticles by using hydrothermal method. Chem. Eng. J. 254 : 106-114.

Zhang, R., Cheng, X., Hou, P., Ye, Z., 2015. Influences of nano-TiO2 on the properties of cement-based materials: hydration and drying shrinkage. Construction and Building Materials 81, 35-41.

Zhang, Z., MacMullen, J., Dhakal, H.N., Radulovic, J., Herodotou, C., Totomis, M., Bennett, N., 2013. Biofouling resistance of titanium dioxide and zinc oxide nanoparticulate silane/siloxane exterior facade treatments. Building and Environment 59, 47-55. doi.org/10.1016/j.buildenv.2012.08.006.

Zhu, W., Bartos, P.J.M., Porro, A.: Application of nanotechnology in construction - Summary of a state-of-the-art report. Mater. Struct. 37(273), 649–658 (2004) 89

EVANGELOS KARAGIANNIS

Master Thesis

HELLENIC REPUBLIC

National and Kapodistrian University of Athens

EST. 1837